

**Thesis for Master's
degree in chemistry**

Christian Wilhelm Mohr

**Monitoring of phosphorus
fractions – Understanding
geochemical and
hydrological processes
governing the mobilization
of phosphorus from
terrestrial to aquatic
environment.**

60 study points

DEPARTEMENT OF CHEMISTRY

Faculty of mathematics and natural
sciences

UNIVERSITY OF OSLO 09/2010



Preface

Acknowledgements

This master thesis has been carried out at the Department of Chemistry, University of Oslo (UiO) in period from January 2009 to August 2010. This study is part of The Research Council of Norway (RCN) - Miljø2015 - TVERS project EUTROPIA (NFR project number: 190028/S30). Part of the study was carried out at the Norwegian Institute for Water Research (NIVA) and The Department of Geosciences, UiO.

I'd like to thank my supervisor and mentor through out this work Rolf D. Vogt. It has been a great pleasure working with you in this project. Your support, guidance and trust in my abilities as chemist, is truly appreciated.

I'd like to thank co-supervisor Oddvar Røyseth, at NIVA, for all his help. Your overwhelming determination and enthusiasm (within limits) has been of great importance to this thesis and the project.

Thanks also to co-supervisor Tom Andersen for your help. Your knowledge at times baffles me. I would have liked to have spent more time to learn from you.

Thanks to Alexander Engebretsen for all the help through out this project. Also thanks to Brian Lutz and Kaja Opland for your work in the field and lab. To Richard Nosa Okungbowa and Yemane Kidanu, thanks for all your work in the lab.

Also thanks to Mesay Mulugeta Wolle for your work with the ICP-AES data.

Thanks to Xie Rukai for instrument technical and analytical help at the Department of Geosciences.

Special thanks to my work colleagues at NIVA, Eva Hagebø and Tomas A. Blakseth and others for all their help.

I'd also like to thank my fellow students, Asfaw Gebresadik Gebru, Goran Khalaf and Kristine Solberg who I have enjoyed spending time with.

My greatest thanks goes without a doubt to my family for all their support, which unfortunately will never be seen in this thesis, but would not be possible without them.

Table of Content

PREFACE	II
ACKNOWLEDGEMENTS	II
SYMBOLS AND ABBREVIATIONS	VI
ABSTRACT	2
1. INTRODUCTION	4
2. THEORY	7
2.1. FRESHWATER EUTROPHICATION	7
2.1.1. CULTURAL VS. NATURAL EUTROPHICATION	7
2.1.2. THE DETERIORATION OF A LAKE	8
2.1.3. CLASSIFICATION OF THE TROPHIC STATE	10
2.2. PHOSPHORUS CYCLING IN AN AQUATIC ECOSYSTEM	13
2.3. PHOTOOXIDATION AND DISSOLVED ORGANIC PHOSPHORUS (DOP)	17
2.4. ALGAE	18
2.5. EUTROPHICATION REMEDIES	20
2.6. VANSJØ	21
2.6.1. VANSJØ MORPHOMETRICS:	21
2.6.2. INTERESTS OF USE	22
2.6.3. VANSJØ-HOBØL CATCHMENT	23
2.6.4. PODZOLS	25
2.7. DIFFUSIVE GRADIENTS IN THIN FILMS (DGT)	28
3. MATERIALS AND METHODS	34
3.1. SAMPLING AT DALEN	34
3.1.2. SOIL WATER AT DALEN	36
3.1.3. DALEN STREAM	40
3.2. LABORATORY LOCATIONS AND FACILITIES	40
3.3. SAMPLE STORAGE AND PREPARATION BEFORE ANALYSIS	40
3.3.1. FILTRATION OF WATER SAMPLES	40
3.4. QUALITATIVE AND QUANTITATIVE ANALYSIS	41
3.4.1. CONDUCTIVITY AND PH	41

3.4.2.	UV AND COLOUR ABSORBANCE	41
3.4.3.	ALKALINITY	41
3.4.4.	ALUMINUM FRACTIONATION AND ANALYSIS	41
3.4.5.	MAJOR ANION ANALYSIS	42
3.4.6.	MAJOR CATION ANALYSIS	42
3.4.7.	PARTICULATE MATTER (PM) IN STREAM WATER	42
3.4.8.	QUANTITATIVE ANALYSIS OF PHOSPHATE	43
3.4.9.	SEAL AUTOANALYZER FOR ORTHOPHOSPHATE	44
3.4.10.	CNP-AUTOANALYZER	44
3.4.11.	PHOSPHORUS FRACTIONATION IN WATER SAMPLES	45
3.5.	SOIL ANALYSIS	46
3.5.1.	SOIL PRE-TREATMENT	46
3.5.2.	PHOSPHORUS FRACTIONATION SOIL SAMPLES	48
3.5.3.	SEQUENTIAL EXTRACTION OF P IN SOIL	48
3.6.	P-DGTs IN FIELD AND LABORATORY	51
3.6.1.	P-DGTs IN THE STREAM	51
3.6.2.	LABORATORY STUDY FOR P-DGT UPTAKE OF ORGANIC P COMPOUNDS.	52
3.6.3.	EXTRACTION AND ANALYSIS OF EXPOSED P-DGTs	54
3.7.	UV IMPACT ON DOM	54
3.7.1.	HUMIC STREAM WATER SAMPLE	54
3.7.2.	ZERO-TENSION SOIL WATER SAMPLE	55
4.	<u>RESULTS AND DISCUSSION</u>	57
4.1.	SOIL P FRACTIONS AND PH IN DALEN	57
4.2.	SOIL AND STREAM WATER	60
4.3.	P-DGT – LABORATORY AND FIELD STUDIES	66
4.3.1.	P-DGT UPTAKE OF AMP IN THE LABORATORY STUDY	66
4.3.2.	CAN P-DGT UPTAKE OF AMP BE USED TO ESTIMATE UPTAKE OF OTHER LMW ORGANIC P COMPOUNDS IN WATER?	69
4.3.3.	SAMPLING ORTHOPHOSPHATE AND SROP IN DALEN AND STØA STREAM.	71
4.4.	UV IMPACT ON DOM	74
4.4.1.	HUMIC STREAM WATER SAMPLE	74
4.4.2.	ZERO-TENSION SOIL WATER SAMPLE	77
4.4.3.	POSSIBLE CNP ANALYSIS PROBLEMS RELATED TO DOM.	79

5.	<u>CONCLUSION</u>	<u>81</u>
6.	<u>FUTURE WORK</u>	<u>82</u>
7.	<u>LITERATURE REFERENCES</u>	<u>83</u>

Symbols and Abbreviations

Al _i	Inorganic labile aluminium
Alk	Alkalinity
Al _o	Organic monomeric aluminium
Al-P	Phosphorus bound to aluminium
AMP	Adenosine monophosphate
Ca-P	Phosphorus bound to calcium
CNP-autoanalyzer	Carbon, nitrogen and phosphorus autoanalyzer
DBL	Diffusive boundary layer
DGT	Diffusive gradients in thin films
DNOM	Dissolved natural organic matter
DOC	Dissolved organic carbon
DOM	Dissolved organic matter
DON	Dissolved organic nitrogen
DOP	Dissolved organic phosphorus
EUTROPIA	Watershed EUTROphication management through system oriented process modeling of Pressures, Impacts and Abatement actions
Fe-P	Phosphorus bound to iron
GF/F	Grade for glass microfiber filter with pore size 0.7 µm
IC	Ion chromatography
ICP-AES	Induced coupled plasma atomic emission spectrometer
LHF	Litter fermentation humus
LMW	Low-molecular-weight
LOI	Loss on ignition
NIVA	Norwegian Institute for Water Research
NO ₃ -N	NO ₃ ⁻ determined as N (NO ₂ ⁻ is also included)
OECD	Organisation for Economic Co-operation and Development
Orthophosphate	The sum of H ₃ PO ₄ , H ₂ PO ₄ ⁻ , HPO ₄ ²⁻ , PO ₄ ³⁻
P-DGT	The DGT sampler with ferrihydrite adsorbent
PIP	Particulate inorganic phosphorus
PM	Particulate matter
PO ₄ -P	Orthophosphate determined as phosphorus
POP	Particulate organic phosphorus
RCF	Relative centrifugal force (RCF (g) = 0.00001118 * r (cm) * RPM ²)
RCN	The Research Council of Norway
RPM	Rotations per minute
RSD	Relative standard deviation
Sol-P	Easily soluble phosphorus

SROP	Soluble reactive organic phosphorus
SRP	Soluble reactive phosphorus
TF	Throughfall sample, water collected under canopy
TOC	Total organic carbon
Tot-N	Total nitrogen
Tot-P	Total phosphorus
Type I water	Ultra pure water
Type II water	Pure water
UiO	University of Oslo
USGS	U.S. Geological Survey
UV	Ultra violet radiation
WFD	Water Framework Directive
ZT	Water sample collected with zero-tention lysimeter (soil water collected under the forest floor)

Abstract

This study was performed in the Vansjø-Hobøl catchment in SE Norway, as part of research related to the transport of phosphorus to the eutrophic lake Vansjø, the largest lake in the catchment. This study is part of The Research Council of Norway (RCN) project EUTROPIA, which aims to improve understanding of geochemical and hydrological processes governing the mobilization of nutrients with special emphasis on phosphorus compounds. This work has examined sampling and fractionating methods for better understanding of phosphorus processes in the catchment, which will further contribute to the studies by other participants in the project.

Considerable research has been conducted on P leaching mechanisms from agricultural land, but little is known about the significance and mechanisms controlling P leaching from forests. Focus of this research has therefore been on forested catchments, comprising 85% of the catchment.

The lack of positive response to the considerable abatement actions is likely due to changes in environmental pressures, such as climate, land use change and long-range transported pollutants.

This monitoring study indicates that the decrease in Al leaching, from acid sensitive forested catchments, due to reduced S deposition may be an important factor governing the flux of P to the lake Vansjø. Aluminium ions are known to be a strong precipitating agent of P.

The monitoring also showed considerable concentrations of dissolved organic matter (DOM) from forested watersheds. The flux of DOM is known to have increased considerably since the 80ties. With this increase there has likely also been an increase in the flux to the lake of P bound to DOM.

The organic P fraction was shown to be a major contributor of the total P to the stream from the catchment. Also it was found that larger than expected amounts of Al was leaching from the soils.

Research on UV exposure to DOM was also conducted to determine the effect on the release of orthophosphate. UV exposure experiments showed up to 17% release of the phosphorus bound to DOM during the first period of UV exposure, indicating a P-fraction, which may easily be released to water. However, the UV decomposition process is complex and more research is needed.

A laboratory study showed that the DGT sampler (Diffusive Gradient in Thin films) specially designed for orthophosphate (P-DGT), also collected small organic molecules with phosphate groups, using the model compound AMP (adenosine monophosphate). The diffusion coefficient of AMP was calculated to $3.3 \times 10^{-6} \text{ cm}^2/\text{s}$ (22 °C), compared to 5.5×10^{-6} for orthophosphate, which agrees with larger molecules having slower diffusion rates. With the P-DGT it was possible to collect LMW organic phosphorus compounds as well as orthophosphate in water from the catchment. LMW organic phosphorus fraction was shown to contribute 6.5% of the total P collected by P-DGTs from an agricultural site. The P-DGT sampler can thus be used to get more information on this fraction in water containing dissolved organic phosphorus (DOP).

1. Introduction

There has been an increasing demand by the public and non-governmental environmental organizations for cleaner rivers and lakes. An opinion poll, cast by the European Commission in 25 EU countries, identified the five main environmental issues Europeans were most concerned about. The average result showed that nearly half responded with worries about “water pollution”. As a result the European Water Policy underwent a thorough restructuring process, and a new Water Framework Directive (WFD) was adopted and set into force as of 22nd December 2000 (European Commission, 2010). In 2006 the WFD was adopted by the Norwegian government, and incorporated into Norwegian law (Vannportalen, 2010). The WFD requires good water status, i.e. that all water reserves should not deviate from their natural conditions. Further deterioration should be prevented, and measures taken to improve conditions should be implemented if financially feasible (The European Parliament and the Council of the European Union, 2000). The national deadline to make plans for abatement procedures has been set for 2015 (Vannportalen, 2010).

Within the last 10 years more than half of the monitored lakes in Norway have been classified to have moderate or bad status with respect to eutrophication criteria. This is an increase by almost 20% since 1980-1997. Amongst the different geographical regions in Norway, eutrophication is greatest in the south-eastern (SE) parts (Solheim and Moe, 2008). Lake Vansjø, located near the city of Moss, SE Norway, has since the 1950's become increasingly eutrophic, with increasing algae growth. Since the 1970's there has been numerous measures taken to reduce the input of phosphorous (P) to Vansjø from agriculture and municipal sewage. Despite all these abatement actions, there has been achieved no reduction in the level of total phosphorous and algae growth (Thuen and Buer, 2003).

This lack of response may partly be due to a lag time of response to the abatement actions. But it is also likely that changes in fluxes of phosphorous from other sources may partly have compensated for the achieved reductions of nutrient losses from agriculture and decreased sewage leakage. Over the past 20 – 30 years the watershed has been experiencing significant changes in climate, land-use and anthropogenic deposition. These factors are conceptually prone to effect the mobilization and transport of nutrients from terrestrial to the aquatic environment, though little is

known of the role of these pressures. This is mainly due to that the mechanisms and chemical processes that govern the fluxes of phosphorous are inadequately understood. Understanding of the chemical processes, along with the hydrological, geological, physical and biological mechanisms governing P leaching and transport, is a prerequisite in order to construct conceptual catchment and lake models. Such models are needed in order to generate predictions of changes in lake water conditions based on abatement actions and scenarios of changes in environmental pressures. This in turn provides government officials with the knowledge needed to make policies that can lead to efficient and cost-effective abatement actions, improving the conditions of the lake.

In early 2009 the research project “Watershed EUTROphication management through system oriented process modelling of Pressures, Impacts and Abatement actions” (EUTROPIA) was launched to investigate the major processes and their governing pressures controlling P fluxes to lake Vansjø. Understanding these processes enable us to understand how changes in environmental pressures will affect the P fluxes from the terrestrial to the aquatic environment. This study is an initial part of the EUTROPIA project.

The main focus of the research on eutrophication has typically been on anthropogenic sources of nutrients, especially from agricultural land. Lake Vansjø, with a watershed situated mainly below the marine limit, is a naturally mesotrophic (possibly eutrophic) lake system. This is due to background leaching of P from marine clays in the watershed. About 85 % of the watershed draining into Lake Vansjø is forests, and it has been estimated that approx. 25% of the total P loading to the lake is from these forested areas.

The focus of this thesis has therefore been to better understand the hydro-geochemical processes that govern the mobilization and transport of P fractions from forests. A small representative forested catchment, draining into western Vansjø, has been equipped with water sampling equipment in different water compartments in order to collect water on its journey through the watershed. The chemistry in the catchment has been determined by performing chemical analysis of the soil, deposition, soil water and stream water from different soil plots in the catchment. By studying different P fraction, a preliminary assessment of sources, mobilization- and transport processes, as well as the fate of the P fractions has been achieved. Especially knowing which P fractions are largest in the soil and what conditions are needed to mobilize

them is of importance. Part of this thesis work has been focused on the development of sampling and soil and water fractionating techniques, with particular interest on the use of diffusive gradients in thin films (DGT). Furthermore, new analytical technology for the accurate determination of low levels of nutrients has been necessary to implement and test in order to enable P fractionation. Finally, the potential for photo-oxidation of organic-P, the dominant P form leached from forested sites, has been investigated in order to assess the fate of this fraction in the lake.

2. Theory

2.1. Freshwater Eutrophication

When aquatic environments receive excess amounts of nutrients they tend initially to develop better growth conditions for micro- and macro organisms. The result is an increase in plant growth, especially large algae blooms. The process is known as eutrophication, and aquatic environments with these conditions are known as being eutrophic (USGS, 2008).

2.1.1. Cultural vs. Natural Eutrophication

Eutrophication is really only considered an environmental problem when the eutrophic conditions are the result of excess nutrients contributed by anthropogenic sources. Even though the word “eutrophication” is usually associated as a man-made environmental problem, it is in fact also a natural process in the “aging” of lakes which may take thousands of years.

Man-made eutrophication, usually described as “cultural eutrophication”. Increased urbanization and agriculture are usually the main cause for anthropogenic changes in the natural chemical balance of waterbodies. The main causes for the strong increase in the input rate of nutrient to many waterbodies (Rast and Holland, 1988) and thereby to the increased eutrophication are:

- The use of excess fertilizers to agriculture that are being washed into the streams and lakes with the rain.
- Increased erosion due to increased runoff intensity due to climate change, landscape changes, straightening of streams and deforesting
- Faulty sewage drainage systems with overflow of sewage that results in rapid influx of high nutrient load to the waterbodies

Sources of Cultural Eutrophication

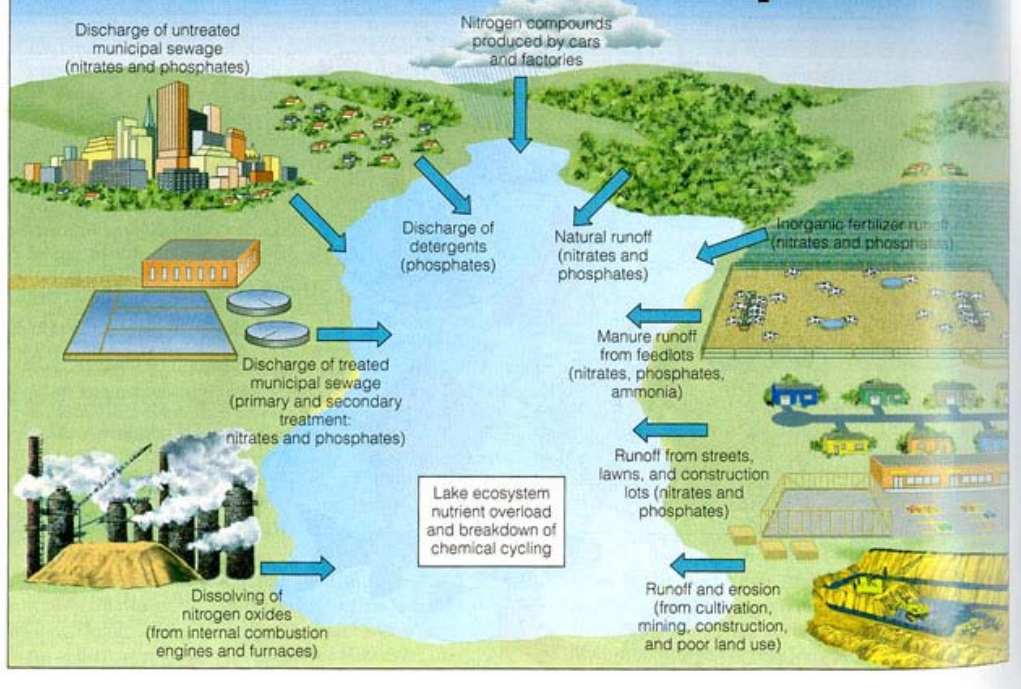


FIGURE 2a Sources of cultural eutrophication (Oracle ThinkQuest, 2008).

2.1.2. The Deterioration of a Lake

High input of limiting nutrients usually results in a high plant growth rate, especially large algae blooms. Phosphorus (P) tends to be the limiting resources in most standing freshwater bodies. The effect is increased P loading is initially limited to being an aesthetic problem, such as poor taste, odour and brown to green colour, but the condition may quickly deteriorate into a health risk (Rast and Holland, 1988).

To a certain point eutrophication can be quite beneficial to many species, such as fish. The increase in plankton gives nourishment for fish, and their photosynthesis provide sufficient oxygen in the water (vanLoon and Duffy, 2005b). Beyond this “optimal point” the growth of plants and plankton becomes so high that the biomass concentration, especially phytoplankton, reduces the lake depth visibility considerably. A reduction of light to the deeper parts of the lake has consequences for the survival of many organisms. Photoautotroph organisms are especially affected, as they are dependent on light for their photosynthesis. Photoautotrophs that live at the bottom of the lake either die or have to migrate towards the surface (if not benthic) in order to achieve sufficient light intensities. The migration to the surface further increases the biomass concentration at the surface, thereby reducing even more the

penetration of the light to the deeper parts of the lake. The upper part of the lake in which more than 1% of surface light can be found is known as the euphotic zone. As eutrophication increases the euphotic zone decreases. The euphotic zone is also decreased by the levels of allochthonous and autochthonous dissolved organic matter (DOM) staining the water yellow and brown (Dodson, 2005c).

The levels of nutrients and light are two major factors controlling the depth at which significant amounts of algae can be found. Algae grow best at light intensities at about $200 \mu\text{E m}^{-2} \text{sec}^{-1}$. The water surface receives about $2000 \mu\text{E m}^{-2} \text{sec}^{-1}$, which is too intense for most algae. In many lakes the major source of bioavailable nutrients are being released from the sediment. The main algae growth is therefore found at the depth in which a preferable balance between light and nutrients can be achieved. Here a thick layer of algae can be found, known as the algal plate. In a low productive lake the algal plate is typically located below the thermocline. In more eutrophic lakes the algal plate can be found above the thermocline as the euphotic zone is restricted to the epilimnion.

Light radiation is also a major source for the heating of most lakes. Temperature plays a role in the saturation of oxygen, where cold water holds more oxygen than warm water. The highest oxygen levels are found at an optimal depth in which a combination between cold temperature and high photosynthesis can be found. In low productive lakes this zone is typically found in the hypolimnion and moves towards the surface as productivity of lakes increase (Dodson, 2005c).

When the algae die they sink to the bottom causing a “drizzle” of dead organic material, which accumulate at the bottom of the lake. Eutrophic lakes have a greater biomass density in the water and therefore have a larger accumulation of organic material at the lake bottoms. The decomposition of dead organic matter by bacteria consumes the oxygen in the water and may eventually create anoxic conditions (Rast and Holland, 1988).

Low oxygen levels will cause fish to suffocate and die if they can not escape these conditions. It has been estimated that the O_2 levels required for maintaining a healthy fish population is about 2-5 mg/L for moderately tolerant fish. For less tolerant fish it is about 5-9 mg/L (Kalff, 2002a). As fish and other organisms die as a result of the anoxic conditions, their biomass add on to the decay of organic matter and consume thereby more oxygen. This is a detrimental positive feedback process, in which the

death of organisms will cause the death of others, accelerating the eutrophication process.

2.1.3. Classification of the trophic state

Productivity or the nutrient richness of lakes is the basis for the trophic concept of classification. It runs from oligotrophic lakes that are nutrient poor and clear, to those eutrophic lakes that are nutrient rich and usually have very poor water clarity. All the negative effects described in chapter 2.1.2 are associated with lakes denoted as being eutrophic. Mesotrophic lakes fall somewhere in between eutrophic and oligotrophic lakes. It is not a simple task to classify the trophic condition of lakes or reservoirs. This is due to that the trophic state is a continuum and that some waterbodies described as eutrophic, do not possess all the negative affects of eutrophication. And visa-versa, where oligotrophic waterbodies can experience occasional algae blooms. Some key parameters commonly used to describe a trophic state are the total phosphorus concentration, chlorophyll *a* concentration, and the Secchi depth (the measurement of water transparency) (Rast and Holland, 1988), see TABLE 2a.

TABLE 2a **Boundary values for fixed trophic classification systems (Organisation for Economic Co-operation and Development (OECD), 1982; Ryding and Rast, 1989a)**

Trophic category	Total phosphorus ($\mu\text{g} \cdot \text{L}^{-1}$)	Chlorophyll <i>a</i> ($\mu\text{g} \cdot \text{L}^{-1}$)		Secchi depth (m)	
		Mean	Maximum	Mean	Minimum
Ultra-oligotrophic	<4.0	<1.0	<2.5	>12.0	>6.0
Oligotrophic	<10.0	<2.5	<8.0	>6.0	>3.0
Mesotrophic	10 – 35	2.5 – 8	8 – 25	6 – 3	3 – 15
Eutrophic	35 – 100	8 – 25	25 – 75	3 – 1.5	1.5 – 0.7
Hypertrophic	>100	>25	>75	<1.5	<0.7

A problem in using total phosphorous (total P) concentration as criteria for eutrophication is that the same level of total P may give a larger ecological response in some parts of the world than others. This is apparent by that all parts of Vansjø,

with an average total P level below 35, would only be classified as mesotrophic according to this system.

Another problem with the OECD classification of trophic state is that it does not address whether or not the trophic level is an environmental problem. There are lakes that are naturally eutrophic, which possess a healthy balance between photosynthesis and respiration.

For this reason the WFD emphasizes that the natural conditions is what defines the good ecological status of water reserves. For Norway the parameters used for classifying the natural type of lake is given in TABLE 2b. Once the lake is classified then other parameter, such as total P, Secchi depth, etc., can be used to determine the ecological status TABLE 2c.

TABLE 2b Parameters used to classify lakes in Norway (Direktoratsgruppen, 2009)

Criteria	Parameter
Ecoregion	Østlandet Sørlandet Vestlandet Midt-Norge Nord-Norge, outer region Nord-Norge, inner region
Altitude typology	High: >800 m a.s.l. (over tree limit) Mid-altitude: 200 to 800 m a.s.l. (under tree limit) Lowland: < 200 m a.s.l.
Calcareous/Alkalinity	Extremely low: Ca < 1 mg L ⁻¹ , Alk < 0.05 mekv L ⁻¹ Low: Ca 1-4 mg L ⁻¹ , Alk. 0.05-0.2 mekv L ⁻¹ Moderate: Ca 4-20 mg L ⁻¹ , Alk > 0.2-1 mekv L ⁻¹ High: Ca > 20 mg L ⁻¹ , Alk.> 1 mekv L ⁻¹
Humus content	Clear: Colour < 30 mg Pt L ⁻¹ , TOC < 5 mg L ⁻¹ Humic: 30-90 mg Pt L ⁻¹ , TOC 5-15 mg L ⁻¹ Extremely Humic: Color > 90 mg Pt L ⁻¹ , TOC> 15 mg L ⁻¹
Turbidity (median value) (used only for lowlands)	Clear: STS < 10 mg L ⁻¹ , (inorganic content ≥ 80%) Strong clay influence: STS > 10 mg L ⁻¹ (inorganic content ≥ 80%)
Lake size (surface area)	Small: 0.5-5 km ² Large: 5-50 km ² Extremely large: >50 km ²
Lake Depth (mean)	Extremely shallow: < 3 m Shallow: 3-15 m Deep: > 15 m

TABLE 2c Ecological status classification for lowland, moderate calcareous, humic lakes such as Vansjø (Direktoratsgruppen, 2009).

Status	High	Good	Moderate	Poor	Bad
Chlorophyll <i>a</i> (µg/L)	3.5	7	10.5	20	40
Secchi Depth (m)	5	3	2	1	0.5
Total P (µg P L ⁻¹)	7	13	19	35	65
Total N (µg N L ⁻¹)	300	450	550	900	1500
O ₂ (mg L ⁻¹) at hypolimnion*	12	9	5	2	1

*Where 50% of observations are below the given border value

2.2. Phosphorus cycling in an aquatic ecosystem

There are many inorganic nutrients important for plant growth, such as nitrogen, phosphorus, carbon, potassium, sulphur, calcium, magnesium and many other trace nutrients. It is however nitrogen and phosphorus that are the main focus regarding eutrophication. Nitrogen and phosphorus are the two nutrients that are most commonly the limiting factor for further growth. This is due to the relatively low availability compared to the high biological demand. Out of the two, phosphorus is least abundant and most commonly limits biological productivity in fresh water lakes (Kalff, 2002b). The soluble reactive phosphorus (SRP), is both the inorganic and organic form considered to be available to algae and macrophytes. Orthophosphate (Sum of H_3PO_4 , H_2PO_4^- , HPO_4^{2-} and PO_4^{3-}) makes up the major component of SRP (Dodson, 2005a). Due to rapid assimilation the concentration of this fraction is however maintained near the detection limit (Ryding and Rast, 1989b). Furthermore, phosphorus in the form of orthophosphate has only a small pH region (4.5 – 7) in which it may be found in significant amounts in most freshwaters (see FIGURE 2b). This is not to imply that it is the pH *per se* that has a large effect on orthophosphate solubility. It is rather the case that pH has an effect on the solubility of other compounds which adsorb or precipitate out orthophosphate. Under pH 4.5 the acidic environment causes the release of iron and aluminium ions, which can adsorb or precipitate with orthophosphate. Above pH 7 the typically high calcium concentrations associated with the neutral to alkaline environment causes orthophosphate to precipitate in the form of $\text{Ca}_3(\text{PO}_4)_2$ ($K_{\text{sp}} = 1.2 \times 10^{-29}$) or $\text{Ca}_5(\text{PO}_4)_3\text{OH}$ ($K_{\text{sp}} = 6.8 \times 10^{-37}$) (Lide, 2004a; vanLoon and Duffy, 2005b).

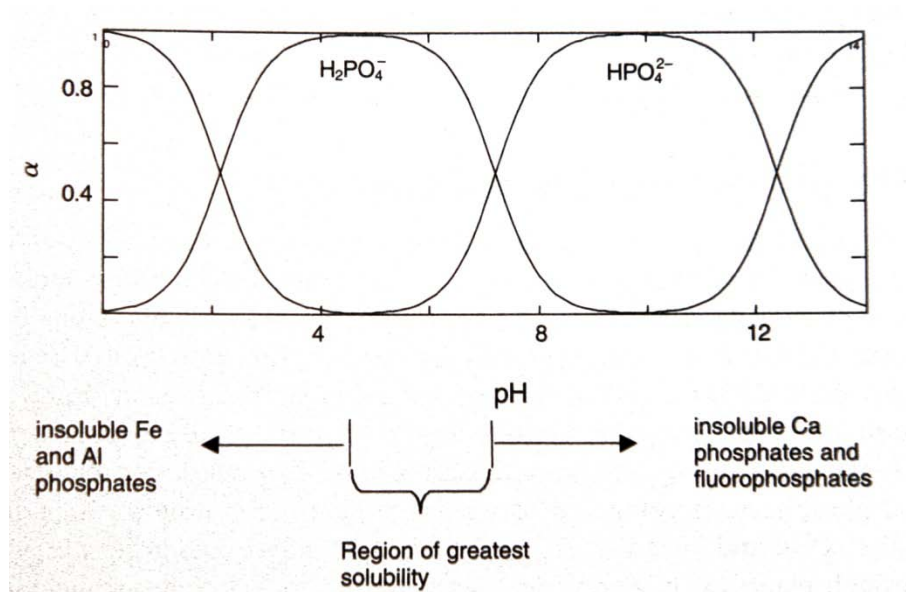


FIGURE 2b pH region of greatest solubility for phosphate (vanLoon and Duffy, 2005b).

Orthophosphate may be released from sediments as a result of reduced redox state as well as increase in pH above pH 7. The effect of reduced redox conditions is discussed below. The release of orthophosphate with increased alkalinity is due to that hydroxide ions compete with orthophosphate in adsorption to FeOOH flocs. This results in orthophosphate being replaced with hydroxide. High pH values are typically found in the epilimnion of eutrophic lakes as heavy photosynthesis consume CO_2 , reducing the amount of carbonic acid, and produce hydroxyl ions (OH^-), raising the water column pH. Thus, photosynthesis increases water column pH (Kalff, 2002b).

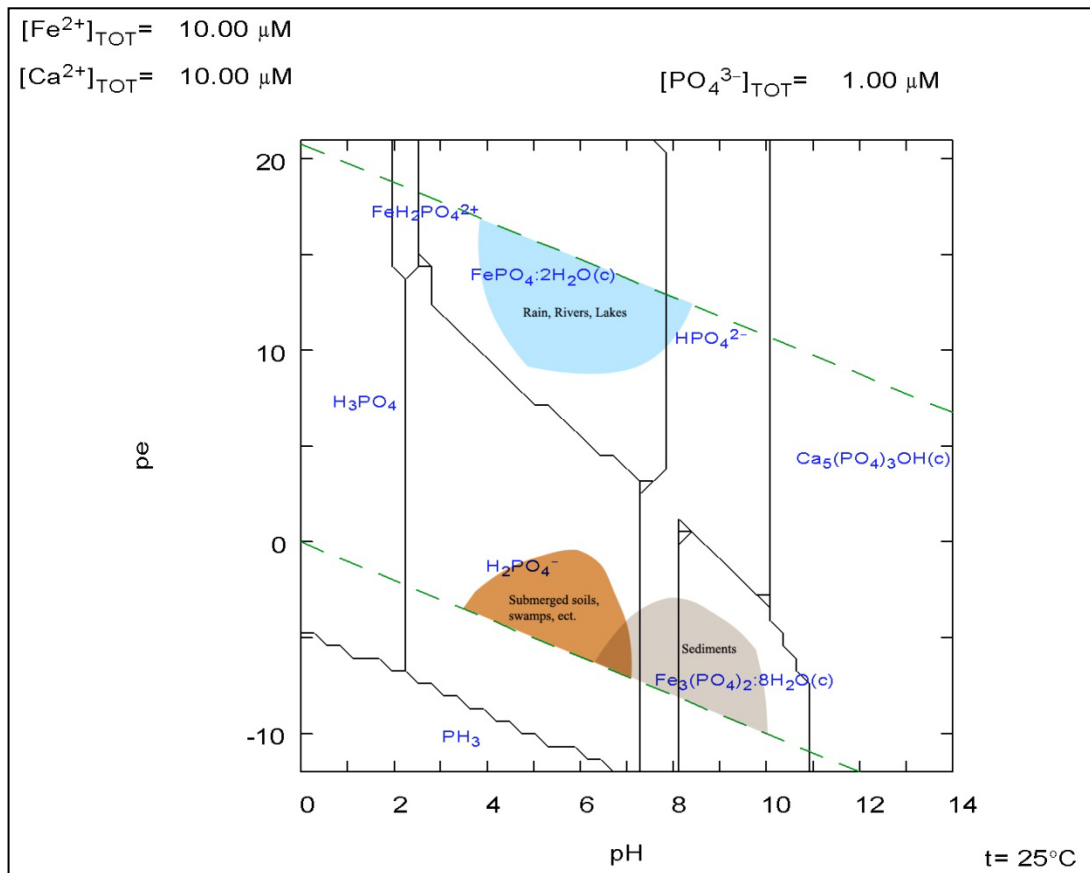


FIGURE 2c Pourbaix diagram for the solubility of orthophosphate in aquatic systems. Coloured areas indicate typical pe and pH values for aqueous, soil, and sediment environments. (Created with computer program Medusa Chemical Equilibrium, 2010)

Most of the phosphorus found in freshwater systems is not readily bioavailable as it is bound up in the biomass, to refractory DOM or bound inorganically/adsorbed to silt and clay particles. The role of dissolved organic phosphorous (DOP) is discussed in the next chapter (2.3).

The fate of the particle bound phosphorous is strongly influenced by the redox conditions. In natural aquatic systems inorganic phosphate exists only in oxidation state +5. It is therefore not considered a redox element. However the oxidation state of iron (and manganese) has an important role when it comes to the insolubility of phosphate. Iron may exist as either Fe(II) and Fe(III) under redox conditions commonly encountered in the aquatic environment. The Fe(III) is insoluble with orthophosphate (FePO_4 , $K_{sp} = 4 \times 10^{-27}$). However, aqueous Fe(III) is not found in significant amounts as it readily precipitates as ferrous hydroxide (Fe(OH)_3 , $K_{sp} = 2 \times 10^{-39}$) in the pH range (4 - 8) of most natural waters. Instead orthophosphate is often adsorbed to Fe(III) hydroxides as FeOOHPO_4 . This is also the case for aluminium, in which orthophosphate is adsorbed as AlOOHPO_4 . Al^{3+} is

known to precipitate out orthophosphate, and is used for this purpose in sewage treatment as well as an abatement action in eutrophic lakes (Cooke et al., 1993; Lewandowski et al., 2003). The orthophosphate concentrations found in natural waters are actually too low to precipitate directly with Al (AlPO_4 , $K_{\text{sp}} = 6.3 \times 10^{-19}$), because Al is far more insoluble with hydroxide. ($\text{Al}(\text{OH})_3$, $K_{\text{sp}} = 3 \times 10^{-34}$) (Kalff, 2002b; Lide, 2004a). Instead the orthophosphate is adsorbed to aluminium hydroxide and precipitated as AlOOHPO_4

Under anoxic conditions, typically found in the lake sediments, Fe(III) in solid complexes reduced to Fe(II). This can result in the release of iron-adsorbed orthophosphate. This is one of the reasons why the redox conditions in the aquatic environment plays such an important role in regards to eutrophication.

In sediments the oxidized surface functions as an effective barrier, hindering the orthophosphate diffusing into the aqueous environment from the anoxic environment below the sediment surface (Kalff, 2002b). Sediment surfaces can become so reduced that they lose their barrier function. This results in the leakage of orthophosphate from the anoxic conditions below. All this contributes to the acceleration of eutrophication as this is a clear case of internal feedback (Kalff, 2002b; Kalff, 2002c). The conditions that control the orthophosphate release are actually far more complex than the pH and redox conditions alone. Fe(II) is in fact also moderately insoluble with orthophosphate (e.g. vivianite; $\text{Fe}_3(\text{PO}_4)_2 \cdot 8\text{H}_2\text{O}$, $K_{\text{sp}} = 1 \times 10^{-36}$). Despite this iron reduction often results in the release of orthophosphate. Unless iron is precipitated as a less soluble mineral Fe^{2+} can easily accumulate to levels that lead to efficient precipitation of iron(II)phosphate. The most likely mineral to trap Fe^{2+} in anaerobic sediments is sulphide, which is generated in such sediments by microbial reduction of sulphate. Iron(II)sulphide is significantly less soluble than iron(II) phosphate and so can sequester Fe^{2+} that is formed by reduction. It is likely that it is the combination of Fe^{3+} reduction and sulphate reduction that leads to the sequestration of iron as iron(II)sulphides and the liberation of phosphate (Pratt, 2006). Furthermore, studies show that redox condition alone are not enough to reduce Fe(III) to Fe(II), partly because iron aggregates are stabilized by a coating of organic matter. Iron-reducing bacteria, using Fe(III) as an electron acceptor, are necessary in order to decompose organic matter. Microorganisms play therefore a major role in the mechanisms that control the release of inorganically bound orthophosphate (Kalff, 2002b).

An overview of major processes that govern the fluxes in the internal phosphorus cycle in a lake is shown in FIGURE 2d. It should be emphasized that the global P cycle, unlike carbon and nitrogen, is far more linear than cyclic. This is due to that the atmosphere does not play a significant role in the movements of phosphorus. The P species are largely restricted to the hydrosphere, lithosphere, and biosphere. Phosphine (PH_3) is the only gas form of P, though its contribution to the P cycle is minor as it is only produced under extreme anoxic condition (see FIGURE 2c), such as may be found in swamps and bogs. For this reason the P transport within any relevant time frame is more one way, i.e. from land to sea.

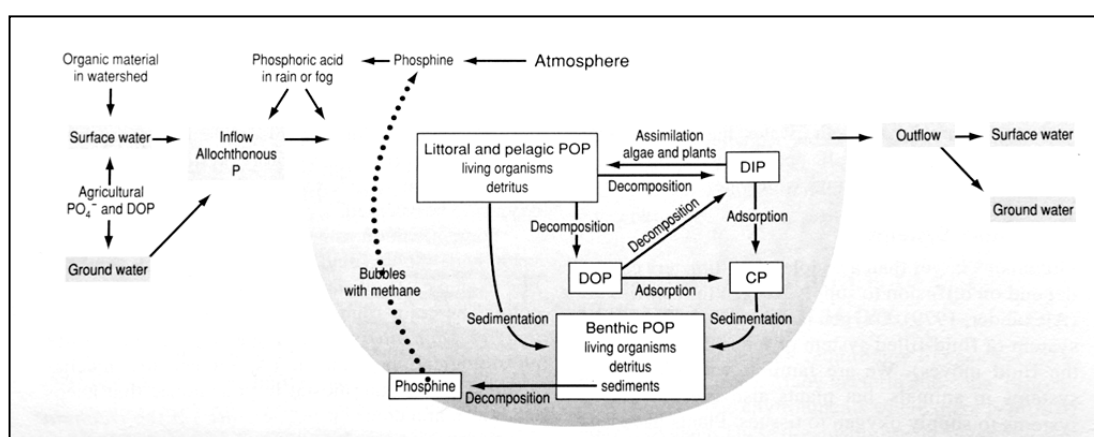


FIGURE 2d Major reservoirs of phosphorus in a stratified lake. TDP = total dissolved phosphorus; SRP = soluble reactive phosphorus; POP = particulate organic phosphorus; DIP = dissolved inorganic phosphorus; CP = colloidal phosphorus; DOP = dissolved organic phosphorus (Dodson, 2005a).

The details regarding the fractions mentioned above are further explained in Dodson 2005a.

2.3. Photooxidation and Dissolved Organic Phosphorus (DOP)

In chapter 2.1.2 it was pointed out that dissolved organic matter (DOM) has an affect on the light penetration down into the water body. DOM strongly absorbs radiation in the ultraviolet (UV) range, protecting aquatic microorganism from the harmful radiation. This UV radiation is also an important factor causing decomposition of DOM in lakes. The absorption of energy rich UV radiation by the chromophores (i.e. conjugated double bonds) breaks down chemical bonds of DOM, thereby affecting the size and structure of the often very complex macromolecule. As a result colouring is reduced, which is known as photo-bleaching. This photo-degradation breaks the

DOM into smaller organic molecule fractions, which are more prone to become bioavailable to microbes. At the same time photo-degradation also yields reactive oxygen species (O^{2-} , H_2O_2 , OH^{\cdot}), and other free radical groups, which are powerful oxidants and toxic to the biota (Kalf, 2002d). The contribution solar radiation has on the release of SRP from DOP is believed to be important. The majority of DOM in a lake comes from the terrestrial environment (allochthonous) (vanLoon and Duffy, 2005a). The fluxes of this allochthonous DOM are known to have increased significantly since the eighties in regions previously suffering heavy loading of acid rain (Gjessing et al., 1998; Haaland et al., 2010; Skjelkvåle, 2009). Along with this increase in DOM fluxes it is likely to believe that also the loading of DOP incorporated in the DOM to the lakes has increased.

More knowledge is therefore needed on the background flux of phosphorous bound to DOM and the fate of this material within in the lakes.

2.4. Algae

Some algae can release toxins, which can be harmful to fish, humans, and other organisms. Most toxic algae, such as *toxic dinoflagellates*, grow mainly in marine environments (Madigan and Martinko, 2006). However the blue-green algae, quite common in eutrophic fresh water lakes, can produce toxins. Blue-green algae are actually not algae, but a bacteria group known as cyanobacteria. The toxin produced by cyanobacteria is part of a toxin family known as microcystins (FIGURE 2e). The toxin is produced by three types of cyanobacteria, *Microcystis*, *Anabaena* and *Oscillatoria* (Oberholster et al., 2004).

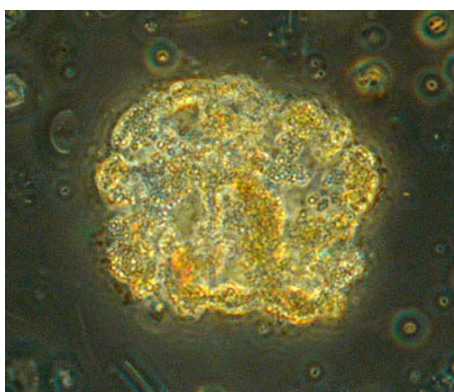


FIGURE 2e *Microcystis aeruginosa* (Smithsonian Environmental Research Centre, 2008).

As stated in section 2.1.2 algae migration may be necessary for its survival at the onset of eutrophication. However, due to the relative poor mobility of pelagic plankton, it becomes more a question of survival of the fittest which determines what species flourish.

Cyanobacteria often dominate above all other plankton in lakes experiencing seasonal eutrophication. This can be seen in FIGURE 2f, where eutrophication takes place during the end of the summer at lake Vansjø in the east-southern part of Norway. The cyanobacteria are marked in red.

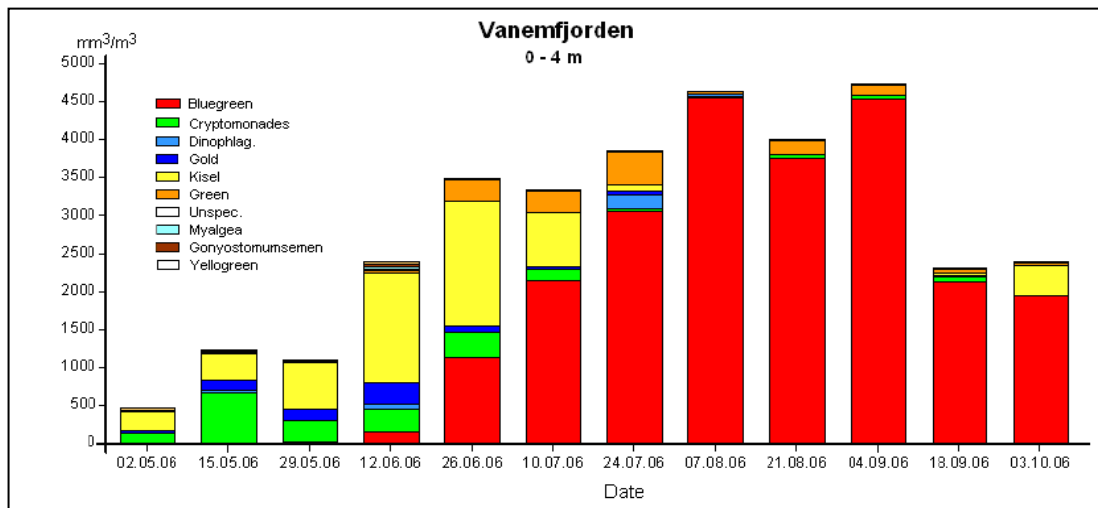


FIGURE 2f Seasonal change in phytoplankton concentrations (mm^3/m^3) for Vanemfjorden, Vansjø. (Bjørndalen et al., 2007).

The dominance during periods of excess phosphorous levels may be due to the fact that they, unlike algae, are not dependent on available reactive nitrogen species (NH_4^+ and NO_3^-) in the environment. They have the possibility of fixating nitrogen directly from the atmosphere, thereby making phosphorus the only limiting factor for their growth (Schindler, 1977).

2.5. Eutrophication Remedies

There are several possible abatement actions that may be used to decrease the problem of eutrophication. One method is to divert or reduce the flux of P from major anthropogenic sources. Improved sewage system management and agricultural regulation are two main areas in which the anthropogenic input of P may be reduced. Better sewage management can be directing the sewage away from the lake and/or treating the sewage before it enters the lake. Important policies regulating agricultural practises are limiting over-fertilization, shifting to less nutrient demanding crops and prohibiting autumn ploughing after the harvest. Soils that are ploughed in the autumn are more prone to erosion due to the absence of a protective cover and reduced infiltration capacity. Setting up sedimentation ponds in nutrient rich streams, which drain into the lake, is another method. Sedimentation ponds are man-made dams in which high nutrient demanding vegetation, such as pond grass, is grown. The principle is to let the pond grass capture most of the nutrients in the stream before the water reaches the lake. This is known as *bottom-up* food chain bio-manipulation. Installation of vegetative filter strips along the edges of the agricultural fields, are another much used abatement action. Vegetative filter strips intercept surface water runoff and are effective in trapping sediments and nutrients.

Another approach is the *top-down* food chain bio-manipulation. By increasing the predator zooplankton population the prey algae population will decrease. The simplest way of doing this is to remove the predators of the zooplankton. The general theory is that species populations alternate from high to low down the food chain. Altering the top of the food chain alters, in theory, the entire food chain (Dodson, 2005b).

A practise used in other countries, such as Germany, is to treat the eutrophic waters with alum ($AlSO_4$) (Lewandowski et al., 2003). This precipitates out phosphorous and is found to also fixate phosphorous in the sediments. The significance of Al as a precipitating agent is especially interesting in respect to the great decrease in concentrations of labile aluminium in runoff from acid sensitive catchments due to the reduction in acid rain (Skjelkvåle, 2009). It is clearly necessary to understand better the possible impact this loss of aluminium leaching may have had on reduced precipitation of phosphate with aluminium hydroxides (Ulrich and Pöthig, 2000).

2.6. Vansjø

2.6.1. Vansjø Morphometrics:

Vansjø is a eutrophic lake near the city of Moss, Norway. The lake covers a surface area of approximately 36 km². It is comprised of multiple waterbodies that are separated by narrow and shallow passages. These are split into two main waterbodies that are referred to as Vanemfjorden and Storefjorden FIGURE 2g.

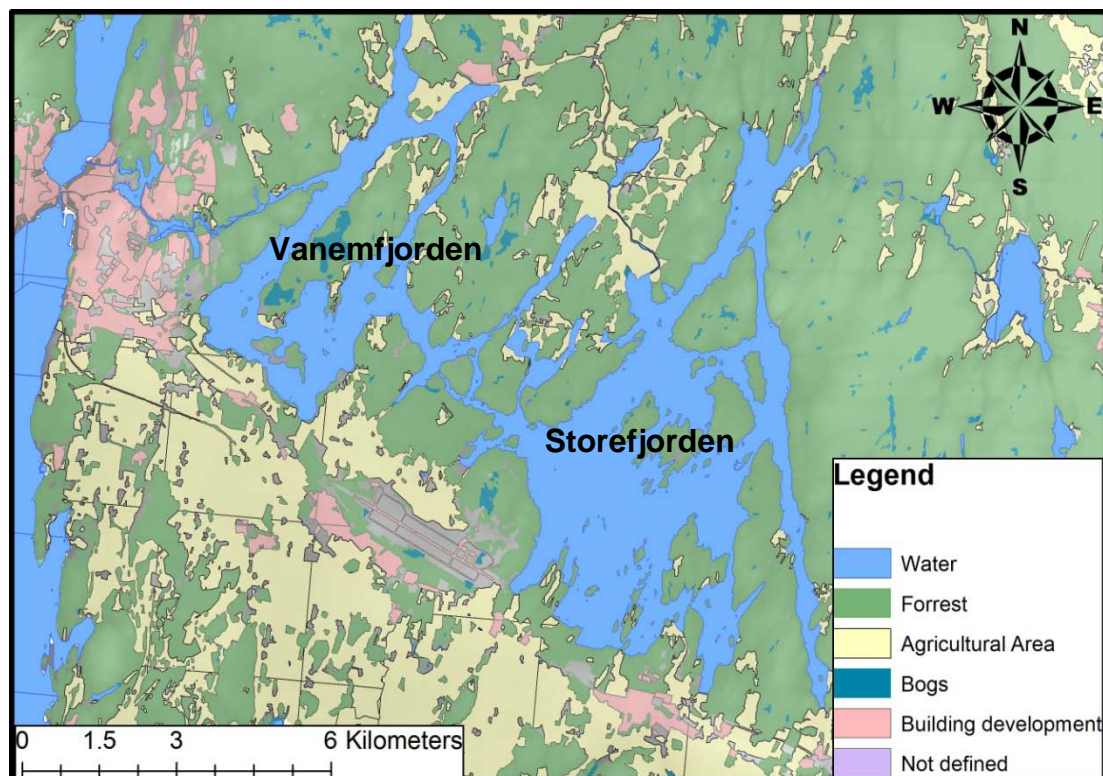


FIGURE 2g Map of Vansjø and its main waterbodies.

Storefjorden is the greater of the two lakes with an area of approximately 24 km² and average depth of 9 m, TABLE 2d (Bjørndalen et al., 2007).

TABLE 2d Morphometrics of Vansjø (Bjørndalen et al., 2007)

Morphometrics	Storefjorden	Vanemfjorden
Surface area (km ²)	23.8	12
Average depth (m)	9.2	3.7
Greatest depth (m)	41	17
Theoretical Water Residence Time (years)	0.85	0.21

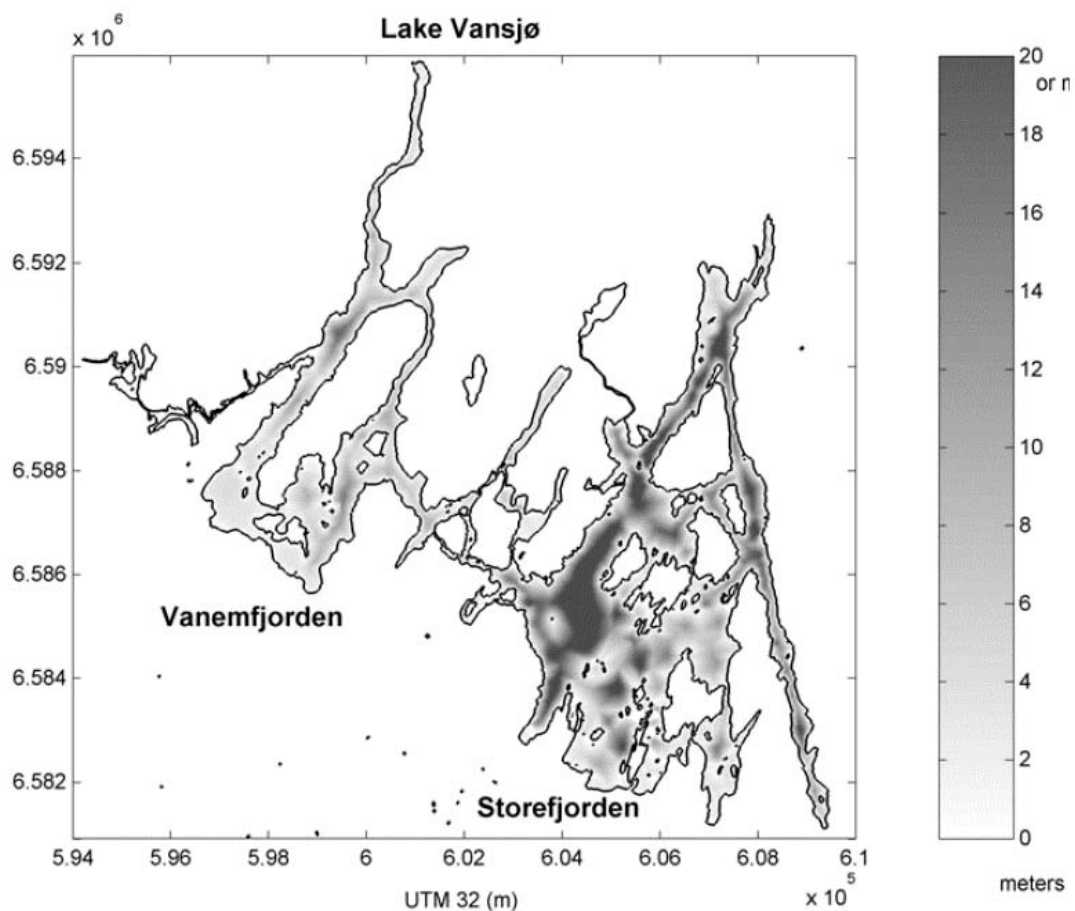


FIGURE 2h Map of Vansjø's depths. (Bjørndalen et al., 2007).

2.6.2. Interests of use

Vansjø has multiple interests of use. Water from Storefjorden is the freshwater source for approximately 60 000 people living in Moss. Vansjø is also a place for recreational activities such as bathing, canoe paddling, boat activities and fishing (Bjørndalen et al., 2007). The water is also still the recipient of nutrient rich runoff

from agriculture as well as likely still some leakage of sewage. There are therefore large conflicts of interest among the different stakeholders.

2.6.3. Vansjø-Hobøl Catchment

Vansjø's water catchment area is known as the Vansjø-Hobøl catchment (Morsa catchment). It has an area of approximately 690 km² in which 15% of the area is agriculture. The rest of the area is mainly forest (FIGURE 2i). It is estimated that these forests contribute to approx. 20-25% of the total P loading to the lake (Solheim, 2001). There are approximately 40 000 people that live within the catchment area. The Hobøl River (Hobølelva) is the largest river in the catchment area. It and other rivers drain mainly into Storefjorden. Lake water flows from Storefjorden to Vanemfjorden. From Vanemfjorden water flows out to Oslofjorden via the Mosse River (Mosseelva) (Bjørndalen et al., 2007).

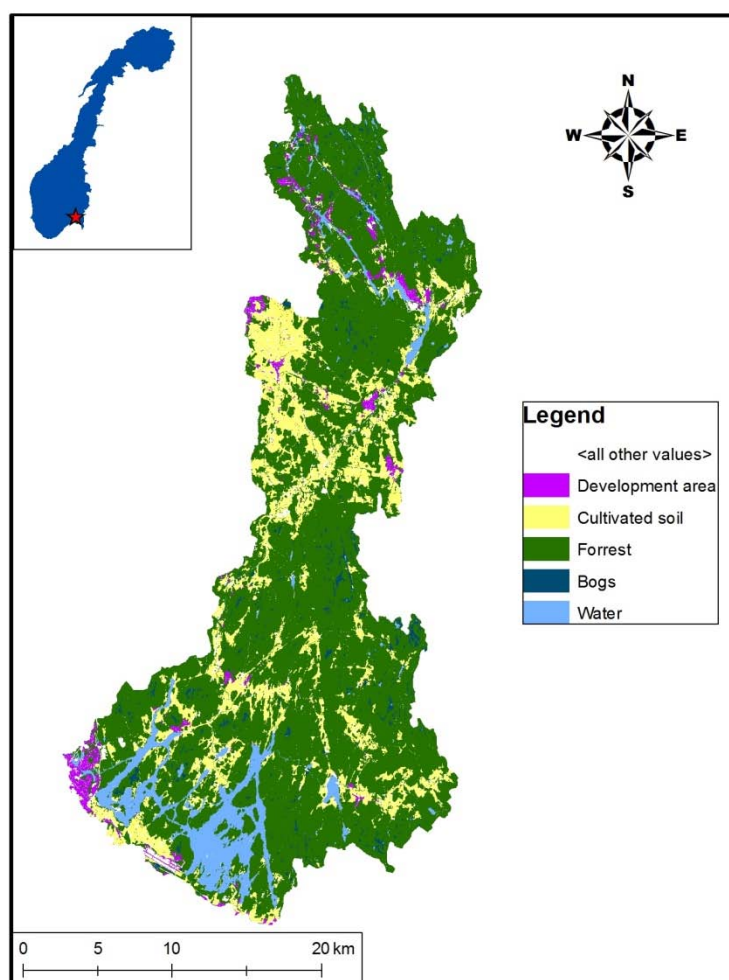


FIGURE 2i Map of the Vansjø-Hobøl watercourse (Bjørndalen et al., 2007).

The geology rock type of the Vansjø-Hobøl catchment consists mainly of gneiss and granite. Both rock types have little water infiltration ability, and little buffering capacity (FIGURE 2j).

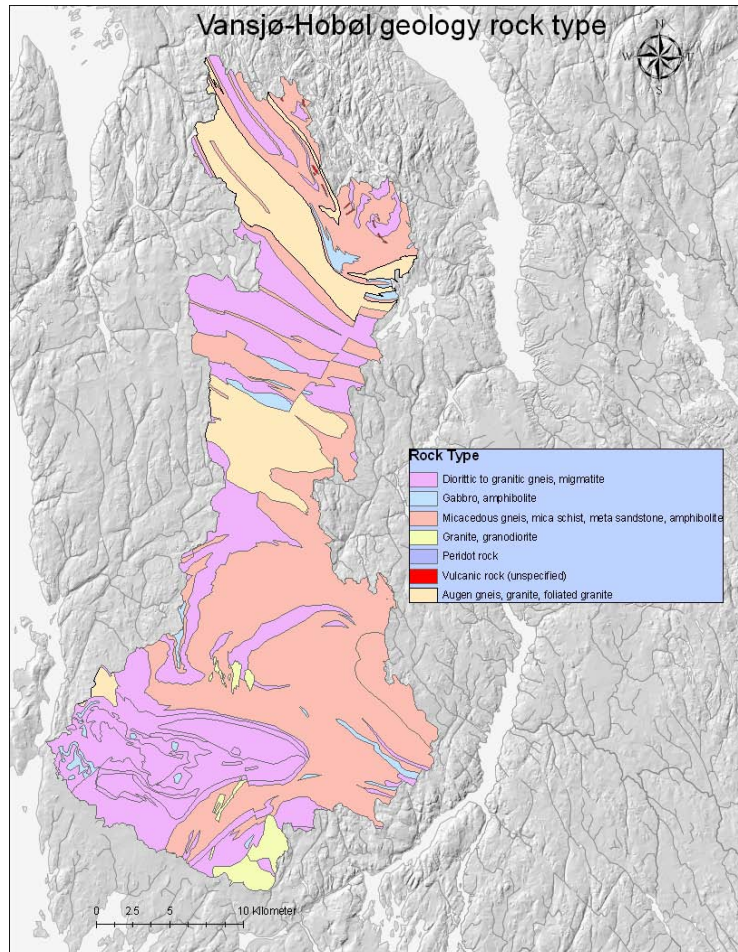


FIGURE 2j Geology rock types of the Vansjø-Hobøl catchment (NGU, 2010).

During the post-glacial ice age period, large parts of Southern Norway have accumulated marine sediments as a result of having been marine limit. The Vansjø-Hobøl is known for having large sediments deposits throughout the region (FIGURE 2k). The sediments play a vital role in buffering the soil water.

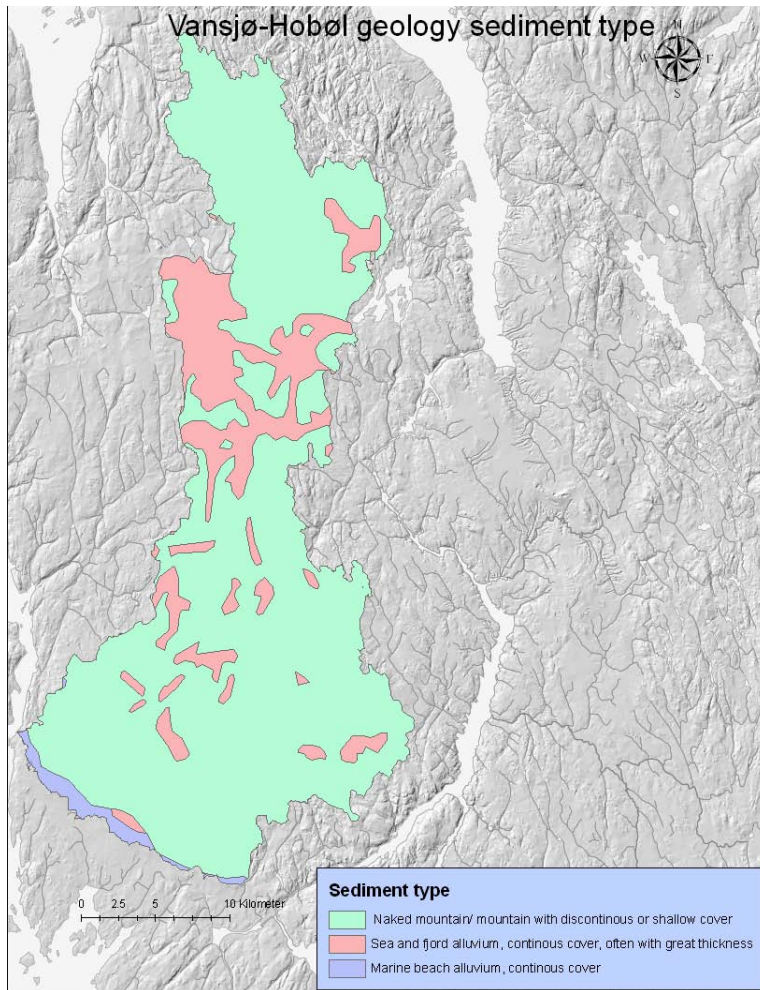


FIGURE 2k Sediment types found in the Vansjø-Hobøl catchment (NGU, 2010).

2.6.4. Podzols

Podzols is the dominating soil type in most of the Vansjø-Hobøl forested catchment. With 85% of the watershed comprised of forest, the chemistry is prone to play a major role in governing the chemistry of Vansjø lake.

Podzols resemble the Spodosols used by USDA Soil Taxonomy system. In podzols, clays, humic acids, iron, and other soluble constituents have been eluviated from the A and E horizons. These constituents have then accumulated to form a spodic illuvial B horizon. The soils are generally recognized as having an ash-grey subsurface horizon (known as E-horizon), with dark brown, red, black horizon below, known as B-horizon. The soils are relatively quite acidic, but the pH tends to increase with depth. The general build up of Podzols, starts with a thin O-horizon. The O-horizon consists mainly of decomposing organic matter, and is known as the litter fermentation humus horizon (LFH). It contains many fine and medium roots. The

bleached E-horizon follows. The soil texture is a cobbly loamy sand, non-sticky and non-plastic. The ash-grey colour is due to the soil being leached of iron by organic acids. The B-horizon usually consists of 2 sub-horizons. The Bh_s is a dusky red, dark brown in colour with a gravelly loamy sand texture. The Bs-horizon is combination between olive grey/light grey in colour and dark brownish yellow colour, with a similar texture to the Bh_s. The 'h' in Bh_s refers to humic matter and the 's' in Bh_s and Bs refers to sesquioxides. Sesquioxides are the iron(III) and aluminium(III) hydroxides and oxides which are abundant in both these horizons. The last horizon is the C-horizon and resembles the original soil material not influenced by the podzolization process. Texture is a loamy sand, and yellowish brown in colour. No roots are found here (ISRIC World Soil Information; United States Department of Agriculture, 1999; vanLoon and Duffy, 2005c).

Some of the inorganic chemical forms found in soil that contain phosphorus are shown in FIGURE 21. In addition there are some common phosphorus containing low-molecular-weight organic molecules, such as phytins, inositols, and nucleotides (Dyer et al., 1940; Yoshida and Kojima, 1940).

The general locations for finding podzols are temperate forested regions (ISRIC World Soil Information). However the type varies. Far more detailed data can be found upon defining the different types of Podzols. The two types that are found around the Vansjø area are *Umbric Endostagnic Podzol (Arenic)* and *Endostagnic Podzol (Ruptic)*. One thing in common with these two types is their high clay content. This is common in SE Norway below 200 m a.s.l. as a result of having been situated below the post-glacial marine limit (Norsk Institutt for Skog og Landskap, 2007). In such regions with marine clays it is common that the lakes are naturally moderately eutrophic (mesotrophic) (Spikkeland, 2003).

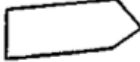


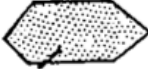
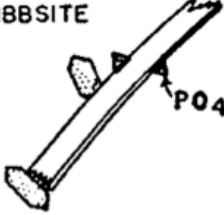







DISCRETE PARTICLES (somewhat available)	DISCRETE PHOSPHATES PRECIPITATED ON SUR- FACES, INCLUDING CHEMI- SORBED PO_4 (Δ) (most available)	OCCLUDED PHOSPHATES (little available)
CALCIUM PHOSPHATE (apatite, dicalcium phosphate, etc.) 	CALCIUM PHOSPHATE PRECIPITATED ON CALCIUM CARBONATE 	CALCIUM PHOSPHATE OCCLUDED IN CALCIUM CARBONATE, SILICA, ETC. 
ALUMINUM PHOSPHATE (variscite-like, wavellite-like, etc.) 	ALUMINUM PHOSPHATE PRECIPITATED ON ALUMINOSILICATE OR GIBBSITE 	ALUMINUM PHOSPHATE OCCLUDED IN IRON OXIDES 
IRON PHOSPHATE (strengite-like, dufrenite-like, etc.) 	IRON PHOSPHATE PRECIPITATED ON IRON OXIDES 	REDUCTANT-SOLUBLE IRON PHOSPHATE OCCLUD- ED IN IRON OXIDES 
ALUMINUM-IRON PHOSPHATE (barrandite-like, etc.) 	IRON PHOSPHATE PRECIPITATED ON IRON OXIDES 	ALUMINUM PHOSPHATE, IRON PHOSPHATE & ALUMINUM- IRON PHOSPHATE OC- CLUDED IN IRON OXIDES 

FIGURE 21 Diagrammatic representation of the physical distribution of the discrete chemical forms of inorganic phosphates present in soils. Diagrammatic representation of the physical distribution of the discrete chemical forms of inorganic phosphates present in soils (Chang and Jackson, 1957).

2.7. Diffusive gradients in thin films (DGT)

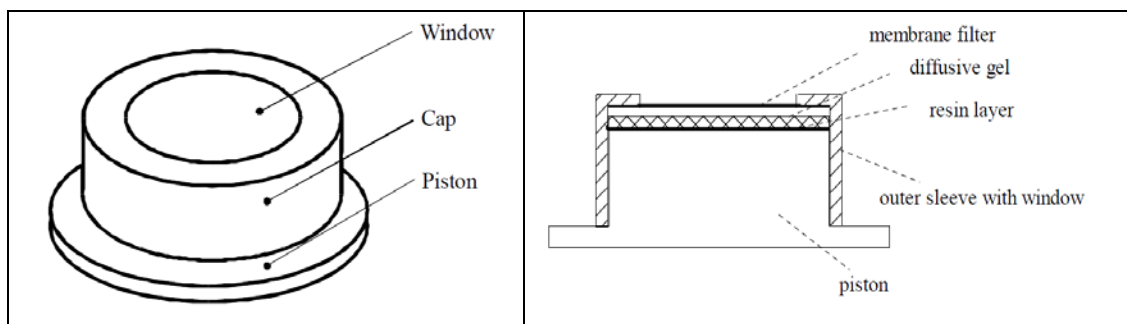
A DGT is a passive sampler that collects ions by diffusion over a diffusion membrane onto a collector, normally referred to as the adsorbent (or receiving sorbent or receiving phase). Several adsorbents have been developed to collect compounds such as trace metal ions (chelex ion exchange resin), phosphate ions (ferrihydrite, $\text{Fe}(\text{OH})_3$), sulphide ions (silver), radionuclide ions (ion exchange resins) (Zhang, 2005). DGTs are used to determine the average concentration over sampling periods, which spans over sampling periods from hours to weeks and even up to months.

DGTs are selective for small ions in solution by excluding large molecules and colloids. Normally only ions or molecules (limited by the pore size of the membrane) can diffuse through the membrane.



FIGURE 2m Photo of disk DGT

DGT samplers are usually in the form of circular discs, with a window of 20 mm in diameter (FIGURE 2n), or in the form of a sediment probe sampler with a window of 20 by 150 mm. DGT disks are suitable for sampling in solution, while DGT probes are used for sampling in sediment and soil, with special emphasis on concentration profiles of ions with depth (Zhang, 2005).



DGT disk overview. The window is the area exposed to the environment, which allows the diffusion to take place. The cap and piston protect the inner content from exposure to the environment. Side profile can be seen to the right. (Zhang, 2005).

The principle of diffusive uptake, is that ions diffuse through the membrane (often denoted as the diffusive gel (FIGURE 2n). On top of the diffusive gel is a low pore size membrane filter to protect the soft diffusive gel. After the ions diffuse past the diffusive gel they end up in the receiving phase membrane known as the resin layer (FIGURE 2n). Here the specified ions bind and accumulate. The type of adsorbent in the receiving phase is critical for the efficiency of the uptake. The receiving phase should have a high K_d (equilibrium constant) for the ions of selection, so that they are quantitatively collected and stored over time. Ferrihydrite is used as the adsorbent for orthophosphate in the receiving phase (Zhang, 2005).

The DGT probes are constructed in such a way that the concentration, of ions being collected, is close to zero at the receiving phase surface. By this the diffusive gradient depends on the concentration of the water only. It is the steady-state concentration gradient, which makes it possible to calculate the average concentration of the ion being sampled based on diffusion theory (Zhang, 2005). Fick's first law of diffusion describes the relationship between the flux of molecules/ions (dm/dt , $\mu\text{g/s}$) through a cross-section (A , cm^2) and the concentration gradient (dC/dx , $\mu\text{g L}^{-1} \text{cm}^{-1}$) multiplied by a diffusion coefficient, D ($\text{cm}^2 \text{s}^{-1}$) specific for the molecule/ion (Equation 2-1).

Equation 2-1

$$Flux = \frac{1}{A} \cdot \frac{dm}{dt} = -D \cdot \frac{dC}{dx}$$

The diffusion coefficient for the specific molecule/ion is a function of a number of physical-chemical variables from the surrounding matrix and the specific molecule/ion. Theoretical calculations can be made to determine D if certain physical-chemical variables are known. For ions this is best described by the electrical mobility equation (Equation 2-2), where q is the electrical charge of the particle, μ_q is the electrical mobility of the charged particle, k_B is Boltzmann's constant, and T is the absolute temperature (Atkins, 1994).

Equation 2-2

$$D = \frac{\mu_q k_B T}{q}$$

For molecules the "Einstein-Stokes equation" can be used (Equation 2-3), which describes the diffusion of spherical particles through liquid with low Reynolds number. η is the viscosity of the medium, and r is the radius of the spherical particle (Atkins, 1994).

Equation 2-3

$$D = \frac{k_B T}{6\pi\eta r}$$

Despite all the theoretical kinetic calculations, the hands on approach is to determine the diffusion-coefficient empirically for the specific molecule/ion. This can be done using the DGT as a test device for uptake vs time, or test of the membrane in a diffusion cell. If the receiving adsorbent is an efficient sink for ions (i.e., the concentration of ions at the adsorbent surface is approximately zero and no back-diffusion occurs), then time-integrated mass uptake can be determined (Equation 2-4). C_O is the concentration outside the DGT, A is the exposed area (DGT window) and L is the combined thickness of the diffusive gel (G , mm), membrane filter (f , mm), and diffusive boundary layer (DBL or δ , mm). The DBL thickness depends on the rate of

water movement, but approximates to ~0.1 mm in well stirred solutions (see FIGURE 2o) (Røyset et al., 2004; Zhang, 2005).

Equation 2-4

$$m(t) = C_o \cdot t \cdot D \cdot \frac{A}{L} = C_o \cdot t \cdot D \cdot \frac{A}{(G + f + \delta)}$$

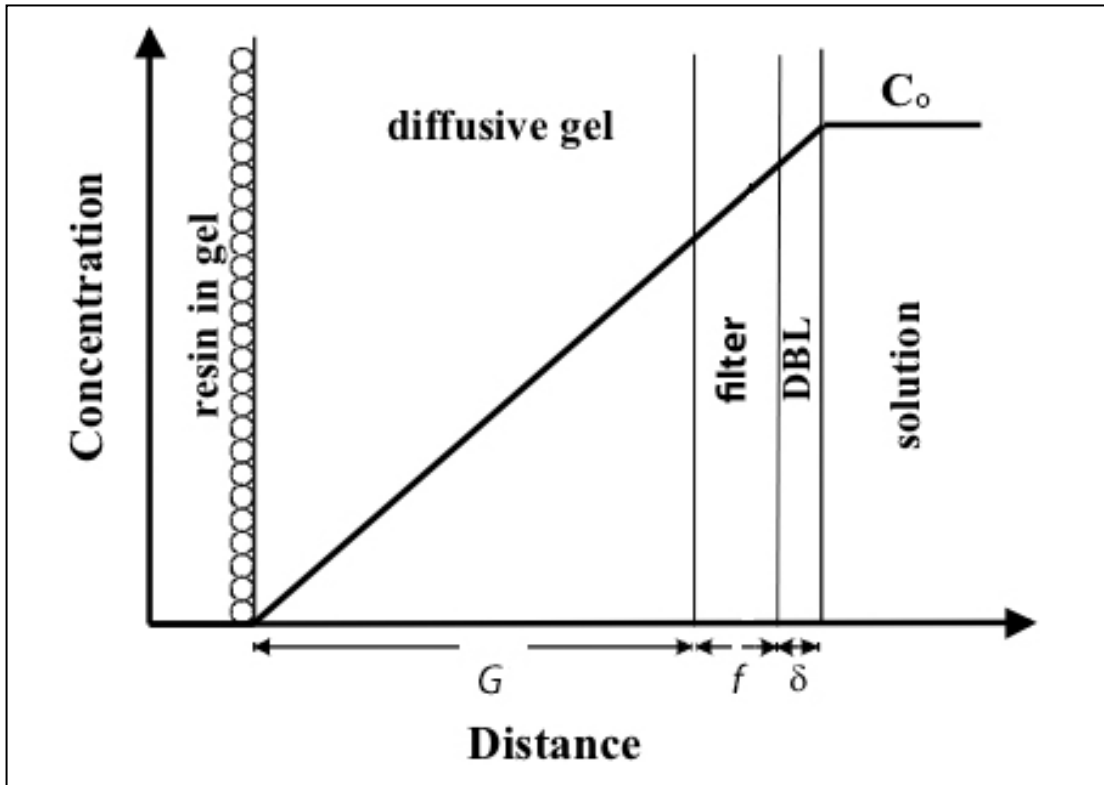


FIGURE 2o Graph shows the concentration gradient as a function of layer thickness.

The mass of molecules/ions adsorbed on the resin membrane, for a given sampling time, can be used to determine D if C_o is known (Equation 2-5),

Equation 2-5

$$D = \frac{m}{C_o t} \cdot \frac{L}{A}$$

C_o can be determined if D is known (Equation 2-6), which is the case when sampling in the environment.

Equation 2-6

$$C_o = \frac{m}{t} \cdot \frac{L}{DA}$$

The maximum exposure time for the DGT-sampler is limited, as the adsorbent membrane has maximum number of binding sites, and therefore saturation of the sampler will occur (Zhang, 2005). Low concentrations and low temperature during sampling will theoretically result in longer sampling time without saturation. The ferrihydrite membrane has an adsorption capacity of 6.7 µg P (Zhang et al., 1998). However even before saturation there is most likely going to be back diffusion. It can therefore be roughly estimated that DGTs can be used for sampling until 50% of the sites are occupied. Beyond 50% saturation it is possible that the net accumulation rate will decrease towards zero at maximum capacity. In FIGURE 2p it is shown how many days it will take to reach 50 % saturation for different temperatures and orthophosphate concentrations.

Saturation is not an issue for orthophosphate concentrations as low as 1 µg P/L, as the time required to reach 50% saturation is way beyond 90 days. At 10µg P/L however, this must be considered, as 50 % saturation occurs between 20 and 40 days.

In a laboratory study it was shown almost linear uptake up to 14 days at a concentration of 10 µg/L at room temperature (Røyset et al., 2004).

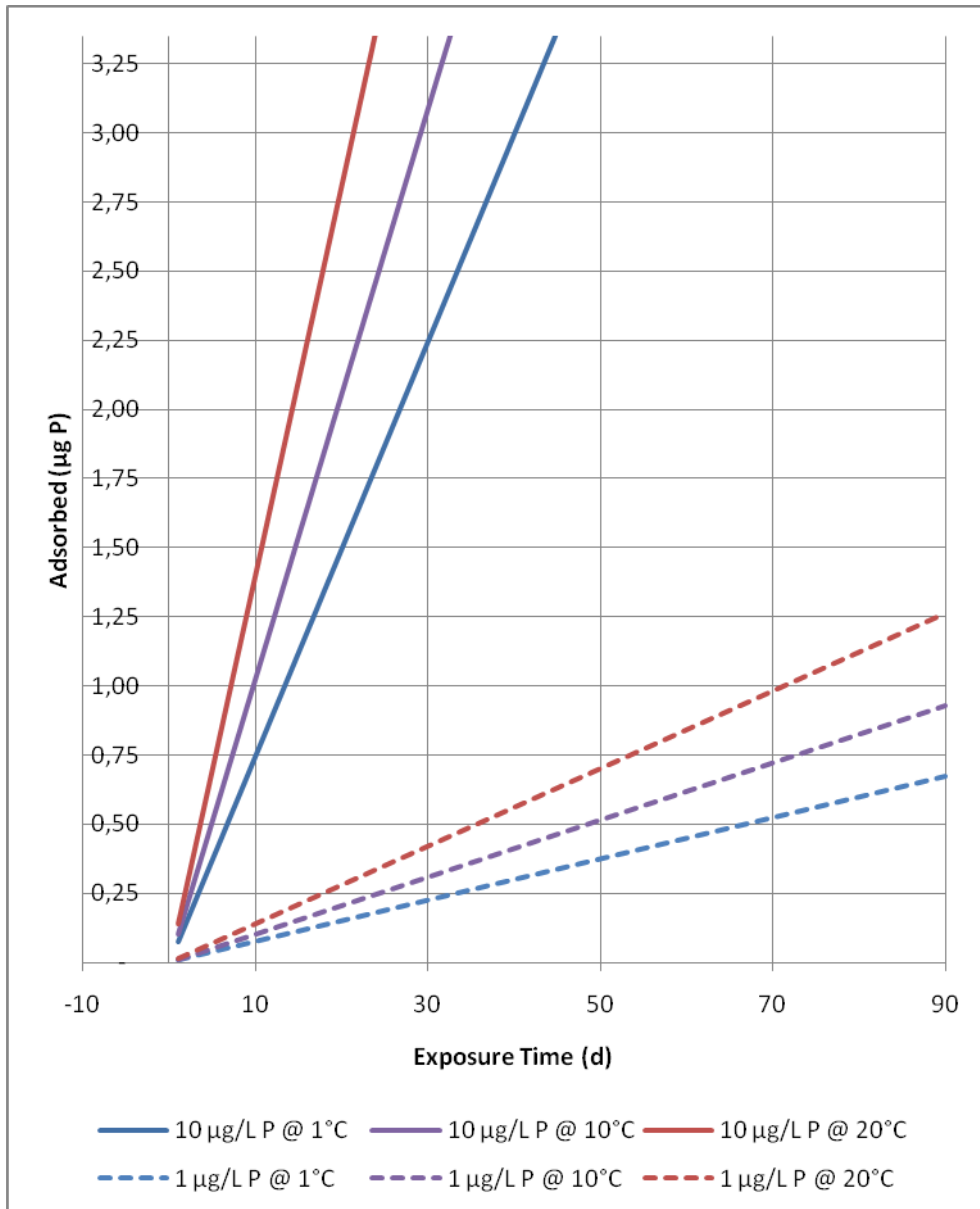


FIGURE 2p The graph illustrates the time required to reach 50% saturation of the ferrihydrite sites with orthophosphate (3.35 µg P, the top of the chart) at different sampling concentrations and temperatures.

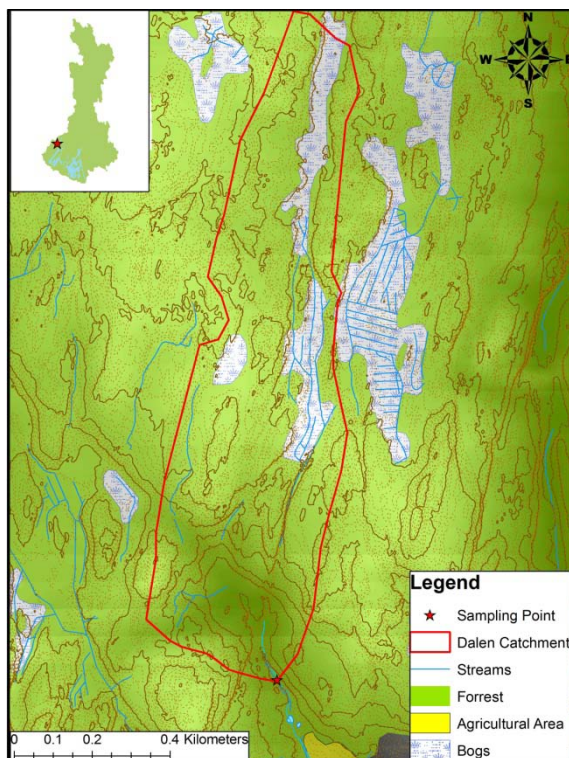
In addition to phosphate, the adsorbent membrane also adsorbs arsenate and selenate. Arsenate is a slight interference when analyzing the amount of phosphate via the molybdate blue method. However, the arsenate interference can be corrected by determining As by mass spectrometry (Røyset et al., 2004). It is presumed that the concentration levels of arsenate (also selenate), in natural surface waters, are normally quite low compared to phosphate, and thereby the error is negligible. For this reason no correction for arsenate interference is assumed needed, and it (and selenate) will not overload the adsorbent capacity.

3. Materials and methods

With an approximate 85% of the entire Hobøl-Vansjø catchment being covered by forest, the need to determine P fluxes from forested catchments is crucial for estimating the total input of P to the lake. Only with this knowledge can the impact on Vansjø from agriculture and other anthropogenic sources be determined. Furthermore, an understanding of the processes governing P leaching and transport is required in order to predict how changes in important environmental pressures have previously affected the P loading to the lake, and how they will influence future trends.

3.1. Sampling at Dalen

Dalen is a typical small forested catchment, located in the north-western part of Vanemfjorden, with an environment believed to be generally representative for most of the forested area of the Hobøl-Vansjø catchment. The small catchment above the stream water sampling point is approximately 556000 m². Of this area 89% is forested area, while bogs in the valley bottom constitute the remaining 11% (FIGURE 3a).



Three soil plots were selected for soil, and soil water sampling. The three plots were set up to represent a topographic gradient, with a plot on the hilltop (the ridge), a plot on the slope and a plot in the valley bottom. The lowest plot is located adjacent to the stream (FIGURE 3b).

FIGURE 3a Red borders show the Dalen Catchment.

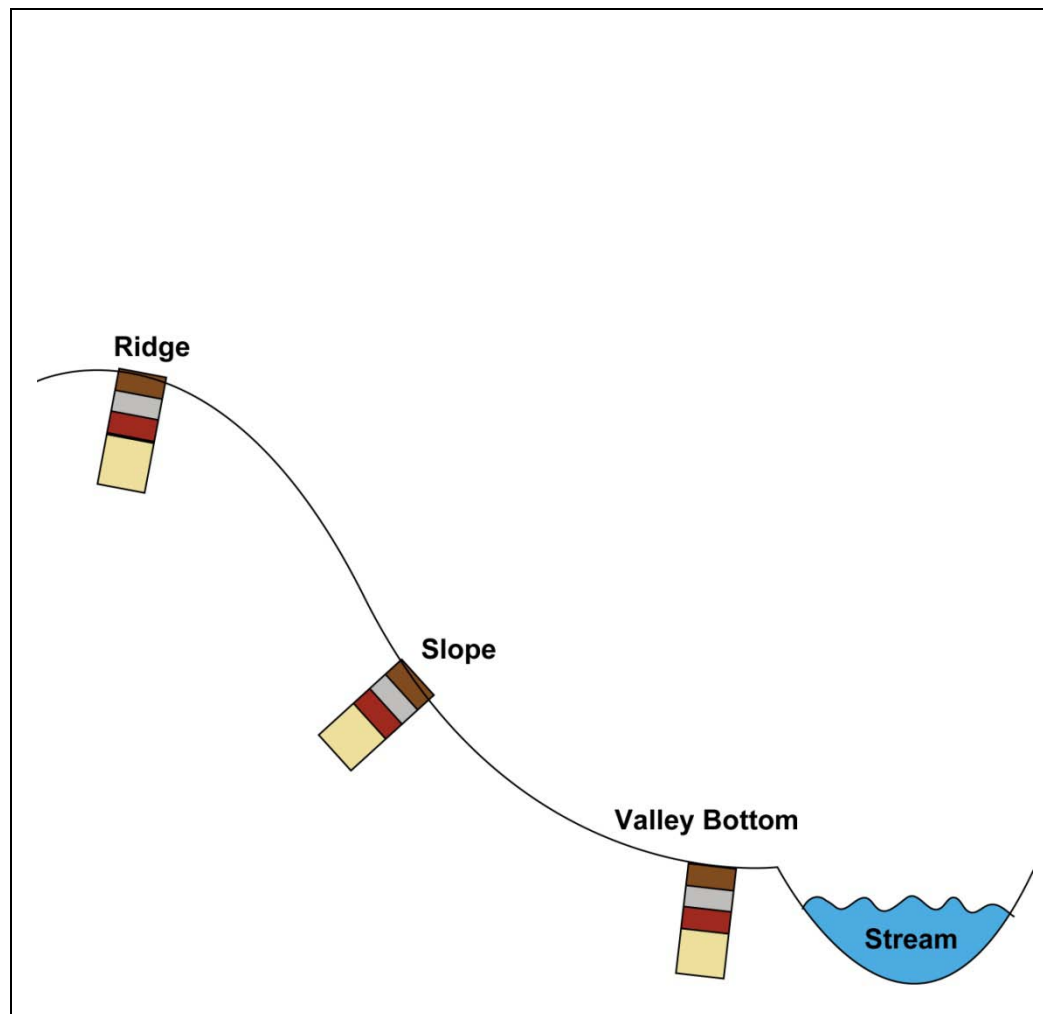
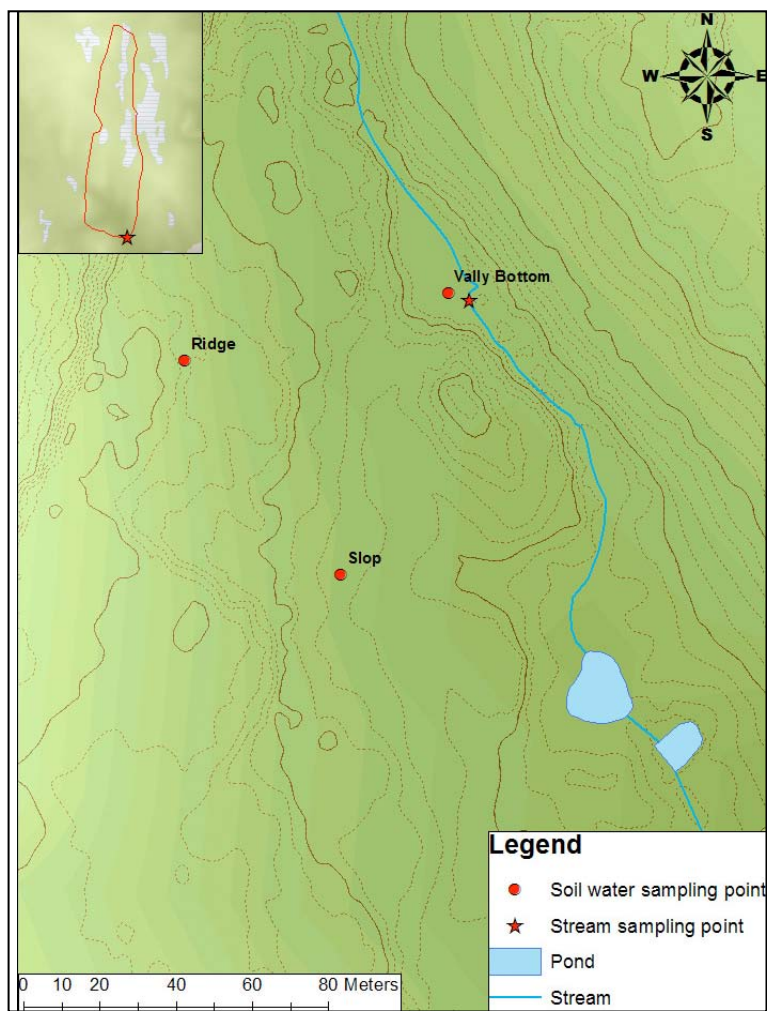


FIGURE 3b Left: Map of sampling points at Dalen catchment. Right: Illustration of the topographic gradient set up for the plots.

The plots not only represent differences in morphology, but also in vegetation and soil characteristics as shown in TABLE 3a and FIGURE 3c.

TABLE 3a Descriptive information of the plots at Dalen

Plot	m.a.s.l.	Vegetation	Soil moisture	Soil characteristics	Total soil depth (cm)
Ridge	47	Spruce, moss, wood-sorrels	dry	Little humus, sand	70
Slope	41	Spruce, litter fall	Wet and dry	Humus, mineral, clay	64
Valley bottom	39	Spruce, moss, wood-sorrels	Wet/moist	Humus, mineral, clay	90



FIGURE 3c Photos of plot locations at Dalen. Left to right: ridge, slope and valley bottom plot.

3.1.2. Soil water at Dalen

Water from different compartments in the watershed is monitored in order to better understand the hydro-biogeochemical processes governing the runoff chemistry and especially the concentrations of P fractions in the stream.

Throughfall collector

Water passing through the forest canopy and ground vegetation is collected in 2 – 3 throughfall collectors placed randomly around the soil plot. These collectors consist of a 11.5 cm in diameter funnel on top of a sample bottle. The top of the funnel is 10 centimetres above the ground. The sampling bottle is kept below the soil surface to protect the collected water from light, which may alter the chemistry of the solution (FIGURE 3d).

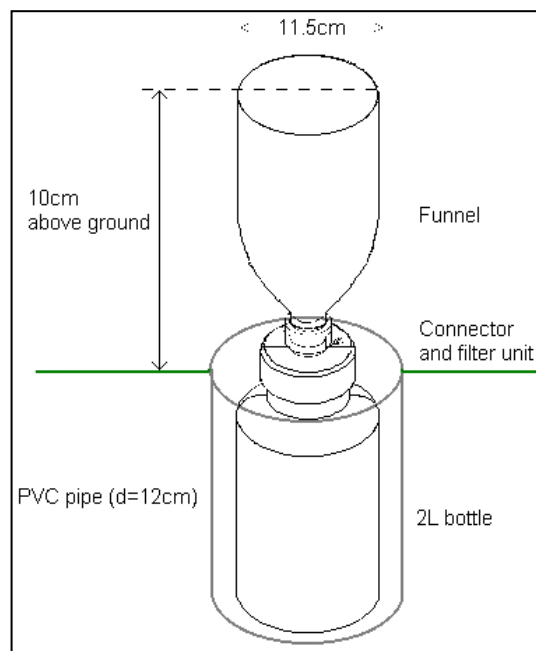


FIGURE 3d Illustration of throughfall collector.

Zero-tension lysimeter

In order to capture water as it passes from the organic forest floor into the mineral soil a simple sieve with a funnel is installed under the O-horizon. Water dripping freely into the funnel is collected into a bottle in the bottom of an adjacent soil pit (FIGURE 3e).



FIGURE 3e Photo of zero-tension lysimeter

Lysimeters

Lysimeters were used in order to sample the soil water from the different genetic soil horizons at each soil plot. The suction lysimeter consists of a porous ceramic cup, which is permeable to water and its solutes. The suction lysimeter is coupled to a flask, which under vacuum sucks soil water through the lysimeter and into the flask. Picture of vacuum flask and lysimeter are shown in FIGURE 3f.

A hole in the soil is dug out and the lysimeters are inserted into the different horizons facing the incoming water from higher altitudes. In addition to the ceramic suction lysimeter, a Teflon suction lysimeter is used for the deepest horizon. The Teflon suction lysimeter is used, because the force required to push the lysimeter to the deepest horizon would break the ceramic cup of the ceramic suction lysimeter. See FIGURE 3f and FIGURE 3g for plot set up.



FIGURE 3f Top left: Ceramic lysimeter and 1 L vacuum sampling flask. Bottom left: Photo of dug out hole used to place lysimeters in soil. Right: Photo of lysimeter placed in the different soil horizons.

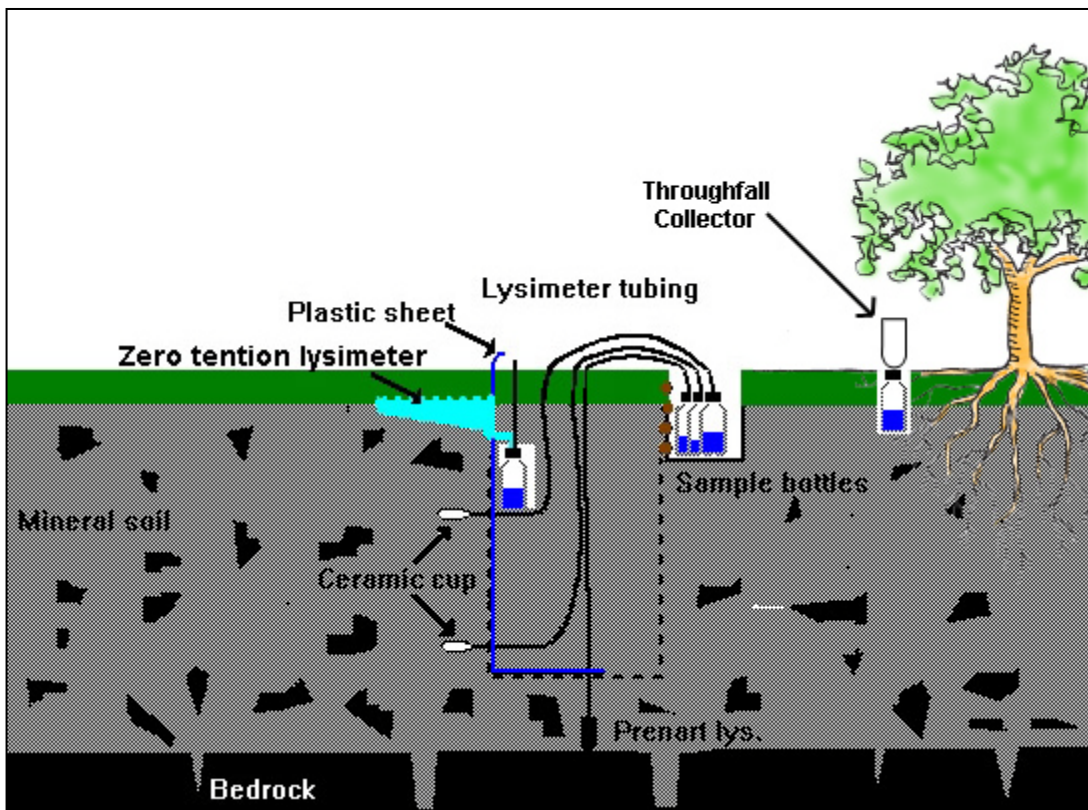


FIGURE 3g Illustration of lysimeters in the different horizons of the soil. The soil water movement is from left to right. A plastic sheet is used to hinder any back flowing water. Sampling bottles kept in a nearby shallow hole to sample. Thoughfall collector is placed under canopy and zero-tension lysimeter under O-horizon.

3.1.3. Dalen stream

The catchment has a single stream, which flows out into Vanemfjorden. The water can be described as extremely humic from the appearance. Sampling of the stream was performed using a field autosampler.

Field autosampler

A Manning autosampler has been installed at the sampling site of the stream and has been set to collect stream water samples at regular preset time intervals. Multiple attempts have been made to capture intense rainfall events causing hydrological discharge episodes. This has only recently been successful and will therefore not be covered by this thesis.

3.2. Laboratory locations and facilities

The majority of the laboratory work in this thesis has been performed in laboratories at the Department of Chemistry, UiO. Part of the work has also been performed at NIVA's Chemical laboratory (determination of C, N and P by NIVA's CNP analyzer) and at the Department of Geosciences (determination of P in the solutions obtained from soil in sequential extractions)

3.3. Sample storage and preparation before analysis

All water and soil samples collected were stored in a cold room at 4 °C. Water samples were collected in prewashed PE bottles. Prior to any analysis, all samples were registered into a common EUTROPIA excel worksheet and given a unique log number.

3.3.1. Filtration of water samples

A number of analytical procedures on water samples require the water to be pre-filtered. This includes analysis of anions and cations by ion chromatography (IC) and Induced Coupled Plasma Atomic Emission Spectrometry (ICP-AES). In addition

filtration was done in order to calculate the quantity of particulate matter (PM) in stream samples. For these reasons aliquots of 200 mL of all water samples, with the exception of lysimeter samples, were filtered through Whatman GF/F 0.7 μm filters. For stream samples these filters are pre-burned at 550°C, weighed and then used.

3.4. Qualitative and quantitative analysis

3.4.1. Conductivity and pH

The measurements of conductivity and pH of water samples were conducted at the laboratory at the University of Oslo. An aliquot of approx. 20 mL of the sample was measured first for conductivity (temperature is included) and then for pH using a Ross combination electrode. The measurements were conducted according to ISO7888 and ISO10523, respectively.

3.4.2. UV and colour absorbance

The water samples were measured for UV (254 nm) and colour (400 nm) absorbance, using 10mm quartz and glass cuvettes (cell), respectively, as a proxy of content of dissolved organic mater (DOM).

3.4.3. Alkalinity

All samples with pH \geq 5.5 were analyzed for alkalinity according to International standard ISO 9963-1 (1994). Water samples were not pre-filtered, as this is sometimes done to avoid interference from suspended matter in the form of carbonate.

3.4.4. Aluminum fractionation and analysis

All samples with pH $<$ 5.5 were analyzed for aluminium fractionations following the operationally defined Barnes/Driscoll procedure (Sullivan et al., 1987). Al-fractionation of monomeric (Al_a) from polymeric forms was accomplished by complexation with 8-hydroxyquinoline at pH 8.3 with subsequent extraction into

MIBK organic phase. Separation of organic bound monomeric aluminium (Al_o) from inorganic mainly labile aluminium (Al_i) is performed by trapping of the Al_i fraction in an Amberlight IR-120 ionexchange column. The Al concentration in the organic extracts are determined photometrically.

3.4.5. Major anion analysis

Chloride, fluoride, sulphate, and nitrate concentrations were determined by a Dionex ICS-2000 Ion Chromatography System with chemical suppression as described in ISO10304-1 and in compliance with the DIONEX manuals.

3.4.6. Major cation analysis

Sodium, potassium, calcium and magnesium were concentrations were determined by inductive coupled plasma atomic emission spectrometer (ICP-AES).

3.4.7. Particulate Matter (PM) in stream water

For stream samples Whatman GF/F 0.7 μm filters are pre-burned at 550°C , weighed (m_0) and then used for filtrating 200 mL (V) of stream sample. The filter is dried at $105\pm 5^\circ\text{C}$ and then re-weighed (m_1).

Equation 3-1

$$PM_T = \frac{m_1 - m_0}{V}$$

The inorganic particulate matter (PM_i) is determined by igniting the filter paper at 550°C for 4h, and weighing (m_2) there after.

Equation 3-2

$$PM_i = \frac{m_2 - m_0}{V}$$

The organic particulate matter (PM_O) is determined by taking the difference between the PM_T and PM_i .

Equation 3-3

$$PM_O = PM_T - PM_i$$

3.4.8. Quantitative analysis of phosphate

The amount of orthophosphate is determined spectrophotometrically by the molybdate blue method. In the molybdate blue method orthophosphate, from the sample, reacts with ammoniummolybdate, creating a yellow coloured product known as phosphomolybdenum acid. This product is then reduced by ascorbic acid, in the presence of antimony, and produces a bright blue complex. The concentration of the blue colour can then be analyzed spectrophotometrically by absorbance at 660 or 880 nm.

Standard phosphate solutions are created using potassium dihydrogenphosphate (KH_2PO_4) solutions as the source of orthophosphate (Murphy and Riley, 1962).

When analyzing orthophosphate in a natural water sample, the analysis of SRP may be a more correct term for this analysis. It has been shown that the reagents used in the analysis hydrolyze labile organic phosphorus, causing it to be measured as orthophosphate (Rigler, 1973). However, this may not always be the case, since the method has many adaptations, usually specific for the instrument or the solution matrix of the analyte.

The range for the spectrophotometric orthophosphate method depends on the instrumentation setup. The normal detection limit is around $1 \mu\text{g P/L}$ and the linear range is up to around $1000 \mu\text{g P/L}$. This can be altered by instrumental parameters such as path length of the cell in the spectrophotometer as well as wavelength used for measurement.

3.4.9. SEAL autoanalyzer for orthophosphate

The SEAL autoanalyzer was used to determine the P fractions from the soil extracts acquired from the Chang and Jackson (1957) and Mørberg and Petersen (1982) methods, see chapter 3.5.2 and 3.5.3. The general setup for the instrument is given in TABLE 3b. Instrument setup details are kept confidential by Seal Analytical and reproduction of information is not permitted without authorization. For more details refer to Seal AutoAnalyzer 3 manual.

TABLE 3b Parameters used in accordance with method no. G-103-93, Seal AutoAnalyzer 3 manual.

Parameters	
Detection Range ($\mu\text{g P/L}$):	0 – 6000
Flowcell (mm):	10
Wavelength (nm):	660
Reagent solutions:	Ammonium molybdate solution Sulfuric acid solution Ascorbic acid solution Wash solution: Same matrix as solution used for extraction (TABLE 3g).
Standard Phosphate Solutions ($\mu\text{g P/L}$):	1000, 500, 250, 125, 62.5, 31.3, 15.6 and 7.8 (All standards are matrix matched with extraction solutions (TABLE 3g).

3.4.10. CNP-autoanalyzer

The CNP-autoanalyzer is a NIVA customized SKALAR San⁺⁺ Automated Wet Chemistry Analyzer. The instrument is used to determine TOC, Total N (Tot-N), Total P (Tot-P), NO₃-N, NH₄-N, PO₄-P and Si simultaneously from a single sample. P-DGT extracts, stream samples and soil water sample were analysed with the CNP-autoanalyzer. Due to confidentiality agreements with NIVA, detail regarding the instrument and its methods will not be disclosed. Only general information on the CNP determination is given in TABLE 3c.

All samples and standards are preserved to 0.04 M H₂SO₄.

TABLE 3c General information regarding analysis with CNP autoanalyzer

Determined	Method	Analyzed	Measurement method	Wavelength (nm)
TOC	Persulphate digestion, CO ₂ stripping.	CO ₂	IR detection	N/A
Tot-N	Persulphate digestion, Cd reduction, Griess reaction	NO ₂ -N	Photometrically	540
Tot-P	Persulphate digestion, Molybdate blue method	PO ₄ -P	Photometrically	880
NO ₂ -N/ NO ₃ -N	Cd reduction, Griess reaction	NO ₂ -N	Photometrically	540
NH ₄ -N	OPA method.	NH ₄ -N	Fluorometrically	450-1200
PO ₄ -P	Molybdate blue method	PO ₄ -P	Photometrically	880
Si	Molybdate blue method	Si	Photometrically	810

3.4.11. Phosphorus fractionation in water samples

Natural water samples have several fractions of P bound to organic and inorganic matter as well orthophosphate (FIGURE 2d and chapter 2.3). The P in the raw sample has to be fractionated to determine the amount of P in different fractions. The method used, splits the raw sample into four P groups, giving up to 5 operationally defined P fractions, see FIGURE 3h and TABLE 3d.

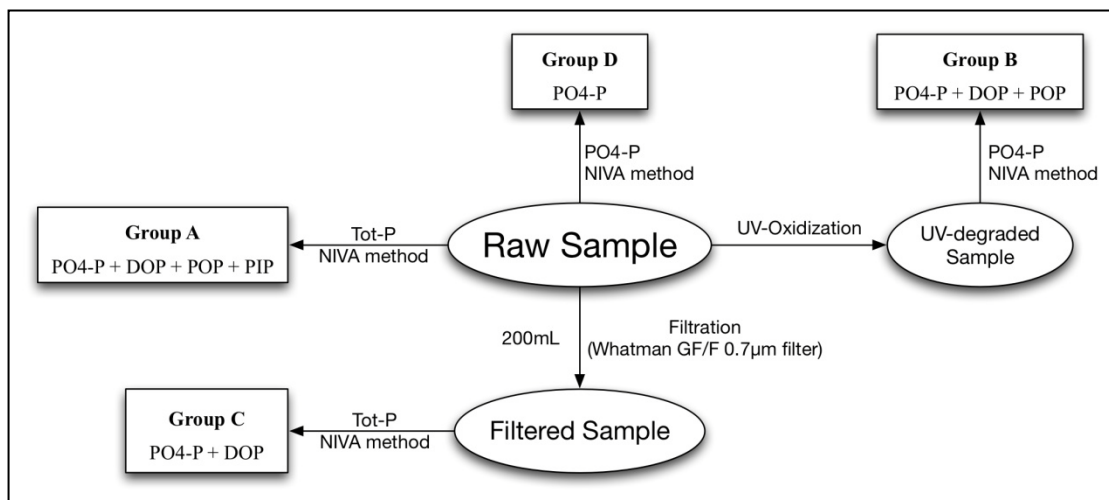


FIGURE 3h Phosphorus fractionation schematics (Vogt, 2008 modified).

The amount of each P fraction can be determined by subtracting the amount of phosphorus found in one group against the amount found in another group (TABLE 3d).

TABLE 3d Determination of different P fractions in stream and soil water.

Fraction	Group
Total-P (Tot-P)	Group A
Particulate inorganic P (PIP*)	Group A - Group B
Particulate organic P (POP = Microbial-P + organic-P macromolecule larger than 0.7 μm^*)	Group B - Group C
Dissolved organic P (DOP)	Group C – Group D
PO4-P	Group D

*As obtained by filtration by Whatman GF/F 0.7 μm filter.

3.5. Soil Analysis

In order to understand the mobility of P in soil one must also know how P is bound in the soil in addition to other chemical and physical soil properties. Analyzing the soil horizon in the terrestrial plots helps give an understanding of how the soil in the catchment interacts with each other and contributes to the input of P in the stream.

3.5.1. Soil pre-treatment

Collected soil samples are placed and distributed evenly on paper plates. The soil is left to dry at room temperature for a few days (paper sheet is put on top of samples as they dry to avoid contamination from air dust). After air drying, the soil is sieved through a 2mm aperture sieve. If necessary the soil aggregates are carefully crushed using a mortar before sieving. The sieved air-dried soil is then stored at room temperature in paper boxes marked with a registration no.

TABLE 3e Soil analysis procedure for water content, LOI and Soil pH.

Parameter	Procedure	Method reference

<p>Dry matter/Water content (w_{H_2O})</p>	<p>Crux is weighed (m_0). Air-dried soil is weighed in crux (m_1), and then heated at $105\pm 5^\circ\text{C}$ for 12h. Thereafter soil sample is placed in dessicator overnight before re-weighing (m_2).</p> <p style="text-align: center;">Equation 3-4</p> $w_{H_2O} = \left(1 - \frac{m_2 - m_0}{m_1 - m_0}\right) \times 100\%$	<p>ISO 11465</p>
<p>Loss on Ignition (LOI)</p>	<p>LOI, crux is weighed (m_0), air-dried soil is heated to 550°C for 4-6 hours. Mass is weighed before (m_1) and after (m_2).</p> <p style="text-align: center;">Equation 3-5</p> $LOI = \left(1 - \frac{m_2 - m_0}{m_1 - m_0}\right) \times 100\% - w_{H_2O}$	<p>(Krogstad, 1992)</p>
<p>Soil pH-H₂O</p>	<p>pH was measured for 10mL soil in 50 mL water suspension.</p>	<p>ISO10390</p>
<p>Soil pH-CaCl₂</p>	<p>pH was measured for 10 mL soil in 50 mL 0.01M CaCl₂ suspension.</p>	

3.5.2. Phosphorus fractionation soil samples

Fractionation between organic bound P and inorganic P was performed by the method of (Mørberg and Petersen, 1982) as explained in TABLE 3f.

TABLE 3f Procedure for organic P and inorganic P fractionation

Fraction	Procedure
Total P	For total P determination, 1 g of previously ignited soil, taken from the soil used for LOI determination, was placed in a 250 mL volumetric flask and added 5 mL 6 M H ₂ SO ₄ . The mixture was heated to 70°C for 10 min. After heating another 5 mL 6 M H ₂ SO ₄ was added. The solution was then diluted with Type I water to 250 mL and PO ₄ -P is determined.
Inorganic P	Determination of inorganic P was performed in the same way, with the exception that the soil used is air-dried and not pre ignited soil.
Organic P	The organic P fraction is the difference between total and inorganic P.

3.5.3. Sequential extraction of P in soil

Fractionation of the inorganic P fraction was performed according to the sequential extraction method by Chang and Jackson (1957), modified by Hartikainen (1979). The method results in the extraction of five P fractions

- Easily soluble P (Sol-P)
- Aluminium bound P (Al-P)
- Iron bound P (Fe-P)
- Calcium bound P (Ca-P)
- Occluded P (Occluded-P)

The procedure for extraction and preparation before determination is shown in FIGURE 3i.

1 g of soil was placed in 85 mL Oak Ridge Polycarbonate Centrifuge Tubes and sequentially extracted according to FIGURE 3i. The Edmund Bühler KS-15 instrument was used for shaking in which extraction occurs. The shaking speed was set at 275 rpm. The Jouan B4i (Thermo Fisher Scientific Inc.) was used for centrifugation.

The relative centrifugal force (RCF) was set for 644 g (2400 rpm, $r = 10$ cm).

Reagents used are given in TABLE 3g.

Determination of P was performed using the Seal orthophosphate AutoAnalyzer 3.

TABLE 3g Reagents used for extraction and preparation for P analysis.

Reagents	Procedure
1 M NH_4Cl	Dissolve 53.5 g NH_4Cl to 1 liter type II water
0.5 M NH_4F	Dissolve 18.5 g NH_4F to 1 liter type II water
0.8 M H_3BO_3	Dissolve 50 g H_3BO_3 to 1 liter type II water
0.1 M NaOH	Dissolve 4.1 g NaOH to 1 liter type II water
0.25 M H_2SO_4	Dissolve 15 mL concentrated H_2SO_4 to 1 liter of type II water
0.1 M KCl with ascorbic acid and EDTA	Dissolve 7.5 g KCl, 12.5 g ascorbic acid and 0.372 g $\text{Na}_2\text{-EDTA}$ in type II water, and dilute to 1 liter in a volumetric flask
Standard 50 ppm P solution	Dissolve 0.2195 g KH_2PO_4 in type I and dilute to 1 liter in a volumetric flask.
Standard 5 ppm P solution	Dilute 50 mL of <i>Standard 50 ppm P solution</i> to 500 mL in a volumetric flask with type I water.
Saturated NaCl solution	400 g NaCl suspended to 1 liter type II water.

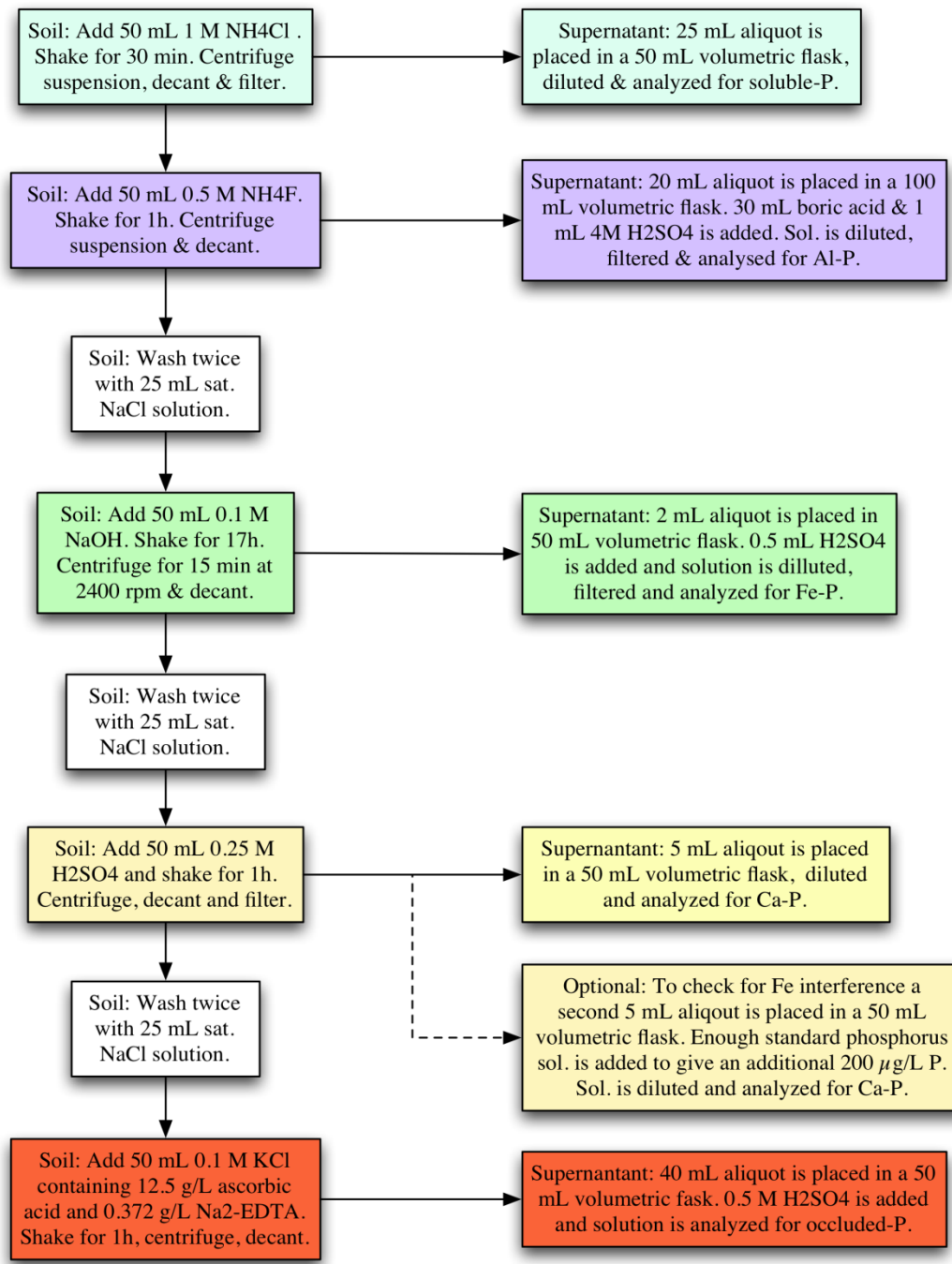


FIGURE 3i Sequential extraction of different inorganic P fractions.

3.6. P-DGTs in field and laboratory

3.6.1. P-DGTs in the stream

In order to sample phosphorus in the stream, P-DGTs were placed in a sealed polypropylene net tube, anchored by a stone on one end and tied on the other end with a rope to a branch or tree, see FIGURE 3j. The P-DGTs were left in the stream for 1 to 2 weeks. Sampling occurred from late October to mid December at two streams near the Vansjø area. One stream is located at Dalen catchment (FIGURE 3b), and the other at Støa catchment. The two catchments are geographically, geochemically and ecologically different. While Dalen is a small forested catchment, Støa is a 100% agricultural catchment. The streams therefore vary significantly from each other in their P concentrations, and P fractions. Analysis was performed at NIVA with the CNP autoanalyzer.



FIGURE 3j Left: Illustration of how the P-DGT is anchored to the stream bed. Right: Photo of Dalen stream, where P-DGTs have been anchored for sampling.

3.6.2. Laboratory study for P-DGT uptake of organic P compounds.

Little is known with regards to if organic phosphorus molecules in water are adsorbed to the ferrihydrite membrane when sampling in the aquatic environment. For this reason a laboratory experiment was performed, at NIVAs chemistry laboratory, to determine the uptake of low-molecular-weight (LMW) organic molecules with ester bound phosphate groups. Adenosine monophosphate (AMP) was chosen, as it is a useful model compound with similar molecular size and properties of common LWM found in soil and surface waters (see FIGURE 3k). The molecule is easily soluble in water and due to its small size and external exposed phosphate group, may possibly be adsorbed by the P-DGTs ferrihydrite receiving phase.

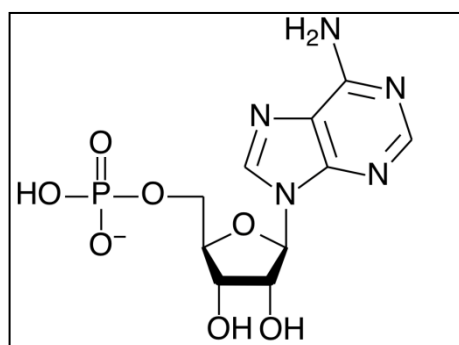


FIGURE 3k Molecule structure of adenosine monophosphate.

The experiment was set up using NIVA's DGT test system. The test system uses a 50 L container with a central rotating disk (rotor) with circular pallets for mounting DGTs. The container is filled with test solutions, DGTs are mounted, and the rotor is set to a fixed rotating speed to ensure a low laminar boundary layer during experiments. The setup is shown in FIGURE 3l.

The experiment was performed by placing 20 P-DGTs in an AMP solution equivalent to 25 $\mu\text{g P/L}$. The P-DGTs were removed individually after different periods of time in order to determine the uptake rate of P.

In the 50 L container (FIGURE 3l) 45 L of the AMP solution equivalent to 25 $\mu\text{g P/L}$ was prepared by diluting 25.6 mL of 558.6 mg/L Na_2AMP stock solution (equivalent to 44.0 mg P/L), with 45 L of Type I water. The stock solution was acidified with

0.04 M H₂SO₄ (pH ~ 1,3), so the pH of the solution was adjusted to reach the desired pH of 5.0. This was done by adding 57 mL of 0.1 M NH₄CH₃COO. The adjustment to pH 5.0 was done to compare with surface water from forest catchments. To slightly increase the ionic strength, 2.63 g of NaCl was added giving a concentration of 1 mmol/L NaCl. The solution was the mixed for a few minutes and then left to stabilize overnight.



FIGURE 31 Left: 50 L container with motorized lid. Bottom-right: Lid for container with 15 Volt electrical motor on top, for rotating a disk containing P-DGTs. Top-right: P-DGTs fit into apertures and are secured to the rotating disk with twistable clips.

Thereafter the P-DGTs were placed and secured onto the rotating disk (speed 6 rpm), which was submerged into the solution (see FIGURE 31).

The sampling time for the individual P-DGTs are listed in TABLE 3h. In addition samples of the solution were taken to control if the AMP concentration was changing throughout the experiment (decomposition, wall adsorption etc). After sampling both P-DGTs and water samples were refrigerated at 4°C, until analysis.

The experiment was performed at NIVA.

Analysis for Tot-P and PO₄-P was performed using the CNP autoanalyser.

TABLE 3h Sampling time for the P-DGTs in AMP solution.

Days	1	2	3	5	7	9	12	14	16	19	21
Number of P-DGTs taken out	1	2	2	2	2	2	2	2	2	2	1

3.6.3. Extraction and analysis of exposed P-DGTs

After exposure the P-DGT samplers were disassembled, and the receiving phase was put in to a 30 ml polypropylene tube and added 0.3 mL of 4M H₂SO₄ and 0.7 mL Type I water and left overnight. By doing this, Fe(OH)₃ in the receiving phase, was dissolved and possible adsorbed P-compounds were released. The solution was then diluted to 30 mL by adding 29 mL Type I water. The determination of Tot-P and PO₄-P was performed using NIVA's CNP autoanalyser.

3.7. UV impact on DOM

3.7.1. Humic stream water sample

The significance of increased leaching of dissolved natural organic matter (DOM), and along with it likely also organic bound phosphorous (DOP), depend on what happens to the material in the lakes. The fate of DOM and DOP in freshwater lakes depends on several factors. Lake Vansjø it a relatively shallow lake system. It may therefore be seen as a large photo-reactor tank where the DOM may be broken down to smaller molecules or mineralized completely. This photo-oxidation is mainly caused by the energy rich UV radiation.

In order to start to assess the importance of this process a pilot experiment was conducted in which DOM from a forested stream (Dalen) was exposed to UV irradiation. The samples were distributed into 14 quartz tubes, placed in a UV reactor tank (FIGURE 3m), and removed, two parallels at a time, from the reactor with increasing time intervals (TABLE 3i). The UV-radiation intensity spatial distribution from the UV-lamp is unknown. For this reason parallels are placed far away from each other to compensate for any uneven UV exposure within the tank.

The decomposition of DOM was measured in the water samples from the tubes as decreased absorbency at λ 254 nm and 400 nm. Absorbency at these wavelengths are

common used proxies for DOM, as the chromophore are responsible for the absorption of radiation (i.e. conjugated double bonds) are assumed to be evenly distributed in natural DOM. Absorbance measurement were also taken for the stream sample with no UV-exposure.

3.7.2. Zero-tension soil water sample

Water from zero-tension lysimeters, capturing water draining freely from the organic forest floor horizon, have very high organic matter content compared to stream samples. Furthermore, the functional characteristics of this DOM are known to be very different than for the DOM that has passed through mineral soil before entering the stream. A similar experiment as for stream water described in chapter 3.7.1 was therefore conducted on a water sample from the forest floor. Here two more longer time intervals were added, because the DOM concentration was higher.

TABLE 3i No. of samples exposed to UV-radiation at different time intervals

UV-exposure time (min)	0	3	6	12	20	40	75	120	240	480
No. of stream sample parallel	2	3	2	2	2	2	2	2		
No. of zero-tension sample parallel	2	2	2	2	2	2	2	2	2	1



FIGURE 3m Top left: UV-reactor tank approx. 50 cm in height. Top right: Insides of the UV-reactor tank. UV light bulb in the centre, and the quartz tubes with sample are placed around (not shown). Bottom: Top of tank where the quartz tubes are inserted (only in the outer holes. Tubes are approx. 3 cm from the UV light bulb.

4. Results and Discussion

4.1. Soil P fractions and pH in Dalen

Pools of phosphorous in the sampled soil horizons in Dalen, fractionated as described in chapter 3.5.2 and 3.5.3, are presented in FIGURE 4a. The largest soil P pool was found in the organic forest floor O horizon where organically bound P was by far the greatest fraction. This is mainly due to that this soil horizon is situated within the forests internal P cycle, receiving high input of orthophosphate leached out of the forest canopies. The P pool in the O horizon decreases down the slope possibly due to loss by sub-lateral flow of water flushing the soil horizon during periods of high runoff.

The organically bound P is the dominant P pool also in all the E and A horizons, as well as in the B horizons on the slope. The acid extractable Ca bound phosphorous is the second largest P pool in these soils. This pools shows a increasing tendency down through the soil profile, with especially large pool in the deepest C or B horizons on the ridge and in the valley bottom, respectively. This is likely due to marine clay deposits relatively rich in phosphorous. A significant pool of phosphorous bound to iron is found in the Bs horizon of the classical podzol on the ridge. This is reasonable as this is a soil horizon especially rich in iron sesquioxides. The eluvial E horizon in the soil plot located at the ridge had the smallest P pool. This soil horizon is depleted of iron and aluminium sesquioxides and clays. It has therefore a very low capacity to adsorb orthophosphate.

From FIGURE 4b the soils in Dalen were found to be acidic with pH well below 6 in all horizons and plots. The pH increases typically down through the soil profile as well as down along the topographic gradient. Lowest pH (3.2) was therefore found in the salt (pH-CaCl₂ suspension) extracts in the acid forest floor horizon on the ridge, while the highest soil pH (5.7) was in the water extract of the deepest clay rich soil horizon in the valley bottom.

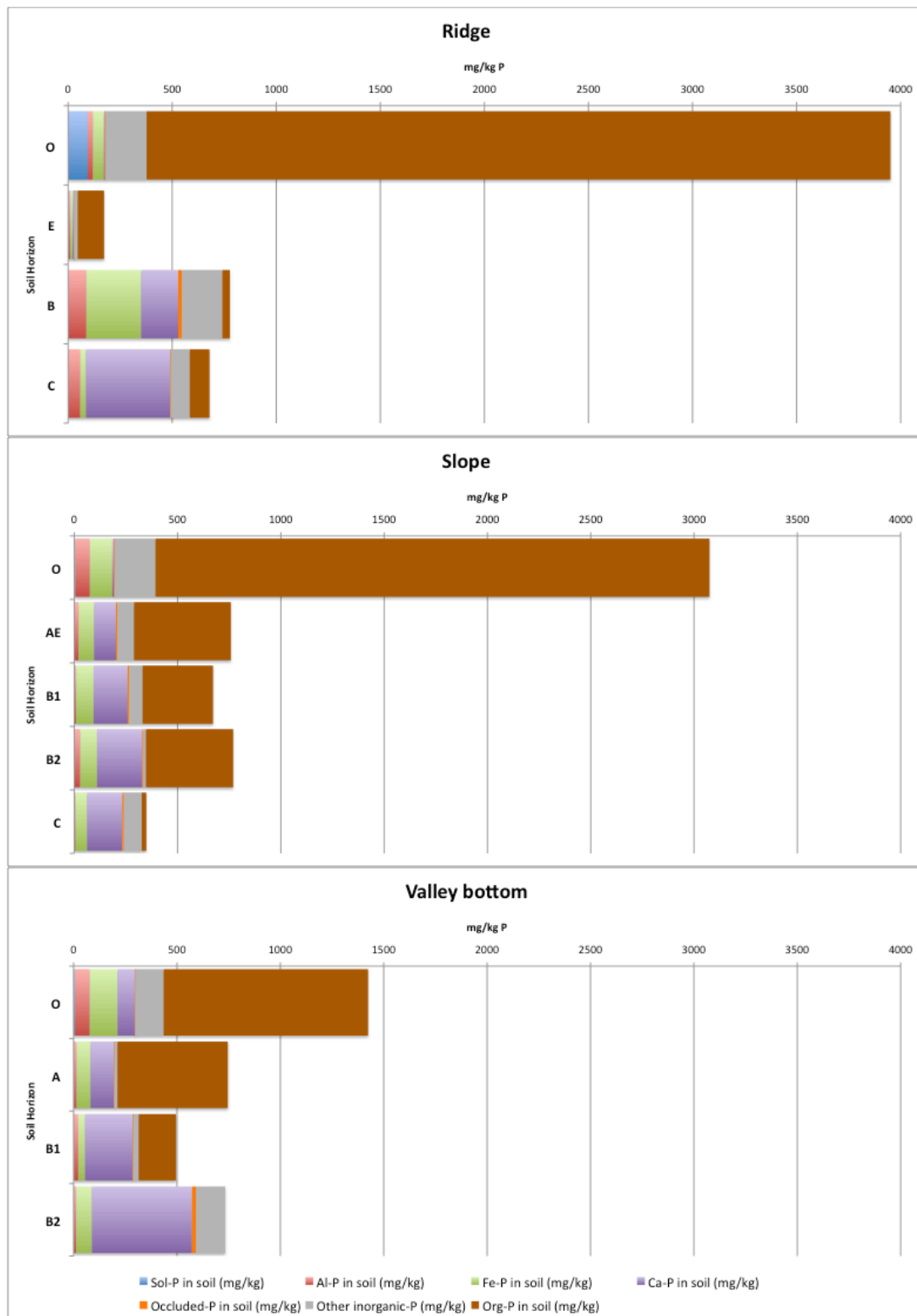


FIGURE 4a Soil pools of phosphorous in different genetic soil horizons at the three soil plots at Dalen. O, E, EA, B and C denote genetic soil horizons.

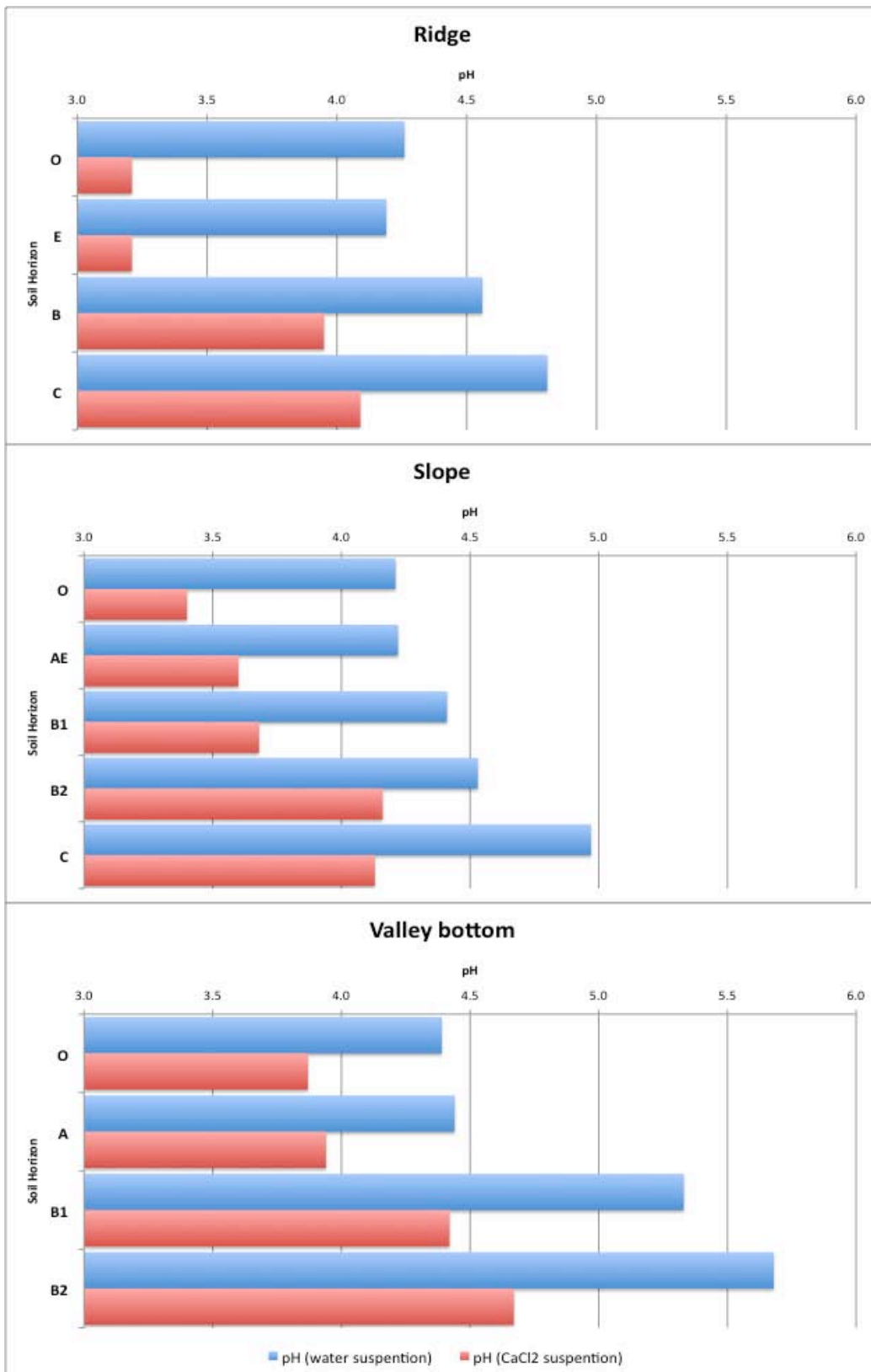


FIGURE 4b Soil pH in water (pH-water suspension) and salt extract (pH-CaCl₂ suspension) in different genetic soil horizons at the three soil plots in Dalen. O, E, EA, B and C denote genetic soil horizons.

4.2. Soil and stream water

Soil water pH in the different soil horizons in the soil plots are given in FIGURE 4c. The results show that the soil water is acidic with approx. pH 4 in the forest floor on the ridge increasing to alkaline pH only in the deepest soil horizons in the valley bottom. As for the soil pH so does the soil water pH increases down through the soil and down the topographic gradient. pH in the throughfall is close to the equilibrium pH with the $p\text{CO}_2$ in air (5.64). The low pH is mainly governed by organic acids in the dissolved organic matter. The DOC concentration generally mirror the variation pH, both down through the soil horizon as well as down the topographic gradient (FIGURE 4d).

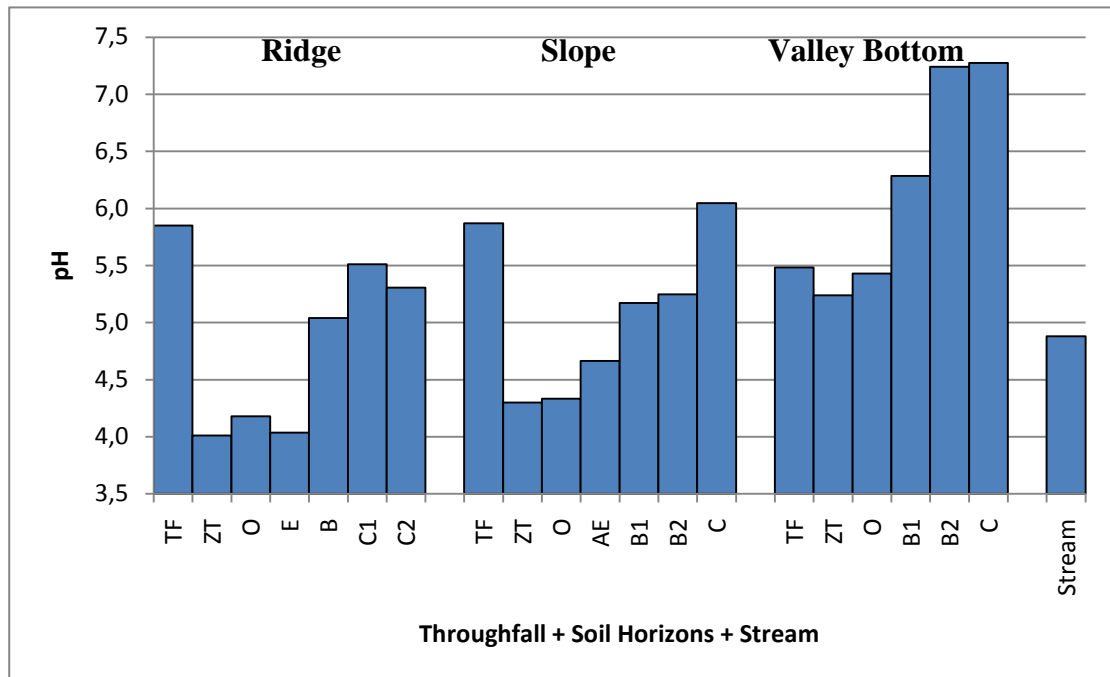


FIGURE 4c Soil water pH in deposition and different genetic soil horizons at the three soil plots in Dalen and stream.

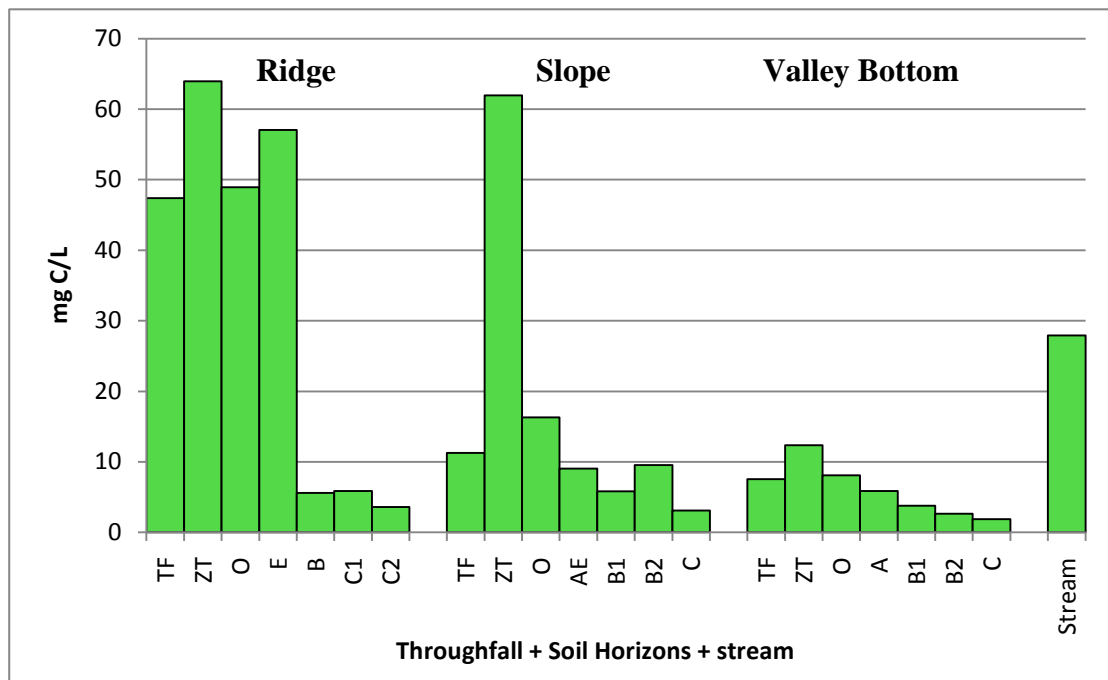


FIGURE 4d Dissolved organic carbon (DOC) in deposition and different genetic soil horizons at the three soil plots in Dalen and stream.

The low pH and high organic content of the soil water allows for very high concentration of organic monomeric aluminium (Al_o) (FIGURE 4e), especially in the eluvial E horizon on the ridge where there is $2 \text{ mg } Al_o \text{ L}^{-1}$. This concentration decreases abruptly down into the B horizon as pH increase to 5. In the soil plot on the slope high Al_o concentrations are also found in the organic forest floor. This suggest sub-lateral water flow transporting aluminium from the mineral soil into the organic soil further downslope. This was also suggested by the spatial distribution of P pools in the soil (chapter 4.1). Considering that sulphur deposition is reduced by about 70% since the end of the 1970s the levels of inorganic labile aluminium (Al_i) found in the soil water, both on the ridge and on the slope, is surprising. More than $30 \mu\text{M } Al_i$ in the AE horizon is similar to what was commonly found in soil water in Birkenes, in southernmost Norway, back in the mid 1980s (Seip et al., 1989). Due to lack of sufficient major anion data it is not possible to assess the speciation of this aluminium and thereby the mobility and transport mechanism. In the organic top horizons in the valley floor, where pH is above 5, the concentrations of aluminium fractions are relatively low. In the mineral soil the pH is higher than 5.5 and Al concentrations are assumed close to detection limit.

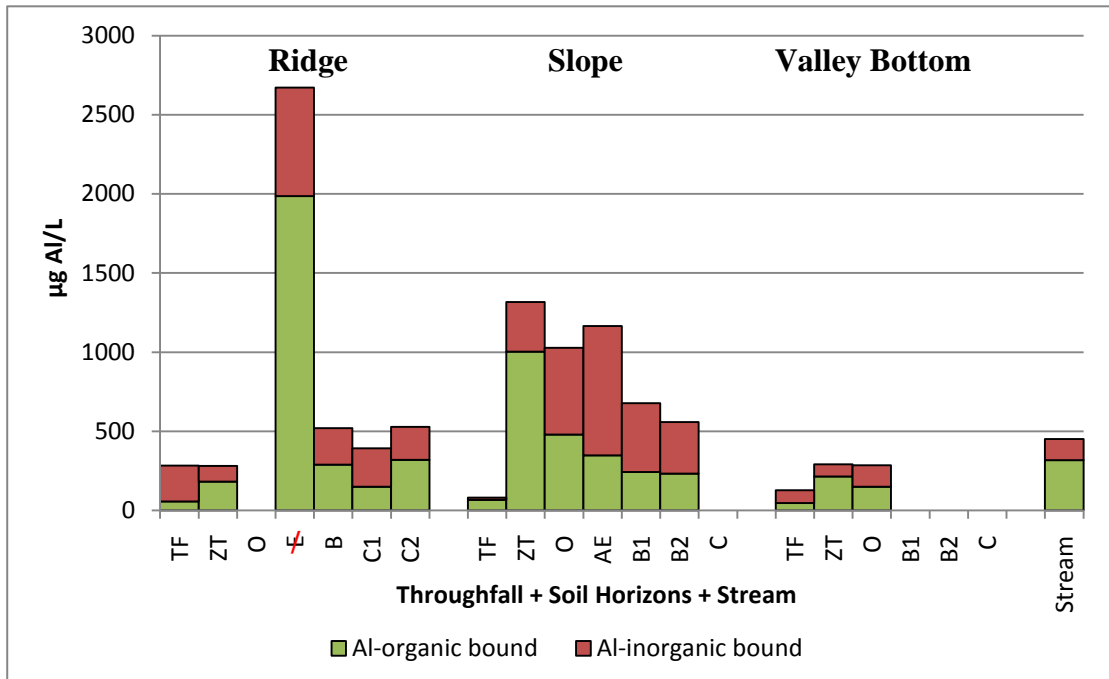


FIGURE 4e Inorganic (Al_i) and organic (Al_o) monomeric bound aluminium in deposition and the different genetic soil horizons at the three soil plots at Dalen. Data for O horizon at the ridge is not available due to lack of data.

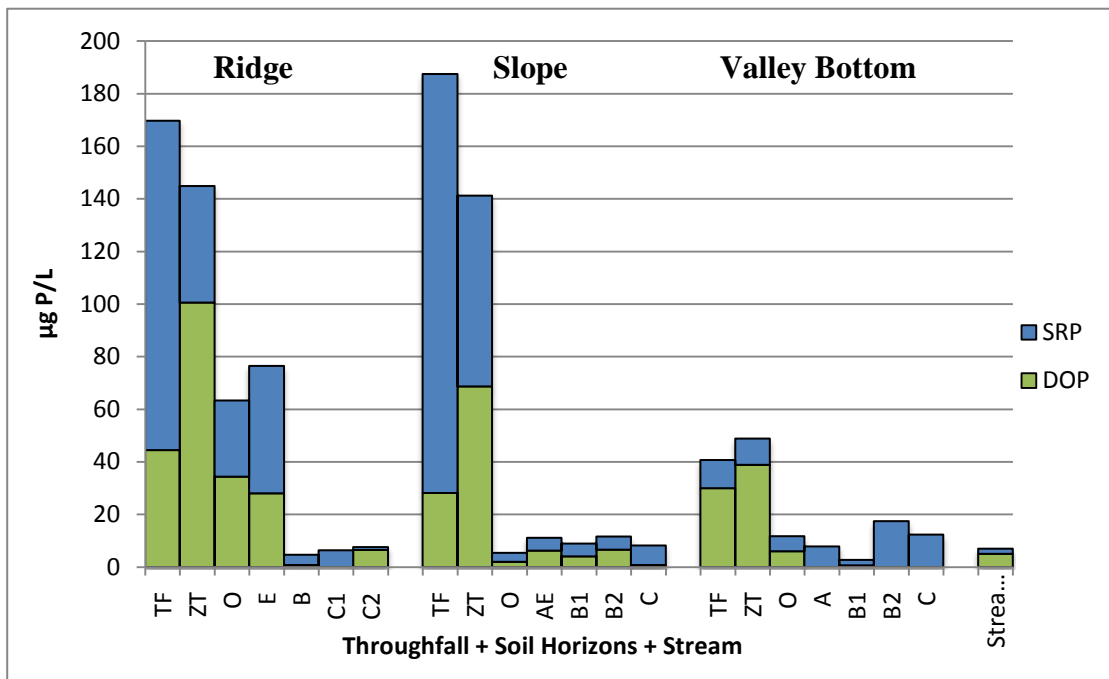


FIGURE 4f SRP and DOP in deposition and different genetic soil horizons at the three soil plots and the stream at Dalen.

Total P concentrations in the different plots and their horizons are given in FIGURE 4f. Concentrations are extremely high in the zone below the canopy and above the roots. This is because of the rapid internal cycling of phosphorous in the vegetation,

where nutrients are leached from the canopy and ground vegetation and assimilated again through the roots. This was also found in the discussion of soil pools of phosphorous (Chapter 4.1). Concentrations in the O-horizons in the slope and valley bottom as well as all horizons in and below the rooting zone remain close to the detection limit.

Spatial distribution of total N show similar pattern as phosphorous with high concentrations below the canopy and above the rooting zone, due to internal nutrient cycling. Significant amounts of ammonia are found in the surface soils on the ridge and slope. In the deeper horizons in the valley bottom significant amounts of ammonium is found, likely due to reducing conditions. Only in the stream due we see a larger amount of nitrate, possibly as a result of ammonia oxidation.

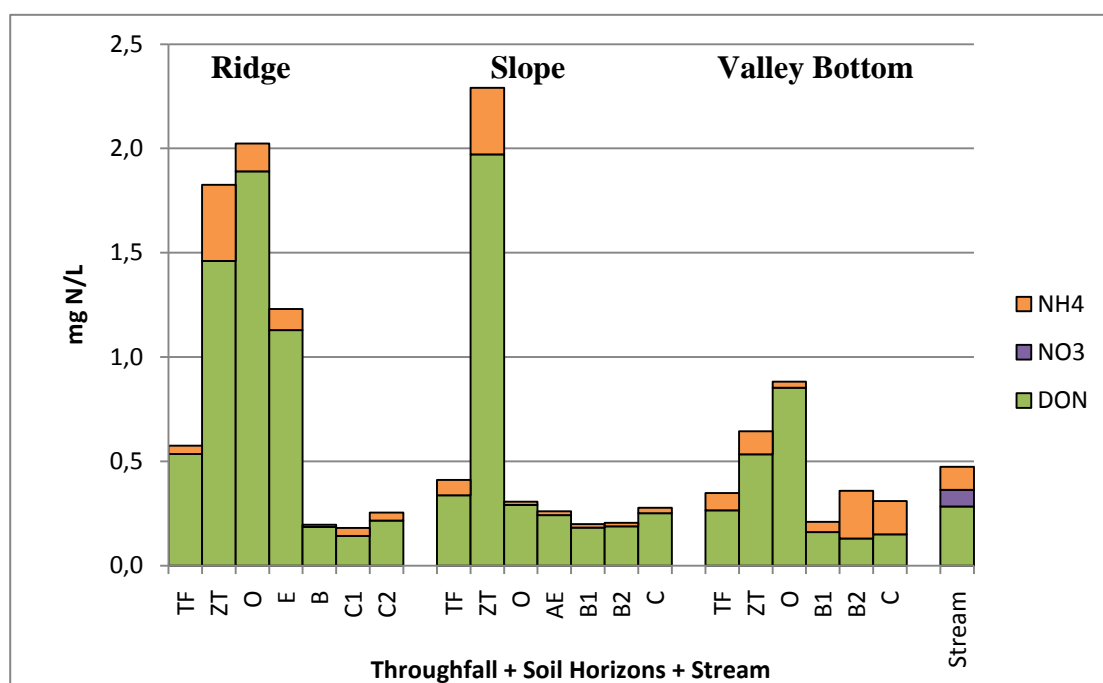


FIGURE 4g Nitrate, ammonia and organic bound N in deposition and different genetic soil horizons at the three soil plots and the stream at Dalen.

Preliminary data of average stream water chemical composition is shown in FIGURE 4h. The water is relatively acid with average pH below 5 (FIGURE 4c) and a high content of Dissolved Organic Carbon (DOC; 30 mg C L^{-1} , FIGURE 4d). This allows for a significant leaching of organic complexed aluminium (Al_o ; 0.4 mg L^{-1}) and inorganic labile aluminium (Al_i ; $5 \text{ }\mu\text{M}$). $5 \text{ }\mu\text{M}$ of Al_i is being leached out of the forested watershed. Aluminium is a strong precipitating agent for P. A rough estimate, assuming that each mol of Al_i precipitates out 1 mol of orthophosphate, and

extrapolated for the forested area of Morsa provides a potential for precipitation of 43 t P yr⁻¹. This is highly significant considering that the total flux of P to Morsa is now approx. 39 t P/yr. During the acid rain period there was likely a 3 times greater Al leaching. This could at that time potentially have precipitated out more than 130 t P yr⁻¹. Clearly the loss of aluminium leaching due to the reduction in sulphur deposition may be a significant contributing factor for the lack of reduced total P levels in the lake, despite considerable abatement actions to reduce the nutrient loading to the lake.

The sea salt ions Na⁺ and Cl⁻ are the dominant cation and anions, respectively, due to strong sea salt influence. Significant amounts of nitrate and ammonium are being leached out of the catchment. Total average P concentration is 7.6 µg P L⁻¹. Of this 1.9 µg P L⁻¹ is SRP (presumed mainly orthophosphate) and 5.1 µg P L⁻¹ is DOP. Approx. 20-25% of the total P loading to the lake is from forests. 85% of total P from forested watersheds is organic P. There has been a significant increase in the concentrations of DNOM over the last 25 years (NORDTEST, 2003). This represents an increased total P loading of 9.5%, suggesting that the increased background flux of organic bound P may be an important factor contributing to holding a high level of total P in the lake.

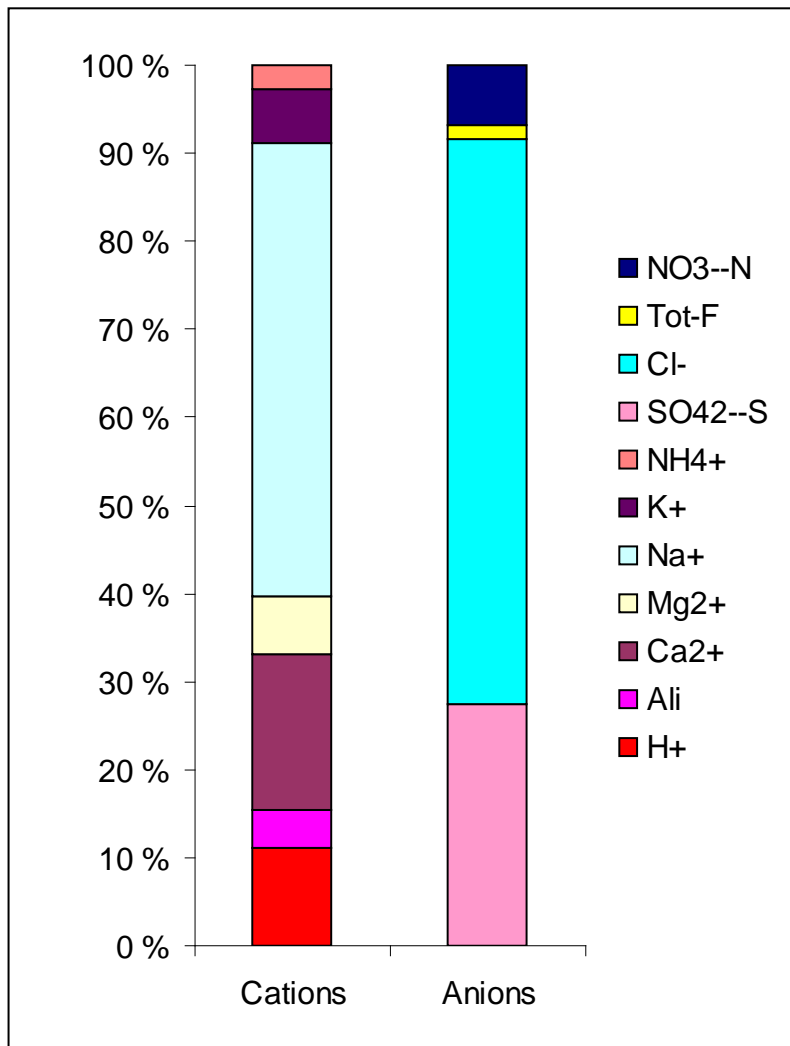


FIGURE 4h Chemical composition of major ions in stream water draining Dalen catchment.

4.3. P-DGT – laboratory and field studies

4.3.1. P-DGT uptake of AMP in the laboratory study

The uptake of AMP is presented in FIGURE 4i. The graph shows a near to linear uptake of AMP determined as total P with the CNP analyser. There is no uptake of free orthophosphate (below the detection limit of the orthophosphate method). This indicates that AMP is adsorbed nearly quantitatively by the P-DGT sampler. The absence of orthophosphate in the extract from the P-DGT, indicates that the AMP is not broken down or altered on the P-DGT samplers adsorption membrane during the sampling period or during the extraction process (by sulphuric acid). If this assumption is true, these data shows that it may be possible to use P-DGTs to collect AMP and orthophosphate together. By determining Tot-P and PO₄-P in the extract from the sampler, it is possible separate the inorganic fraction (PO₄-P) and the organic fraction (here AMP) by difference (Tot-P – PO₄-P).

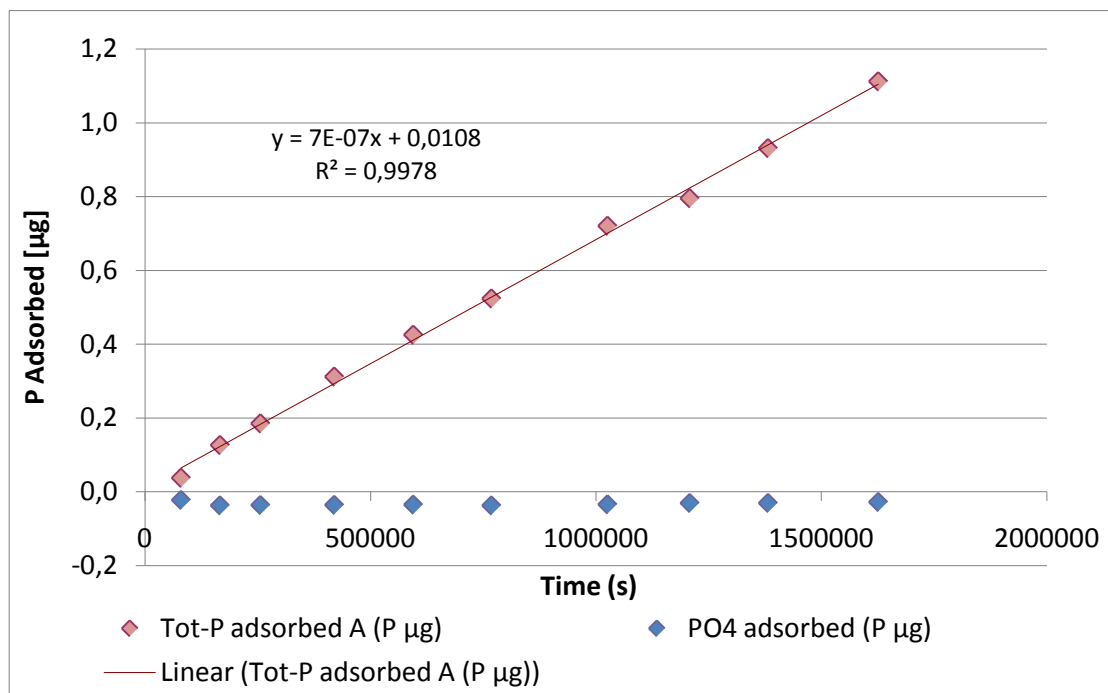


FIGURE 4i Uptake curve for AMP and orthophosphate (PO₄-P) for the P-DGT sampler. Orthophosphate concentrations are below detection limit.

The diffusion coefficient for AMP can be calculated by Equation 2-5, from each point in the curve of Figure 4c. For each calculation we need to know the concentration of

AMP in the exposure solution during course of the experiment. This was done by water samples taken at some intervals during the laboratory test. The results in Figure 4d show a slow decrease in AMP concentration during the exposure period.

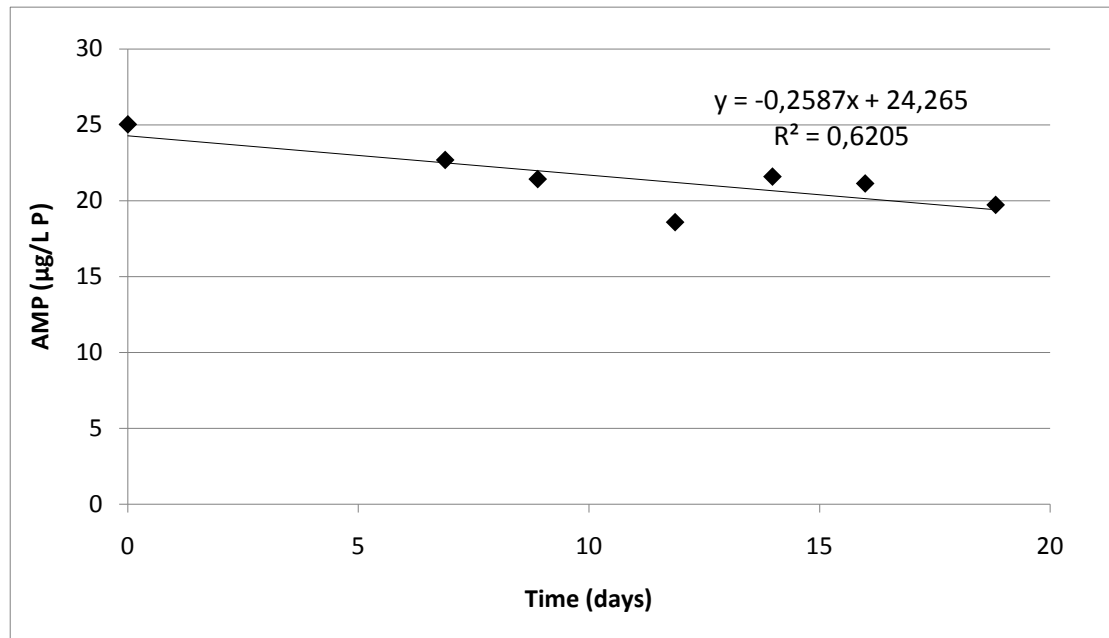


FIGURE 4j AMP concentration in the laboratory test container during the exposure time of the P-DGT experiment.

The reduction in AMP concentration from the initial 25 to approx. 19.5 µg P/L means that the diffusion coefficient must be calculated for the each of the time periods. The average AMP concentration for each sampling period was calculated (as average of 25 and the estimated end concentration from the end of each period) using the linear regression equation in FIGURE 4j. The average concentrations of AMP thus calculated were used as input to calculations, and the diffusion coefficient obtained are shown in TABLE 4a.

TABLE 4a Average AMP concentration for the exposure time intervals and diffusion coefficients obtained.

Sampling Time (days)	C _O , average AMP conc. (µg P/L)	D _{DC} AMP (10 ⁻⁶ cm ² /s)
1	24.5	1.96
2	24.4	2.71
3	24.3	2.96
5	24.0	3.38
7	23.8	3.29
9	23.5	3.04
12	23.1	3.30
14	22.8	3.32
16	22.6	3.32
19	22.2	3.33
Average (all sampling days)		3.06
Standard deviation		0.44
RSD %		14.5
Average (day 5 to 19)		3.26
Standard deviation		0.13
RSD %		4.0

The results show that the diffusion coefficient increases from the first days but then stabilises at a level around $3.3 \times 10^{-6} \text{ cm}^2/\text{s}$. The relative standard deviation (RSD%) for all data points are 14.5 %. When the data for the 3 first exposure periods are excluded, the standard deviation decreases to 4.0 %.

The relatively low diffusion coefficient from the first days may be attributed to analytical errors in determining the Tot-P concentrations in the extracts from the P-DGTs due to the small amounts collected in the beginning: Another error may be difficulties in estimating the correct Tot-P in the test chamber, as the correlation coefficient for the estimated line is relatively poor ($R^2 = 0.621$) in Figure 4d.

Based on the data in TABLE 4a the best value for the diffusion coefficient for AMP is estimated to be $3.3 \pm 0.1 \times 10^{-6} \text{ cm}^2/\text{s}$. The temperature of this diffusion coefficient is 22.5 °C, which was the average temperature at the laboratory during the test period.

Based on the decrease in concentration of AMP in the test solution during the experiment, it was calculated a total loss of of 236 $\mu\text{g P}$ as AMP from the solution (TABLE 4 m). By calculating the uptake of AMP into the P-DGTs, this only accounted for 36 $\mu\text{g P}$. Thus, there is an unexplainable loss of 203 $\mu\text{g P}$ (TABLE 4b). This loss may be explained by adsorption of AMP onto the walls the polyethylene container during the exposure period. AMP is a relatively low-polar organic compound that may adsorb on such surfaces. Another explanation may be growth of microorganisms in the solution during the course of the experiment. The latter assumption was supported by a noticeable odour from the solution and small amounts of white “slime” in the solution toward the end of the exposure period.

TABLE 4b Loss of AMP from the test solution in the test container

Initial mass AMP in container (P μg)	1126
End mass AMP in container (P μg)	887
SUM AMP collected by all P-DGTs (P μg)	36
Unexplained Loss of AMP (P μg)	203

4.3.2. Can P-DGT uptake of AMP be used to estimate uptake of other LMW organic P compounds in water?

Based on the results above we may conclude that AMP is adsorbed very well by the ferrihydrite adsorbent. The important question is whether other LMW organic phosphorus containing molecules, similar in size and charge to AMP, may also be adsorbed to the P-DGTs. This cannot be stated based on these experiments alone and further investigations is needed. However, the diffusion coefficient is in reasonable agreement with the values obtained for single ions in solution, with typical values in the range of $5\text{-}6 \times 10^{-6} \text{ cm}^2/\text{s}$. Due to the larger molecular size of AMP compared to single ions, a lower diffusion coefficients are expected.

When sampling in surface waters and streams, these molecules are referred to as soluble reactive organic phosphorus compounds (SROP). If it is estimated that if the size and electrical charge of a SROP-molecule is similar to AMP, the diffusion coefficient will be approximately the same range. To apply this theory to sampling in water, the effect of temperature must considered. Using the “Einstein-Stokes

equation” (Equation 2-3), we can calculate the diffusion coefficient at different temperatures. First we need to estimate the radius of the AMP molecule. By rearranging the ”Einstein-Stokes equation”, as in Equation 4-1, the radius was calculated to be 6.5 Å (0.65 nm).

Equation 4-1

$$r = \frac{k_B T}{6\pi\eta D}$$

This was used to calculate the AMP diffusion coefficient as a function of temperature, as shown in FIGURE 4k. This curve is also compared to the corresponding curve for PO4-P (maybe in the form of $H_2PO_4^-$ based on data from Zhang, 2005, see Appendix D, D-2 for more data). The smaller PO4-P molecule has a diffusion coefficient of $5.3 \times 10^{-6} \text{ cm}^2/\text{s}$ compared to $3.1 \times 10^{-6} \text{ cm}^2/\text{s}$ for AMP at a temperature of 20 °C. This curve is used in the calculations of concentration of SROP collected by the P-DGTs in the field, where the temperature varies.

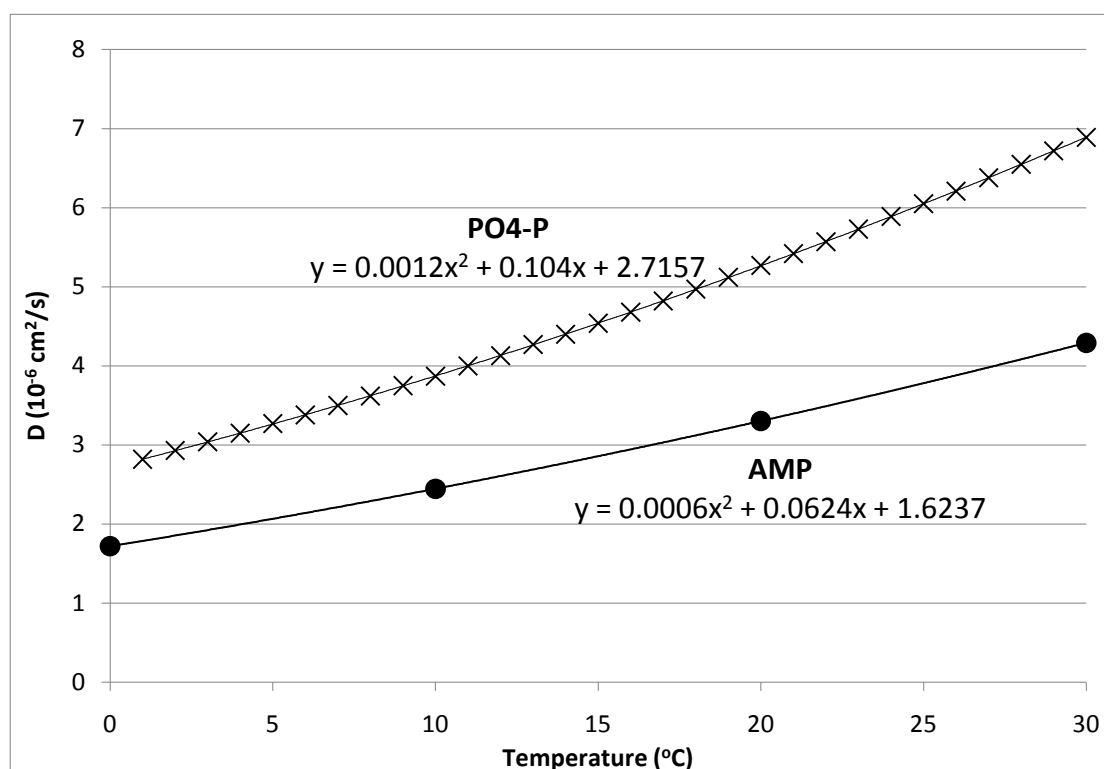


FIGURE 4k Diffusion coefficient shown as a function of temperature for a spherical molecule with a radius of 6.5 Å, like AMP and similar for PO4-P.

4.3.3. Sampling orthophosphate and SROP in Dalen and Støa stream.

P-DGTs were used to estimate the average phosphorus concentration in streams and determine the accuracy of P-DGT sampling compared to direct water sample collecting and analysis. Initially 5 parallel P-DGTs were used in each stream to determine the standard deviation of the sampling process. Parallels were placed in the same net. The results in (TABLE 4c) show a RSD of 27.4% and 15.4%, respectively. Based on statistical data from CNP-analyzer shown in Appendix B, B-7, it seems possible that the RSD from the analyzed concentration for Dalen in TABLE 4c, may be partly the result of uncertainty of the laboratory analysis by the CNP analyzer. The concentrations determined in the DGT extracts at Dalen, are only 4 times above the limit of detection (LOD) of the Tot-P method, and for that reason may have a large contribution to a large RSD. The P-DGTs from the Støa sites show a RSD of 15.4 % at a concentration where the analytical uncertainty of the CNP laboratory method is expected to be below 10%. These results may therefore be an indication of the sampling precision of the P-DGTs themselves. As a first test for field sampling of P-compounds using this type of P-DGTs, this can be considered as satisfactory. Future work will show if this can be lowered, when we get more training in handling the P-DGT both in the field and in the laboratory.

TABLE 4c Data for sampling precision of P by P-DGT at the two locations Dalen and Støa stream (12 days sampling, 5 parallells)

P-DGT	Dalen stream		Støa stream	
	Determined in P-DGT extract (µg P/L)	Calculated stream concentration from P-DGT (µg P/L)	Determined in P-DGT extract (µg P/L)	Calculated Stream concentration from P-DGT (µg P/L)
Parallel 1	6.5	1.2	131.3	24.0
Parallel 2	3.4	0.6	164.2	30.0
Parallel 3	4.7	0.9	117.0	21.4
Parallel 4	3.5	0.6	163.3	29.8
Parallel 5	4.9	0.9	166.7	30.5
Average	4.6	0.8	148.5	27.1
Stdev	1.3	0.2	22.8	4.2
RSD %		27.4		15.4

In FIGURE 4I the average concentration for stream samples collected during the sampling period and the P-DGT calculated average stream concentration, are shown . Dalen stream have very low levels, but shows almost identical results of 1.2 and 1.3 $\mu\text{g P/L}$, respectively. At Støa, however, the deviation is large between average stream water concentration and P-DGT concentration. At this site the variations in stream water concentration were large during the exposure period. This is a site with much particle transport, and a large fraction of P may be bound to particles and colloids in the water. This fraction is not taken up by the P-DGT. It is also difficult to determine $\text{PO}_4\text{-P}$ accurately by the molybdate method, as at the colloidal fraction may be included in the fraction determined, and free $\text{PO}_4\text{-P}$ may be overestimated. This may explain at least some of the deviation observed.

FIGURE 4I also show the results for the SROP fraction collected by the P-DGT .At Støa there is a noticeable SROP fraction of about 6.5 % of the total P-DGT fraction. If this SROP fraction is an organic fraction, this is interesting as it shows that the P-DGT can collect both inorganic and organic fractions of P (LMW P organic compounds). For Dalen stream the SROP was so low that calculations resulted in negative value (i.e. Tot-P is smaller than orthophosphate due to lower analytical accuracy for Tot-P than $\text{PO}_4\text{-P}$). SROP was therefore below the detection limit so no conclusion can be drawn, See TABLE D7 and TABLE D8 from D-3 in Appendix D.

Still, these data show that the P-DGT sampler may have a potential to give additional information for improved phosphorus fractionation in water. The results are preliminary, but some preliminary indications of the new potentials of the P-DGT sampler can be given:

At Støa the deviation between stream water $\text{PO}_4\text{-P}$ concentrations and P-DGT concentration may be used to estimate more accurately the “free” $\text{PO}_4\text{-P}$ fraction in samples with noticeable contents of particles and colloids, where orthophosphate may be adsorbed. This assumption may be supported by the good agreement at the Dalen site, where the particle content is very low.

The significant fraction of SROP at Støa, shows that we may use P-DGTs to estimate the organic fraction of LMW organic compounds in water

These initial findings must be supported by future research, but as a first test the results are promising.

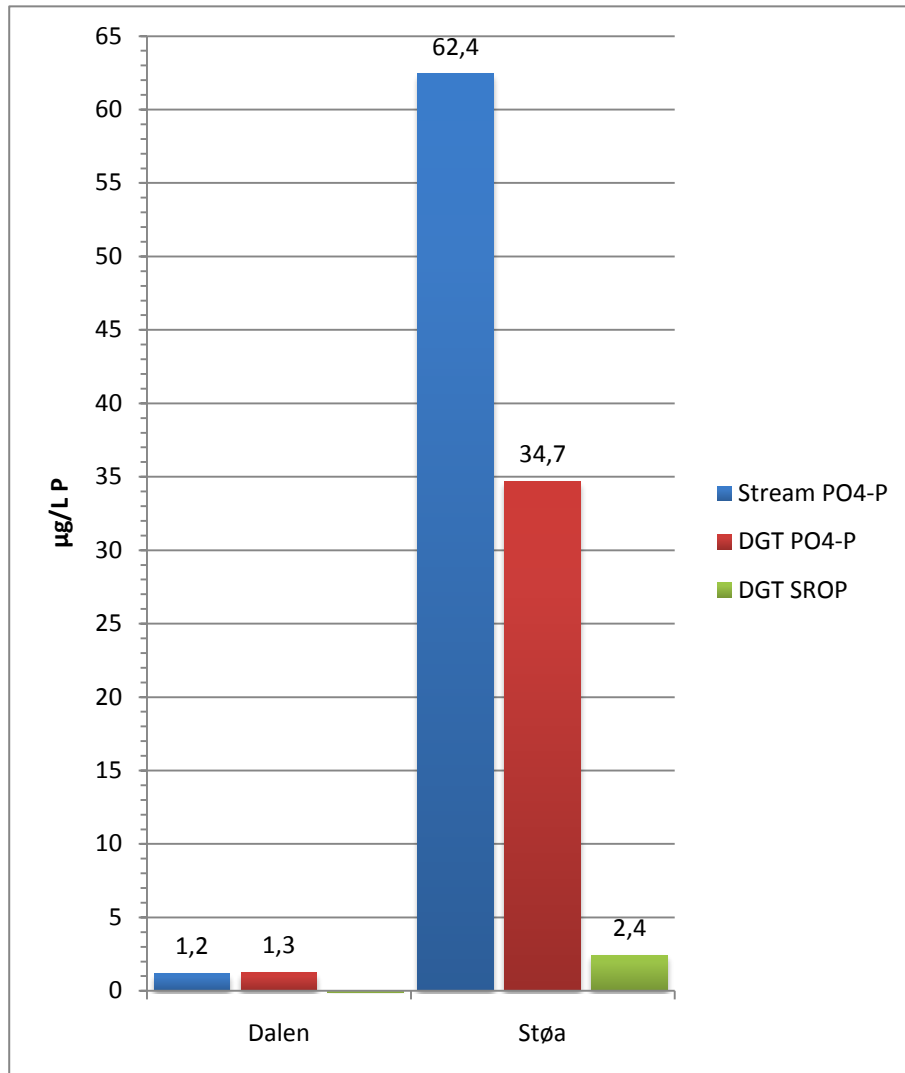


FIGURE 4I Comparison of average stream sample concentration vs average stream concentration determined from P-DGT. Average SROP concentrations from P-DGTs are also shown.

4.4. UV impact on DOM

4.4.1. Humic stream water sample

The absorbencies plotted against the UV exposure time are shown in FIGURE 4h. Concentrations of orthophosphate (PO₄-P) and total P (Tot-P) were plotted in the same graph (FIGURE 4m.) in an attempt to assess the release of orthophosphate from DOP

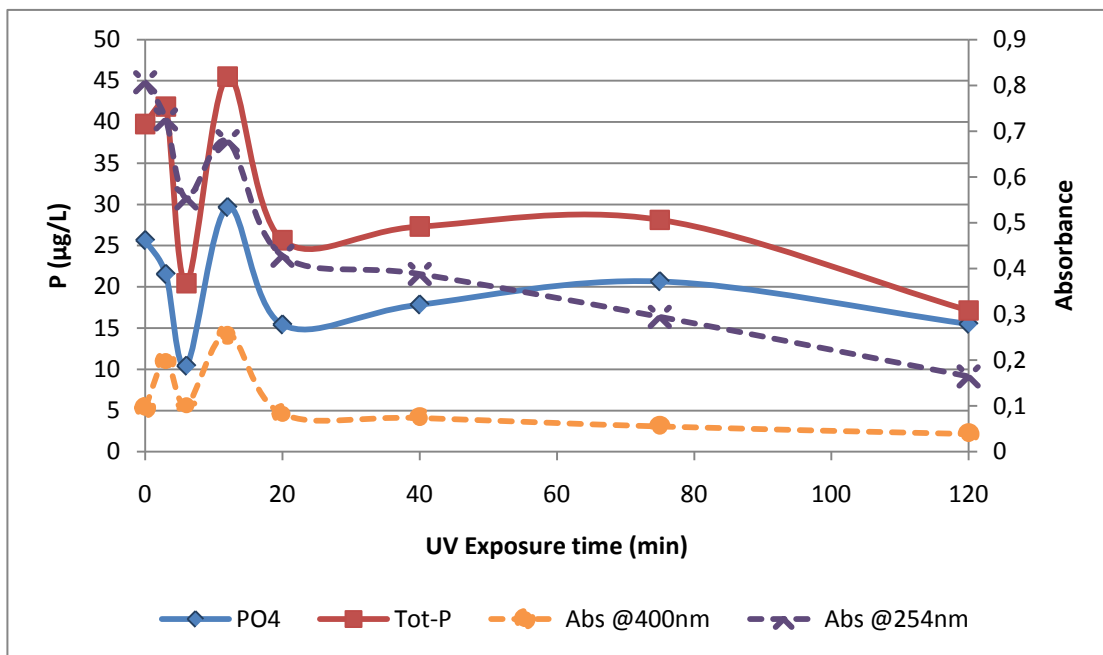


FIGURE 4m Graphs showing the variation in absorbencies and variations in P fractions in the tubes with stream water that were treated with increasing length of UV exposure time.

Unfortunately the results of the UV exposure show an error with the experiment. The total P analysis is the key to discovering this error. In theory the total P should have remained constant with increasing exposure time. The cause for the error appears to be in the CNP analyzer and may be related to precipitation of DOM (see chapter 4.4.3). A confounding issue is that the absorbencies co-vary with the erroneous total P. Another way of looking at the P data is to compare PO₄-P as a fraction of the total P. This way, regardless of whether the homogeneity varies with each sample, the total P will be constant ($\text{Tot-P} / \text{Tot-P} = 1$) and PO₄-P as a fraction of the total P will possibly illustrate a possible trend of DOP mineralization in the experiment, see FIGURE 4n.

From FIGURE 4n it appears to be a clear increase in orthophosphate relative to the total P. The orthophosphate, which initially accounted for about 60% of the total P increased to constitute 90% of the total-P. However we need to consider that the samples were exposed to abnormally (relative to the environment) high intensities of UV radiation for up to 120 minutes.

Despite considerable abnormalities throughout the experiment, the overall effect on DOM of 120 min of intense UV irradiation appears to be between 80% decrease based on UV adsorbency, and 50% reduction based on absorbency of colour at λ 400 nm.

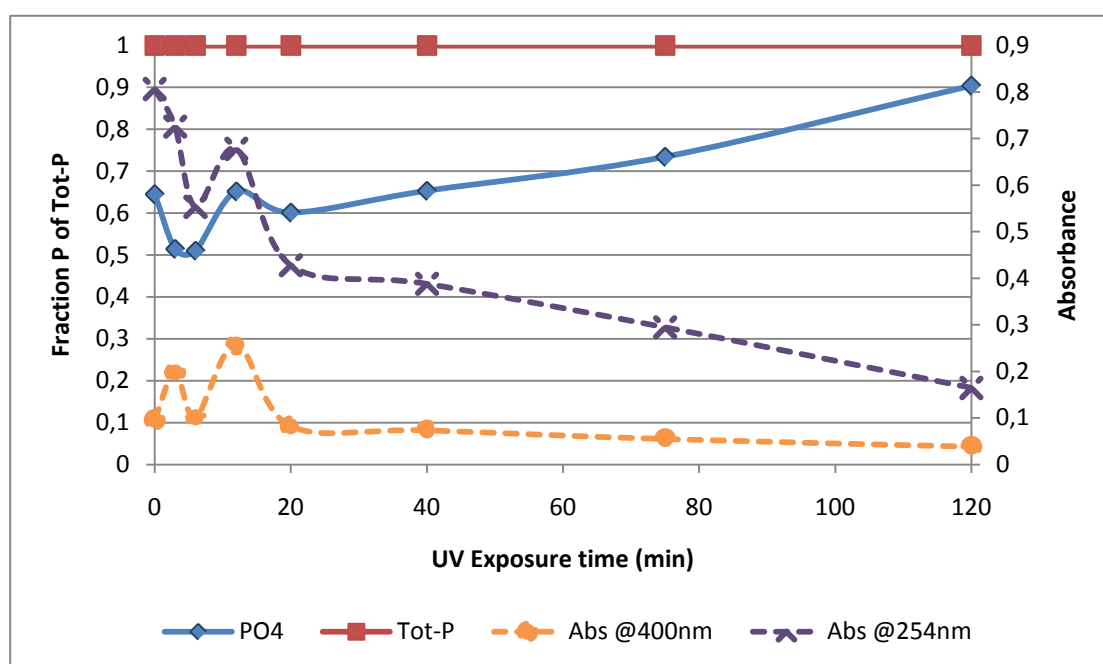


FIGURE 4n Graphs showing the effect of photo-degradation of DOM on P fractions and DOM absorbencies as a function UV exposure time for a stream sample. PO4-P is presented as a fraction of the total P.

Included in the analysis scheme of the experiment was the determination of total nitrogen (tot-N) as well as ammonium (NH_4^+) and nitrate (NO_3^-). The tot-N varied in an unreasonable manner, similar to the tot-P addressed above. In order to assess these N data is to compare the NH_4^+ and NO_3^- as fractions of the total N. When examining the effect of UV exposure on these parameters (FIGURE 4o and FIGURE 4p) a different pattern is found. NH_4^+ increases as NO_3^- decreases with increasing UV irradiation time. One may speculate that the DOM requires an electron acceptor to continuously remove electrons as UV irradiation breaks the chemical bonds. NO_3^- might be that electron acceptor. NO_3^- would then be reduced to NH_4^+ , which may explain why the graphs mirror each other. However it does not explain why the PO4-

P graph seems to initially follow the pattern of the UV and colour absorbance, while the N-species do not.

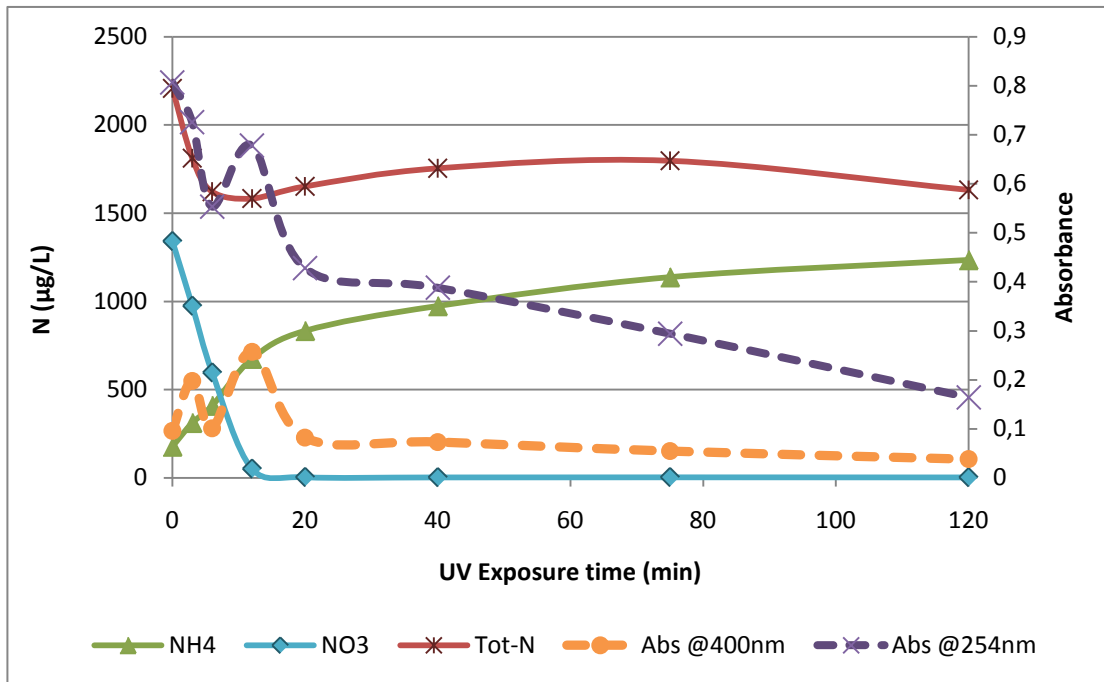


FIGURE 4o Graphs showing the variation in absorbencies and variations in N fractions in the tubes with stream water that were treated with increasing length of UV exposure time.

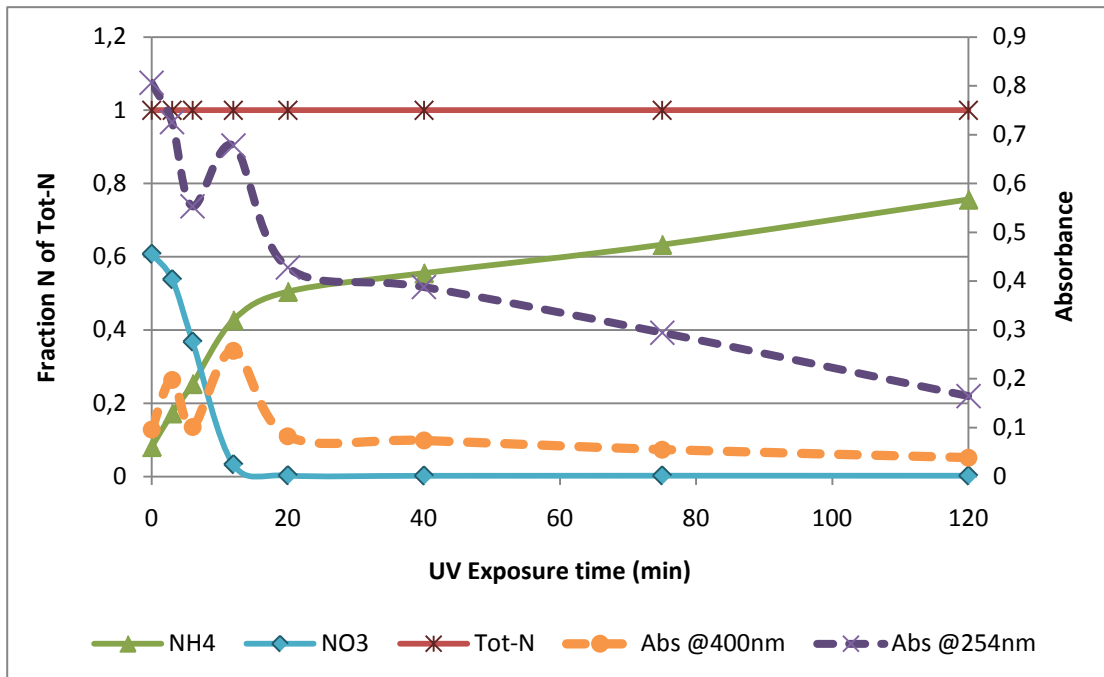


FIGURE 4p Graphs showing the effect of photo-degradation of DOM on N fractions and DOM absorbencies as a function UV exposure time for a stream sample. NH_4^+ and NO_3^- are presented as fractions of the total N.

4.4.2. Zero-tension soil water sample

The results presented in FIGURE 4q. show an unusual trend with the absorbance at 400 nm. Instead of the absorbance decreasing as would be expected due to photo-bleaching, it was found to increase. This may be because DOM from the organic soil water contains very large organic macromolecules which fold upon them selves hindering light to be full absorbed. Another speculation is that many small chromophore groups in individual molecules absorb more light than one giant molecule with many chromophores groups. Correcting for variation in Tot-P we see in FIGURE 4r that the orthophosphate increases rapidly from about 50% of the tot-P to about 67%. The initial increase in orthophosphate concentration seems to indicate an approximate 0.7% orthophosphate release per minute from DOM within the first 40 minutes. It is difficult to interpret the environmental impact this may have as zero-tension water is not naturally exposed UV light.

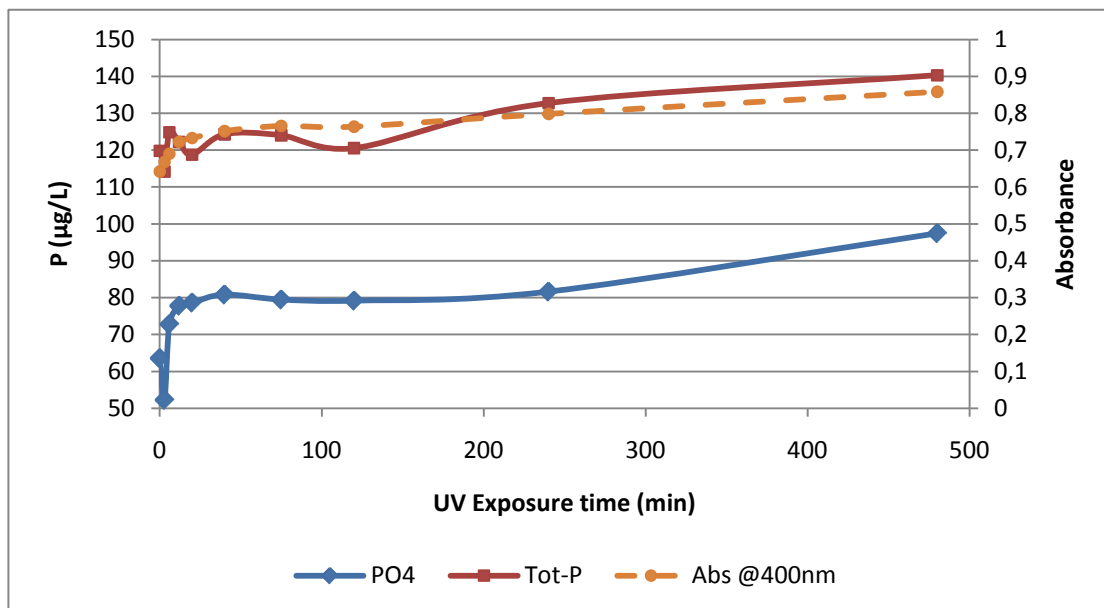


FIGURE 4q Graphs showing the variation in absorbency and variations in P fractions in the tubes with soil water (from the organic forest floor horizon) that were treated with increasing length of UV exposure time.

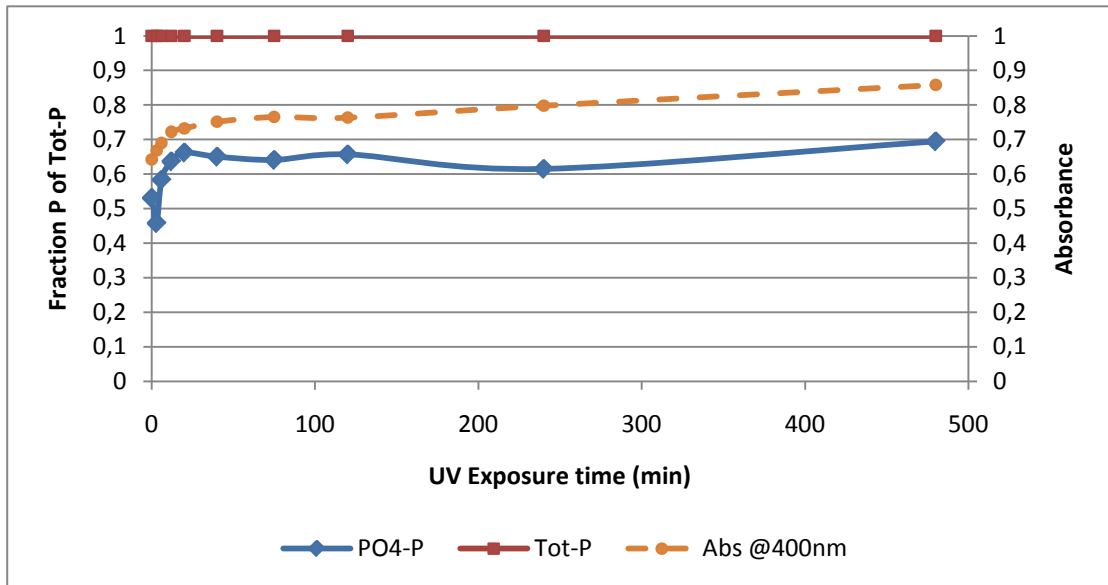


FIGURE 4r Graphs showing the effect of photo-degradation of DOM on P fractions and DOM absorbencies as a function UV exposure time for a soil water (from the organic forest floor horizon) sample. PO4-P is presented as a fraction of the total P.

The pattern of N fractions shown in FIGURE 4s seems to indicate a release of NH_4^+ from the organic material due to the UV as no nitrate was found initially in the sample.

This experiment clearly shows that more studies are needed to determine the effects of UV irradiation of DOM.

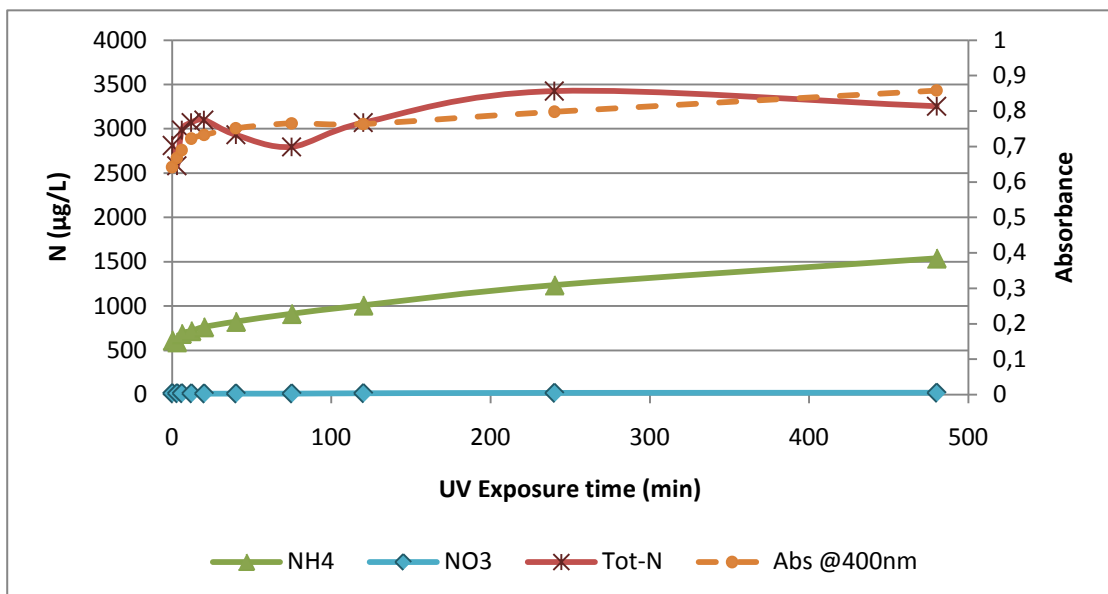
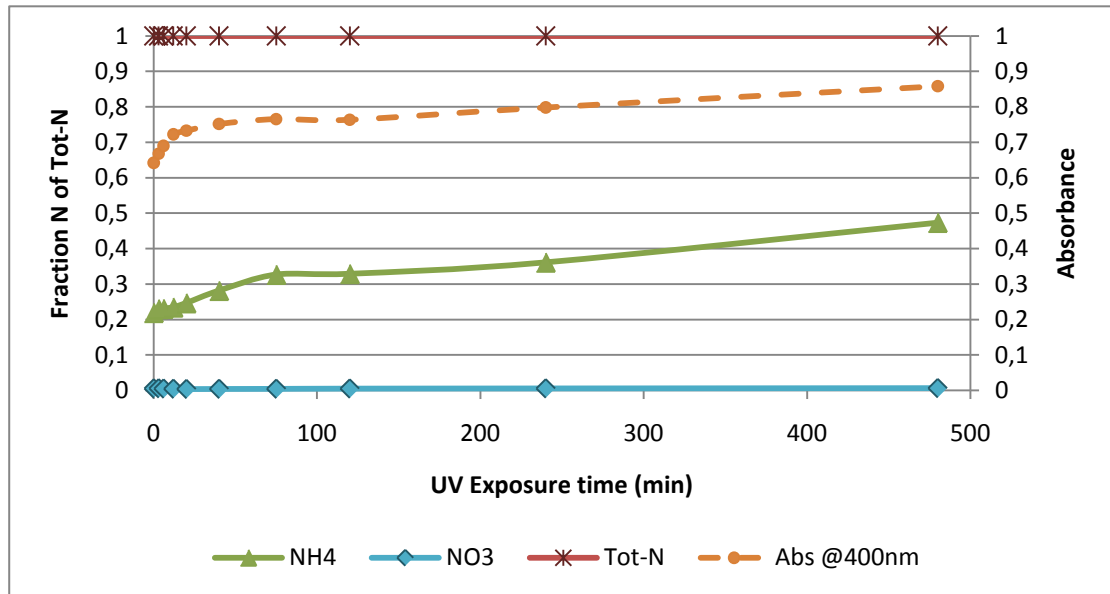


FIGURE 4s Graphs showing the variation in absorbency and variations in N fractions in the tubes with soil water (from the organic forest floor horizon) that were treated with increasing length of UV exposure time.



4.4.3. Possible CNP analysis problems related to DOM.

pH is known to affect the solubility of humic matter. Low pH result in protonation of the hydroxylic group making the humic molecule more non-polar and therefore less soluble in water. One of the issues analysing with the CNP analyzer is that the sample are acidified with 1% 4 M H₂SO₄ prior to analysis. This results in small precipitation of humic matter at the bottom of the vials. By coincidence it was noticed that the zero-tension solutions that were exposed the longest to the UV irrigation had the greatest precipitation under acidic conditions, see FIGURE 4t. This is in fact very surprising as it is the humic fraction that is precipitated upon acidification to pH 1, while the fulvic fraction remains in solution. This therefore suggests that the UV irradiation makes the DOM more humic, which is contradictory to what we may expect.

Anyway, this is believed to have resulted in part of the error for total N and total P. It seems possible that the CNP autosampler does not manage to mix (intake needle blows air out before intake, resulting in mixing) the solution in the tube effectively enough to get a homogenous solution. It is also possible that once the material has precipitated the CNP analyzer is at least partly incapable of dissolving the material within the time of digestion.

This gives cause for concern and we need resolve this problem by revising the sample pre-treatment method.

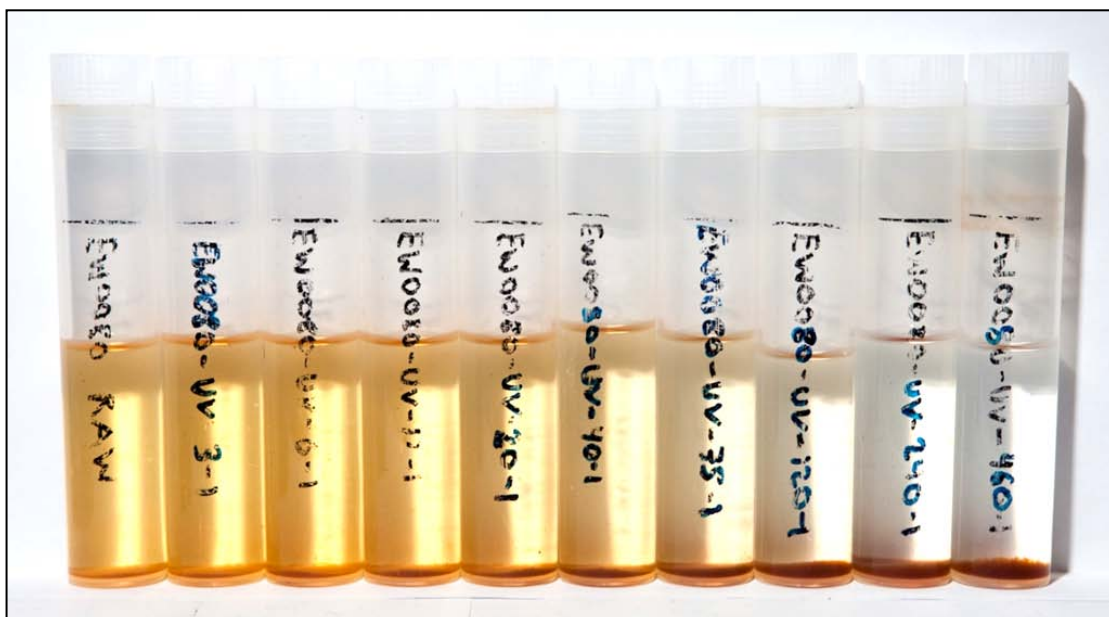


FIGURE 4t The effect of UV exposure on DOM. Solubility decreases as function of UV exposure for acidified samples.

5. Conclusion

Aluminum is known as a strong precipitating agent of orthophosphate. With the reduction in Al leaching, due to a massive reduction in acid rain deposition since the 1980s, it seems possible that less orthophosphate is being precipitated with $\text{Al}(\text{OH})_3$ in the water than before. This may be the reason the no considerable improvements have been noticed in Vansjø's status. More data and research using geochemical modelling is needed to determine Al effect on orthophosphate solubility in the catchment and lake.

The P-DGT sampler seem to be a promising new sampling tool both for sampling of free orthophosphate in water, and also for separation of orthophosphate from low molecular weight (LMW) organic phosphorus compounds in water.

Laboratory experiments showed that AMP (adenosine monophosphate) was efficiently taken up by the P-DGT sampler. When extracting the P-DGT adsorbent, it was shown that AMP was not degraded, but probably released in its original form. The organic fraction could then be determined as the difference between Total-P and $\text{PO}_4\text{-P}$ in the extract.

The diffusion coefficient of AMP was also determined in the laboratory study, and was found to be $3.3 \times 10^{-6} \text{ cm}^2/\text{s}$ at $22.5 \text{ }^\circ\text{C}$, compared to about $5.3 \times 10^{-6} \text{ cm}^2/\text{s}$ for the free $\text{PO}_4\text{-P}$ ion. Diffusion coefficients are temperature dependant. Correction for average temperatures during the sampling period must be done when using DGTs in the field.

If other LMW organic phosphorus compounds behaves similarly as AMP, the P-DGT sampler may be used to collect and calculate concentrations of organic phosphorus compounds in water (denoted SROP in this work). This is a new result in which as far as we know, have not been reported before.

In a smaller field test of P-DGTs at a site with high loads from an agricultural area, a noticeable SROP fraction of 6.5 % of the total P-DGT fraction was observed. This is also an important new finding, as we earlier have limited data for the organic fraction in water. The SROP fraction may be an important P fraction, which may be both biologically available, and an important fraction of soluble P compounds necessary in understanding geochemical mechanisms of phosphorus in water as well as in catchment modelling of phosphorus transport.

The DOM UV-experiment shows that there is a need to revise the experimental conditions to draw clear conclusions from this work. However, the experiment does indicate an initial release of up to 17% SRP from DOP in the zero-tension soil water sample, after UV-exposure. There seems also to be differences in the molecular composition of DOM in soil water versus DOM in stream water on how they react to UV irradiation. This is seen as the absorbency in soil water increased, while stream water decreased at 400 nm with increasing UV-exposure time up 120 min.

6. Future work

Promising results on the use of the P-DGT sampler in this work, shows potential for further work.

We need more data on uptake of other LMW organic P compounds on the P-DGT. This can be done by examining uptake by model compounds of typical LMW P compounds in water (inositols or phytins). Diffusion coefficients need to be calculated by laboratory studies. Diffusion coefficient may also be estimated theoretically by molecular weight/size versus diffusion coefficient models.

Another step may be to separate the different SROP compounds in water from each other. This may be possible using liquid chromatographic techniques coupled to powerful detection techniques such as ICP-MS.

It may also be of interest to combine the DOM UV-experiment, with P-DGTs.

Possibly there are a great number of SROP species being released from DOM, which may be collected by a P-DGT. Such processes may also be studied by LC-ICP-MS.

7. Literature References

- Atkins, P.W., 1994. Molecules in motion, Physical chemistry. Oxford University Press, pp. 846-850.
- Bjørndalen, K., Andersen, T. and Færøving, P.-J., 2007. Utredninger Vansjø - Kartlegging av vannkvalitet i 2006, NIVA, Norwegian Institute for Water Research.
- Chang, S.C. and Jackson, M.L., 1957. Fractionation of soil phosphorus. *Soil Science*, 84: 133-44.
- Cooke, G.D. et al., 1993. Effectiveness of aluminum, calcium, and iron salts for control of internal phosphorus loading in shallow and deep lakes. *Hydrobiologia*, 253(1-3): 323-35.
- Direktoratsgruppen, 2009. Veileder 01:2009 - Klassifisering av miljøtilstand i vann, pp. 1-184.
- Dodson, S.I., 2005a. Aquatic Ecosystems: Chemical Cycles, Introduction to Limnology. McGraw-Hill Higher Education, pp. 239-245.
- Dodson, S.I., 2005b. Community Ecology: Freshwater Communities Changing Through Time, Introduction to Limnology. McGraw-Hill Higher Education, pp. 201-203.
- Dodson, S.I., 2005c. Setting the Stage: Water as an Environment, Introduction to Limnology. McGraw-Hill Higher Education, pp. 39-56.
- Dyer, W.J., Wrenshall, C.L. and Smith, G.R., 1940. Isolation of phytin from the soil. *Science (Washington, DC, United States)*, 91: 319-320.
- European Commission, 2010. Introduction to the new EU Water Framework Directive.
- Gjessing, E.T., Riise, G. and Lyndersen, E., 1998. Acid rain and natural organic matter (NOM). *Acta Hydrochimica et Hydrobiologica*, 26(3): 131-136.
- Haaland, S., Hongve, D., Laudon, H., Riise, G. and Vogt, R.D., 2010. Quantifying the Drivers of the Increasing Colored Organic Matter in Boreal Surface Waters. *Environmental Science & Technology*, 44(8): 2975-2980.
- ISRIC World Soil Information, PODZOLS (PZ).
- Kalff, J., 2002a. Dissolved Oxygen. In: T. Ryu (Editor), *Limnology: Inland Water Ecosystems*. Prentice-Hall Inc., New Jersey, pp. 236-237.

- Kalff, J., 2002b. Phosphorus Concentration and Cycling. In: T. Ryu (Editor), *Limnology: Inland Water Ecosystems*. Prentice-Hall Inc., New Jersey, pp. 247-256.
- Kalff, J., 2002c. Redox Reactions and Nutrient Cycling. In: T. Ryu (Editor), *Limnology: Inland Water Ecosystems*. Prentice-Hall Inc., New Jersey, pp. 239-242.
- Kalff, J., 2002d. Ultraviolet radiation and its effects, *Limnology: Inland Water Ecosystems*. Prentice-Hall Inc., New Jersey, pp. 143-144.
- Krogstad, T., 1992. Tørrstoff og glødetap. In: I.f. Jordfag (Editor), *Metoder for Jordanalyser*. Norges Landbrukshøgskole, Ås, pp. 10-11.
- Lewandowski, J., Schauser, I. and Hupfer, M., 2003. Long term effects of phosphorus precipitations with alum in hypereutrophic. *Water Research Pergamon Press*, 37(13): 3194-3204.
- Lide, D.R., 2004a. In: D.R. Lide (Editor), *Handbook of Chemistry and Physics*. CRC Press LLC, Boca Raton, Florida.
- Lide, D.R., 2004b. Properties of water in the range 0-100 degrees Celsius. In: D.R. Lide (Editor), *Handbook of chemistry and physics*. CRC Press LLC, pp. 3.
- Madigan, M.T. and Martinko, J.M., 2006. Algae. In: G. Carlson (Editor), *Brock Biology of Microorganisms*. Pearson Prentice Hall, New Jersey, pp. 472-477.
- Mørberg, J.P. and Petersen, L., 1982. Øvelsesveiledning til geologi og jordbundlære. Part 2. Den Kongelige Veterinære- og Landbohøyskole, København, pp. 136.
- Murphy, J. and Riley, J.P., 1962. A modified single solution method for the determination of phosphate in natural waters. *Analytica Chimica Acta*, 27: 31-36.
- NGU, 2010. karttjenesten, <http://www.ngu.no/no/hm/Kart-og-data/Kart/>.
- NORDTEST, 2003. Increase in colour and amount of organic matter in surface waters, The Nordic Council of Ministers.
- Norsk Institutt for Skog og Landskap, 2007. Podzol.
- Oberholster, P.J., Botha, A.-M. and Grobbelaar, J.U., 2004. *Microcystis aeruginosa*: source of toxic microcystins in drinking water. *African Journal of Biotechnology*, 3: 159-168.
- Oracle ThinkQuest, E.F., 2008. Eutrophication, <http://library.thinkquest.org/04oct/01590/pollution/culturaleutroph.jpg>, Modified [2008].

- Organisation for Economic Co-operation and Development (OECD), 1982. Trophic Terminology, Eutrophication of Waters, Monitoring, Assessment and Control. OECD, Paris, pp. 75-78.
- Pratt, A.J., 2006. The Curious Case of Phosphate Solubility. *Chemistry in New Zealand*, 70(3): 78-80.
- Puigdomenech, I., 2010. Medusa Chemical Equilibrium. KTH Royal Institute of Technology, Stockholm.
- Rast, W. and Holland, M., 1988. Eutrophication of Lakes and Reservoirs: A Framework for Making Management Decisions. *Ambio*, 17(1): 2-12.
- Rigler, F.H., 1973. A Dynamic View of the Phosphorus Cycle in Lakes. In: E.J. Griffith, A. Beeton, J.M. Spencer and D.T. Mitchell (Editors), *Environmental Phosphorus Handbook*. John Wiley and Sons., New York, pp. 539-572.
- Røyset, O., Bjerke, E., Eich-Greatorex, S., Sogn, T.A. and Almås, Å.R., 2004. Simultaneous sampling of phosphate, arsenate and selenate in water by Diffusive Gradients in Thin Films (DGT), NIVA, Norwegian Institute for Water Research.
- Ryding, S.-O. and Rast, W., 1989a. Characteristics of Eutrophication, The Control of Eutrophication of Lakes and Reservoirs. *Man and the Biosphere Serie*. UNESCO, Paris, pp. 37-40.
- Ryding, S.-O. and Rast, W., 1989b. The Control of Eutrophication of Lakes and Reservoirs. *Man and the Biosphere Serie*.
- Schindler, D.W., 1977. Evolution of Phosphorus Limitation in Lakes. *SCIENCE*, 195: 260-262.
- Seip, H.M., Andersen, D.O., Christophersen, N., Sullivan, T.J. and Vogt, R.D., 1989. Variations in concentrations of aqueous aluminum and other chemical species during hydrological episodes at Birkenes, southernmost Norway. *Journal of Hydrology*, 108(1-4): 287-405.
- Skjelkvåle, B.L., 2009. Overvåkning av langtransporterte forurensinger 2008, NIVA.
- Smithsonian Environmental Research Centre, 2008. Phytoplankton Guide to the Chesapeake Bay & other Regions, Cyanobacteria, *Microcystis aeruginosa*, http://www.serc.si.edu/labs/phytoplankton/guide/other_phyla/microaerug.jsp, Modified [04.11.08].
- Solheim, A.L., 2001. Tiltaksanalyse for Morsa (Vansjø-Hobøl-vassdraget), NIVA.

- Solheim, A.L. and Moe, J., 2008. Eutrofierings-tilstand i norske innsjøer og elver 1980-2008. 1042/2008, Statlig program for forurensningsovervåking.
- Spikkeland, I., 2003. Der det er vann er det liv. Ferskvann og våtmark i Østfold. *Natur i Østfold*, 22(1-2): 27-33.
- Sullivan, T.J., Christophersen, N. and Muniz, I., 1987. Soil and streamwater chemistry during snowmelt at Birkenes catchment, southern most Norway. SI-report 850701-1, Oslo.
- The European Parliament and the Council of the European Union, 2000. Directive 2000/60/EC of the European Parliament and of the Council of 23 October 2000 establishing a framework for Community action in the field of water policy, *Official Journal of the European Communities*, pp. 1-73.
- Thuen, G. and Buer, J., 2003. Handlingsplan for Morsa 2002-2005, Morsa.
- Ulrich, K.-U. and Pöthig, R., 2000. Precipitation of aluminum and phosphate affected by acidification. *Acta Hydrochimica et Hydrobiologica*, 28: 313-322.
- United States Department of Agriculture, 1999. Spodosols, *Soil Taxonomy*, pp. 695-698.
- USGS, 2008. Eutrophication, <http://toxics.usgs.gov/definitions/eutrophication.html>, Modified [24.10.08.].
- vanLoon, G.W. and Duffy, S.J., 2005a. Organic matter in water, *Environmental Chemistry a global perspective*. Oxford University Press Inc., New York, pp. 254-272.
- vanLoon, G.W. and Duffy, S.J., 2005b. Phosphorus environmental chemistry, *Environmental Chemistry a global perspective*. Oxford University Press Inc., New York, pp. 311-319.
- vanLoon, G.W. and Duffy, S.J., 2005c. Soil Properties, *Environmental Chemistry a global perspective*. Oxford University Press Inc., New York, pp. 411-415.
- Vannportalen, 2010. Om vanndirektivet - EUs rammedirektiv for vann.
- Vogt, R.D., 2008. Phosphorus Fractionation (unpublished work). Department of Chemistry, UiO, Oslo.
- Yoshida and Kojima, R., 1940. Studies on organic phosphorus compounds in soil; isolation of inositol. *Soil Science*, 50: 81-89.
- Zhang, H., 2005. DGT - for measurements in water, soil and sediments, DGT Research Ltd, Lancaster.

Zhang, H., Davidson, W., Gadi, R. and Kobayashi, T., 1998. In situ measurement of dissolved phosphorus in natural waters using DGT. *Analytica Chimica Acta*, 340: 29-38.

List of appendixes

<u>APPENDIX A : WATER QUALITY.....</u>	<u>89</u>
<u>APPENDIX B : LABORATORY EQUIPMENT AND INSTRUMENTS.....</u>	<u>90</u>
B-1 PH.....	90
B-2 CONDUCTIVITY	90
B-3 ALKALINITY.....	90
B-4 UV AND COLOR ABSORBANCE	90
B-5 ION CHROMATOGRAPHY (IC)	91
B-6 INDUCED COUPLED PLASMA ATOMIC EMOTION SPECTROMETER (ICP-AES)	91
B-7 CNP AUTOMATED ANALYZER	91
B-8 PHOSPHATE AUTOMATED ANALYZER	94
<u>APPENDIX C : WATER SAMPLING.....</u>	<u>94</u>
C-1 CERAMIC LYSIMETER	94
<u>APPENDIX D : P-DGT CALCULATIONS</u>	<u>95</u>
D-1 CALCULATIONS FOR DIFFUSION FOR ORTHOPHOSPHATE AS A FUNCTION OF TEMPERATURE.	95
D-2 CALCULATIONS FOR DIFFUSION FOR AMP AS A FUNCTION OF TEMPERATURE.	96
D-3 P-DGT CALCULATIONS FOR P IN STREAM.	97

Appendix A: Water quality

TABLE A1 Water quality information

Type	Water Purification System	Resistivity (M Ω cm at 25°C)	TOC (μ g C/L)	Product of
Ultra pure water (Type I)	Milli-Q water	18.2	≤ 5	Millipore
Pure water (Type II)	Elix UV deionized water	5-15	< 30	Millipore

Appendix B: Laboratory equipment and instruments

B-1 pH

Electrode: 8102 ROSS[®] Combination pH Electrode. pH range 0-14. Glass body.

Product of Thermo Fisher Scientific Inc.

Signal measurement device: Orion Research, Expandable ionAnalyzer EA920

Product of Thermo Fisher Scientific Inc.

B-2 Conductivity

Instrument: FiveGo[™] (FG3) hand held operating device.

Product of METTLER-TOLEDO Inc.

B-3 Alkalinity

Instrument: 716 DMS Titrino.

Product of Metrohm AG.

B-4 UV and color absorbance

Instrument: Digital Double-Beam Spectrophotometer UV-150-2

Wavelength range: 200 – 1000 nm

Monochromator: Czerny-Turner type, grating monochromator

Detector: Silicon photo-cell

Cell: 10 mm square quartz cell

Product of SHIMADZU corporation

B-5 Ion Chromatography (IC)

Instrument: ICS-2000.

Product of Dionex Corporation.

Operated by Alexander Engebretsen at the Department of Chemistry, UiO.

B-6 Induced Coupled Plasma Atomic Emission Spectrometer (ICP-AES)

Instrument: Varian Vista AX CCD simultaneous axial view ICP-AES.

Product of Varian Ltd

Operated by Mesay Mulugeta Wolle at the Department of Chemistry, UiO.

All samples were acidified with 1% HNO₃.

TABLE B2 Instrumental ICP-AES conditions used for analysis

Parameter	
RF Power	1.30 kW
Plasma Ar flow	15 L min ⁻¹
Auxiliary Ar flow	1.5 L min ⁻¹
Nebulizer Ar flow	0.75 L min ⁻¹
Sample flow rate	1.5 mL min ⁻¹
Reading time	10 sec

B-7 CNP Automated Analyzer

Instrument: Customized San⁺⁺ Automated Wet Chemistry Analyzer

Software: "Flow Access"

Product of SKALAR.

Operated by Tomas A. Blakseth, Eva Hagebø and Christian W. Mohr at NIVA, Oslo.

TABLE B3 Uncertainty and accuracy calculations for CNP autoanalyzer

Date	Tot-N ppb N	NO3 (low) ppb N	NO3 (high) ppb N	NH4 (low) ppb N	NH4 (high) ppb N	Tot-P (low) ppb P	Tot-P (high) ppb P	PO4 (low) ppb P	PO4 (high) ppb P	TOC (low) ppb C
February 5, 2010	497.61					5.34		4.06	42.71	
March 2, 2010	363.58	44.29	395.40		191.47	5.31	47.27	3.30	40.00	0.526
March 15, 2010	395.42	50.08	396.80	8.61	192.28	4.97	54.53	4.05	41.53	0.50
March 17, 2010				6.85	189.52	4.57	46.76			
March 17, 2010				7.41	191.04					
May 5, 2010	390.55	44.12	394.66	7.53	204.03	5.46	49.10	3.84	40.14	
May 5, 2010	386.69	44.10	395.62	8.03	203.43	5.37	49.84	3.82	39.83	
May 5, 2010			393.58	6.28	195.71					
May 5, 2010			393.54	6.31	198.60					
May 12, 2010	501.08	47.33		8.13	194.62	4.78	46.96	4.16	38.32	
May 27, 2010	469.90	48.80		7.10	210.40	6.40	48.50	4.10	39.80	0.34
June 3, 2010						5.0		4.0	36.3	
July 15, 2010		48.6	394.9			5.0	49.2	3.1	38.1	
Average	429.26	46.75	394.92	7.36	197.11	5.22	49.02	3.82	39.64	0.46
Stdev	58.10	2.55	1.15	0.81	6.87	0.50	2.50	0.38	1.89	0.10
RSD	13.5%	5.4%	0.3%	11.0%	3.5%	9.6%	5.1%	9.9%	4.8%	22.1%
True Value	400	50	400	6	200	4.85	48.5	4	40	0.5
Accuracy	-7.32%	6.50%	1.27%	-22.67%	1.45%	-7.68%	-1.07%	4.45%	0.90%	8.6%

TABLE B4 Calculations for limit of detection

Date	Tot-N ppb N	NO3 ppb N	NH4 ppb N	Tot-P ppb P	PO4 ppb P	TOC ppm P
February 5, 2010	-19.98	-2.77		-0.60	-0.36	
February 5, 2010	-6.96	-0.64		-0.27	-0.27	
February 5, 2010	-9.08	0.26		-0.74	-0.31	
February 5, 2010	-5.23	-0.88		0.12	-0.38	
February 5, 2010	-5.12	-0.90		-0.94	-0.37	
February 5, 2010	-7.20	-0.25		-1.20	-0.38	
March 2, 2010	-3.84	-3.04		0.02	0.96	-0.02
March 15, 2010	-0.64	2.48	-0.10	2.13	-0.11	0.08
March 17, 2010	9.88	1.36	9.77	0.16	0.02	-0.06
May 5, 2010	-3.32	-1.71	3.49	-0.35	-0.11	
May 12, 2010	18.19	1.06	26.54	0.27	0.35	
May 27, 2010		0.50	-0.40	-0.20	0.20	-0.05
June 3, 2010				0.60	-0.26	
July 15, 2010		-5.91		0.55	0.12	
Average	-3.03	-0.80	7.86	-0.03	-0.06	-0.01
Stdev	9.95	2.20	11.22	0.82	0.38	0.06
LOD (k=3)	29.8	6.6	33.6	2.5	1.1	0.2

B-8 Phosphate Automated Analyzer

Instrument: AutoAnalyzer 3

Software: AACE 6.04

Product of SEAL Analytical

Operated by Ruikai Xie and Christian W. Mohr at the Department of Geosciences, UiO.

Appendix C: Water sampling

C-1 Ceramic lysimeter

The ceramic lysimeters are built according to the schematics in FIGURE C1.

Ceramic cup is made of a special porous alumina material known as “P80” developed from CeramTec AG.

The tubing is of type Tygon® R-3603, with the inner and outer diameter 1.52 and 3,02 mm respectively. Tygon® R-3603 is a product of Saint-Gobain Performance Plastics.

Vacuum grease and two-component glue is used to seal all air leaks and hold the lysimeter together.

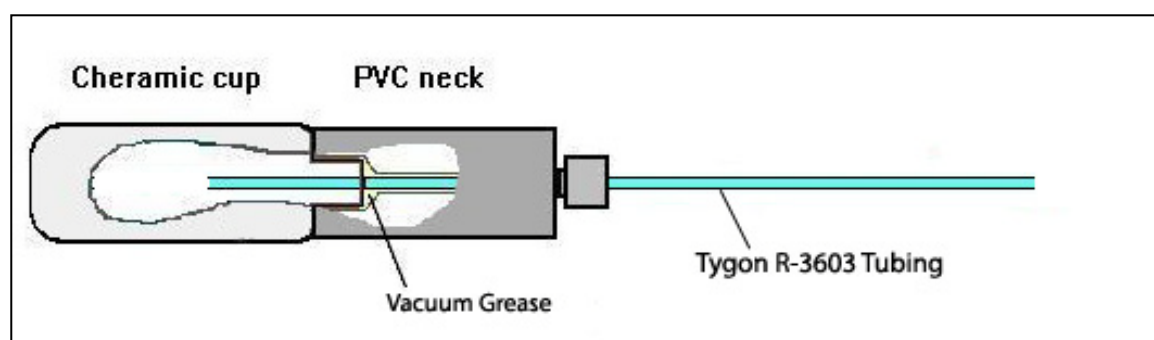


FIGURE C1 Schematics of the ceramic lysimeter.

Appendix D : P-DGT calculations

D-1 Calculations for diffusion for orthophosphate as a function of temperature.

TABLE D5 List of diffusion coefficients for H_2PO_4^- at different temperatures (Zhang, 2005).

Temperature (°C)	D (10^{-6} cm ² /s)
1	2.82
2	2.93
3	3.04
4	3.15
5	3.27
6	3.38
7	3.50
8	3.62
9	3.75
10	3.87
11	4.00
12	4.13
13	4.27
14	4.40
15	4.54
16	4.68
17	4.82
18	4.97
19	5.12
20	5.27
21	5.42
22	5.57
23	5.73
24	5.89
25	6.05
26	6.21
27	6.38
28	6.55
29	6.72
30	6.89

D-2 Calculations for diffusion for AMP as a function of temperature.

TABLE D6 Viscosity for water at different temperatures (Lide, 2004b). Calculation of diffusion coefficient (D) from “Einstein-Stokes equation” for AMP, Equation 2-3.

T (°C)	η ($\mu\text{Pa s}$)	η ($\text{kg m}^{-1} \text{s}^{-1}$)	D ($\text{m}^2 \text{s}^{-1}$)
0	1793	0.00179	1.72286E-10
10	1307	0.00131	2.45002E-10
20	1002	0.00100	3.30865E-10
30	797.7	0.00080	4.29781E-10

D-3 P-DGT calculations for P in stream.

TABLE D7 Calculations of average P concentration in Dalen stream from P-DGTs.

LOG NO.	Date Start	Date End	Sampling Time (s)	Average Temperature (°C)	P-DGT analysis conc. PO4-P (µg P/L)	P-DGT analysis conc. tot-P (µg P/L)	Analysis volume (mL)	Adsorbed PO4-P (µg P)	Adsorbed P (µg P)	Adsorbed SROP (µg P)	D _{DC} PO4-P (10 ⁻⁶ cm ² /s)	D _{DC} SROP (10 ⁻⁶ cm ² /s)	Average Stream PO4-P (µg P/L)	Average Stream SROP (µg P/L)
Average of 5 parallels	30.10.2009 13:05	11.11.2009 14:50	1043100.0	4.3	4.6	4.6	20	0.09	0.09	0.000	3.45	2.27	0.8	0.0
ED011	11.11.2009 14:50	21.11.2009 14:40	863400	6.75	3.2	2.1	20	0.06	0.04	-0.022	3.72	2.43	0.6	-0.3
ED014	21.11.2009 14:40	04.12.2009 14:30	1122600	4.94	20.5	18.1	20	0.41	0.36	-0.048	3.52	2.31	3.4	-0.6
ED016	04.12.2009 14:30	11.12.2009 13:35	601500	3.44	1.6	0.9	20	0.03	0.02	-0.014	3.36	2.21	0.5	-0.3
ED018	11.12.2009 14:30	18.12.2009 12:20	597000	1.00	2.6	2.4	20	0.05	0.05	-0.005	3.10	2.06	0.9	-0.1
Average													1.3	-0.1

TABLE D8 Calculations of average P concentration in Støa stream from P-DGTs.

LOG NO.	Date Start	Date End	Sampling Time (s)	Average Temperature (°C)	P-DGT analysis conc. PO4-P (µg P/L)	P-DGT analysis conc. Tot-P (µg P/L)	Analysis volume (mL)	Adsorbed PO4-P (µg P)	Adsorbed P (µg P)	Adsorbed SROP (µg P)	D _{DC} PO4-P (10 ⁻⁶ cm ² /s)	D _{DC} SROP (10 ⁻⁶ cm ² /s)	Average Stream PO4-P (µg P/L)	Average Stream SROP (µg P/L)
Average of 5 parallels	30.10.2009 14:50	11.11.2009 13:22	1031520.0	4.3	148.5	158.0	20	2.97	3.16	0.190	3.45	2.27	27.1	2.6
ED012	11.11.2009 13:22	21.11.2009 15:30	871680	6.75	170.7	172.8	20	3.41	3.46	0.042	3.72	2.43	34.2	0.6
ED013	21.11.2009 15:30	04.12.2009 12:40	1113000	4.94	260.4	262.4	20	5.21	5.25	0.041	3.52	2.31	43.2	0.5
ED015	04.12.2009 12:40	11.12.2009 12:20	603600	3.44	37.5	38.7	20	0.75	0.77	0.024	3.36	2.21	12.0	0.6
ED017	11.12.2009 13:35	18.12.2009 11:45	598200	1.00	162.3	174.9	20	3.25	3.50	0.252	3.10	2.06	56.8	6.6
Average													34.7	2.4